UNIVERSITY OF CALGARY

Identification of a Novel Conserved Region in ING1 Tumor Suppressors as a Lamin Interacting Domain

by

Xijing Han

A THESIS

SUBMITTED TO THE FACULTY OF GRADUATE STUDIES

IN PARTIAL FULFILMENT OF THE REQUIREMENTS FOR THE

DEGREE OF MASTER OF SCIENCE

DEPARTMENT OF BIOCHEMISTRY AND MOLECULAR BIOLOGY

CALGARY, ALBERTA

JULY, 2007

UNIVERSITY OF CALGARY

FACULTY OF GRADUATE STUDIES

The undersigned certify that they have read, and recommend to the Faculty of Graduate Studies for acceptance, a thesis entitled "Identification of a Novel Conserved Region in ING1 Tumor Suppressors as a Lamin Interacting Domain" submitted by Xijing Han in partial fulfilment of the requirements of the degree of Master of Science.

Supervisor, Dr. Karl Riabowol
Department of Biochemistry and Molecular Biology

Dr. Julie Deans
Department of Biochemistry and Molecular Biology

Dr. Justin MacDonald
Department of Biochemistry and Molecular Biology

Dr. David Schriemer
Department of Biochemistry and Molecular Biology

External Examiner, Dr. Brian Burke
Department of Anatomy and Cell Biology, University of Florida

Date

Abstract

Since the discovery of the ING1 gene, five ING genes named ING1-5 and several different splicing isoforms of ING1, ING2, and ING4 have been identified. ING proteins interact with methylated core histones and with histone acetyltransferase and histone deacetylase complexes to modify chromatin structure. Through comparative sequence analyses, I identified and further characterized a novel region conserved among all ING family members as a Lamin Interacting Domain (LID) that specifically binds to lamin A/C. ING1 colocalized with lamin A/C and expression of lamin A/C was indispensable for nuclear localization of ING1, suggesting ING1 is tethered by lamins to function. Lamin-ING1 interactions were found to be necessary for efficient ING1-induced apoptosis and maintenance of nuclear architecture. Expression of dominant negative LID peptides induced changes in chromatin and the nuclear envelope reminiscent of Hutchinson-Gilford progeria syndrome (HGPS). These data support the idea that loss of lamin-ING1 interactions may be a major effector of lamin A loss leading to the HGPS phenotype.

Acknowledgements

I would like to thank my graduate supervisor, Dr. Karl Riabowol, for all his support and encouragement. I would also like to thank the members of my supervisory committee, Dr. Julie Deans, Dr. Justin MacDonald, and Dr. Dave Schriemer for their helpful comments and guidance. In addition, I thank Dr. Brian Burke for being the external examiner and for providing the useful reagents. I would also like to thank all members in the lab for their help on my research and Dr. Jerome B. Rattner for his assistances with electron microscopy. Finally and importantly, I wish to thank my parents for their love, understanding and encouragement.

This work was supported by grants from the Canadian Institutes of Health Research to Dr. Riabowol.

Table of Contents

List of Tables

List of Figures and Illustrations

CHAPTER ONE: INTRODUCTION

Section I. The ING tumor suppressor

The founding member of the **IN**hibitor of **G**rowth (ING) gene family ING1 was isolated using subtractive hybridization of cDNAs between normal human breast epithelial cells and transformed cancerous cells followed by an *in vivo* selection assay (Garkavtsev et al., 1996). ING family members are present throughout eukaryotic proteomes (He et al., 2005). To date, studies from multiple groups have implicated ING1 as well as other ING family members in the regulation of a variety of cellular processes, including promotion of apoptosis (Scott et al., 2001b;Vieyra et al., 2002b), DNA damage repair (Scott et al., 2001b;Berardi et al., 2004), negative regulation of cell proliferation (Garkavtsev et al., 1996;Nagashima et al., 2001), chromatin remodeling (Feng et al., 2002;Vieyra et al., 2002b), epigenetic regulation (Pena et al., 2006;Shi et al., 2006), and cellular senescence (Garkavtsev et al., 1998b). Reports have identified various splicing isoforms of ING1, ING2, and ING4. The human ING1 gene has three exons which can be alternatively spliced to generate at least three and perhaps a fourth, currently potential transcript, encoding p47ING1a, p33ING1b, p24ING1c, and p27ING1d, among which p33ING1b is the most abundant isoform in human cells and is the best characterized so far (Vieyra et al., 2002b;He et al., 2005).

ING gene products possess distinct, but in some cases overlapping functional properties and unique expression profiles in eukaryotic systems. Ectopic overexpression of ING1 has been found to block cell cycle progression by arresting cells in G1 phase of the cell

cycle, and longer term expression promotes apoptosis. Consistent with a role as a tumor suppressor, inhibition of ING1 expression with antisense RNA promotes focus formation *in vitro* and tumor formation *in vivo* (Garkavtsev et al., 1996;Feng et al., 2002). Loss of ING1 expression has been implicated in a broad range of human cancer types, including primary breast tumors, lymphoid malignancies, testis tumors, squamous cell cancers, and head and neck cancers (Vieyra et al., 2003;Tallen et al., 2003;Gong et al., 2005), whereas mutations of ING1 genes are relatively rare, suggesting that ING1 functions as a class II tumor suppressor.

A) Structural features of the ING family

Since the initial description of ING1, four additional ING family genes named ING2-5 have been identified, primarily through sequence homology searches (Feng et al., 2002;Nagashima et al., 2003;Vieyra et al., 2003;Berardi et al., 2004;He et al., 2005). ING sequences have also been reported in mouse, rat, *C. elegans*, *Drosophila*, yeast, fish, etc., but most of the orthologs are not characterized yet. The chromosomal locations of the ING1-5 genes have been respectively assigned to chromosome bands 13q34, 4q35, 7q31, 12p13.3, and 2q37.3 (He et al., 2005). All ING family members share relatively similar architectural features, containing a conserved region encoding a plant homeodomain (PHD) finger module (He et al., 2005) and a nuclear localization signal (NLS) (Scott et al., 2001a;He et al., 2005).

The most highly conserved feature of the ING family, the PHD motif, is characterized by a Cys4-His-Cys3 zinc finger sequence, and recent studies suggest that the PHD finger of

ING2 directly binds di- and tri-methylated histone H3K4, with a preference on H3K4me3, an epigenetic mark for active chromatin and gene expression (Pena et al., 2006;Shi et al., 2006). In contrast, ING4 also binds to histone H3, but the interaction is not sensitive to the methylation status of the lysine residue K4 (Palacios et al., 2006). The association of ING2 PHD finger together with an H3K4me3 peptide has been studied by Nuclear Magnetic Resonance (NMR), and Y215, E237, and W238 residues of the PHD finger were found to be important in this interaction (Pena et al., 2006). Following the PHD finger, there is a polybasic region which is thought to be involved in stress-induced phosphoinositide (PI) binding (Kaadige and Ayer, 2006). The nuclear localization signal is located upstream of the PHD motif, and contains two functional nucleolar targeting sequences (NTS) RRKR and KKKK that have been shown to be individually sufficient to target p33ING1b to the nucleolus following UV irradiation in human fibroblasts. The ability of p33ING1b to translocate to the nucleolus appears to be important for the efficiency of promoting apoptosis (Scott et al., 2001a).

The p33ING1b isoform is distinguished from other ING1 members by a partial bromodomain and a specific sequence named the PCNA-Interacting-Protein (PIP) domain. PCNA (Proliferating Cell Nuclear Antigen) is an essential factor involved in both DNA replication and nucleotide excision repair (Maga and Hubscher, 2003). After UV treatment, a rapid and significant increase in the colocalization of ING1 with PCNA was observed, and mutations in the PIP region inhibited this interaction (Scott et al., 2001b). While several lines of evidence have suggested that the bromodomain motif may be involved in chromatin remodeling and protein-protein interactions (Roth et al., 2001),

the PIP domain which functions in binding PCNA has also been found in other proteins involved in growth inhibition (p21), growth arrest after DNA damage (GADD45), and DNA replication and repair (FEN-1) (Scott et al., 2001b;Feng et al., 2002). Furthermore, p33ING1b interacts with members of the 14-3-3 family in a phosphorylation status-dependent manner. Binding to 14-3-3 requires the serine 199 of p33ING1b and this interaction targets a significant portion of p33ING1b to the cytoplasm (Gong et al., 2006). Consistent with localizing to chromatin, recent studies have suggested that human ING family proteins are involved in chromatin remodeling functions via physical binding with histone acetyltransferases (HATs), histone deacetylases (HDACs), factor acetyltransferases (FATs), and DNA methyltransferases (DNMT) protein complexes (Loewith et al., 2000;Skowyra et al., 2001;Kuzmichev et al., 2002;Feng et al., 2002;Vieyra et al., 2002a;Xin et al., 2004;Doyon et al., 2006). Fig. 1 shows some of the structure features of p33ING1b and its binding partners.

B) ING associations with chromatin remodeling factors

Chromatin is the DNA-protein complex packed inside the nucleus of living cells. Chromatin associated proteins are responsible for the impressive feat of packaging approximately two meters of DNA within a cell nucleus of only a few micrometers. The first level of compaction is wrapping DNA into nucleosomes. Each nucleosome core consists of two molecules each of histones H2A, H2B, H3, and H4. A 146-bp segment of acidic DNA is wrapped around the outside of this core of basic histones, forming a 10-nm nucleosome fiber. Chromatin is further packed into higher-order structures known as 30-nm chromatin fibers that require the addition of histone H1 in inter-nucleosomal

regions (Feng et al., 2002;Marmorstein, 2004;Han et al., 2006). Chromatin structure is very dynamic and can be affected by various modifications of chromatin-associating proteins, for example, histones and their remodeling cofactors. Histones are basic proteins with a large proportion of positively charged amino acids, mainly arginine and lysine, and are subject to numerous post-translational modifications including acetylation, methylation, phosphorylation, ubiquitination, and ADP-ribosylation that take place primarily on their 'tail' domains (Marmorstein, 2004;Bannister and Kouzarides, 2005;Mai et al., 2005). These modifications, performed by histone acetyltransferases (HATs), histone deacetylases (HDACs), histone methyltransferases (HMTs), and histone kinases (HKs) among others, offer a mechanism through which upstream signaling pathways converge on common targets to regulate gene expression. Acetylation of histones neutralizes their positively charged lysine-rich amino-terminal tails, thus destabilizing the binding of histones to the negatively charged DNA. Then, other protein complexes are capable of unwinding the chromatin, accessing DNA at certain sites, and initiating gene transcription (Fig. 2) (Han et al., 2006). The dynamic modification of histones through the enzymatic actions of HAT/HDAC complexes is able to alter the degree of DNA relaxation and subsequently modify the accessibility of DNA regions to transcription factors. As a result, HAT/HDAC complexes are believed to serve as relatively general activators or repressors of gene expression. Most HATs have now been identified as transcriptional adapters or co-activators, while many HDACs usually act as co-repressors for transcription (Sterner and Berger, 2000). The state of histone acetylation affects gene expression significantly, and as a result it plays important roles in DNA repair, DNA recombination, apoptosis, and cell cycle progression. Alterations of

HDACs have been identified in tumor cells and contribute to the massive perturbations of gene expression in numerous tumors. Nowadays, HDAC inhibitors (HDACi) represent a new class of targeted anti-cancer agents currently in clinical development and their inhibition of HDACs frequently leads to selective differentiation, cell cycle arrest, and apoptosis in tumor cells (Mai et al., 2005;Peixoto and Lansiaux, 2006). Methylation of histones has been correlated with both positive and negative effects on transcription regulation. Certain modifications (e.g. H3K4 methylation) are strongly indicative of transcriptional activation, whereas other methylation events, such as H3K9 or K27 methylation, are usually associated with repression of transcription (Cao et al., 2002;Kobza et al., 2005).

To date, many studies have indicated that ING1 proteins are involved in epigenetic regulation of gene expression through chromatin remodeling, by physical interactions with protein complexes possessing HAT or HDAC activities. It was initially reported that Yng2, an ING1 ortholog in yeast, was able to interact with Tra1. Tra1 is a yeast ortholog of human TRRAP and a protein component of HAT complexes such as SAGA (Spt-Ada-Gcn5 acetyltransferase) and NuA4 (nucleosomal acetyltransferase of H4) (Loewith et al., 2000). The NUA4 complex preferentially acetylates histone H4, and H2A to a lesser extent, and is vital for cell cycle progression (Allard et al., 1999;Choy et al., 2001). Human ING1 proteins are also found to associate with both HAT and HDAC complexes. On one hand, immunoprecipitated endogenous human ING1 complexes contain HAT activities towards histones H3 and H4, and they co-precipitate with several different HAT enzymes or associated proteins, including CBP (CREB binding protein), PCAF

(p300/CBP-associated factor), p300, and TRRAP (transformation/transcription domain-associated protein) (Vieyra et al., 2002a). The two major isoforms of ING1, p33ING1b and p47ING1a, seem to play distinct roles in regulating gene expression. p33ING1b could selectively increase histones H3 and H4 acetylation when it was microinjected into individual cells, while p47ING1a inhibited histone acetylation. p33ING1b associates with HAT complexes that contain p300/CBP components with a greater affinity than p47ING1a, and p47ING1a has a preference in interaction with HDAC complexes that contain HDAC1 (Vieyra et al., 2002a). On the other hand, p33ING1b has been shown to inhibit the deacetylation of p53 on K382 by physical binding with SIRT1, a NAD^+-dependent type III HDAC that interacts with histone H1 and deacetylases H1 K26 (Vaziri et al., 2001). SIRT1 has been identified as a component of a previously undescribed polycomb repressive complex, PRC4 (Polycomb Repressor Complex 4), and both sirtuins and polycomb proteins have been strongly implicated in regulating senescence (Kataoka et al., 2003;Vaquero et al., 2004). In addition, another group found that the N-terminal 125 amino acids of p33ING1b were responsible for linking ING1 to the Sin3/HDAC complex through direct interaction with Sap30. Sap30 is a specific component of Sin3 complexes and it mediates interactions with different polypeptides providing specificity to Sin3/HDAC complexes which are thought to repress chromatin structure and associate with subunits of the Brg1-based SWI/SNF chromatin remodeling complex (Kuzmichev et al., 2002).

Besides ING1, all other ING family members have also been reported to associate with diverse groups of HAT/HDAC complexes. ING2 was shown to co-localize with post-

translationally modified p53 and p300 during replicative senescence. More p53 was detected with immunoprecipitated p300 in cells co-transfected with ING2, suggesting that ING2 might be able to enhance the acetylation of p53 by p300 (Pedeux et al., 2005). Moreover, a recent study carried out by the purification of TAP-tagged ING family proteins followed by mass spectrometry proposed their involvement in several novel HAT/HDAC complexes. While ING2 was found in an HDAC complex similar to ING1, ING3 associated with the human NuA4/Tip60 HAT complex. ING4 and ING5 were both present in a HBO1 HAT complex (histone acetyltransferase binding to ORC1), and ING5 was also identified in H3-specific HAT complexes containing MOZ/MORF (Monocytic Leukemia Zinc Finger Protein/MOZ-Related Factor) leukemogenic proteins (Doyon et al., 2006). Such associations between INGs and HAT/HDAC complexes not only support the idea that INGs are able to regulate gene expression, but also link chromatin remodeling to other biological functions of ING proteins such as cell cycle regulation, apoptosis, cellular senescence, and DNA repair. Although such associations have been observed by our and other groups for several years, and the ING proteins may play key roles in regulating tumor cell growth, the regions and mechanisms of ING proteins that interact with HAT/HDAC complex proteins are still unknown.

C) ING proteins in cell cycle regulation and apoptosis

ING1 protein was initially identified as a tumor suppressor since ectopic expression of ING1 arrests cells at the G0/G1 phase of the cell cycle (Garkavtsev and Riabowol, 1997) and later induces apoptosis (Helbing et al., 1997). Overexpression of p33ING1b can activate the p21/WAF1 promoter, a cyclin-dependent-kinase inhibitor (CDKi)

(Garkavtsev et al., 1998a). Distinct isoforms of ING1 may be involved in different ways in regulating cell cycle progression. Cells transfected with ING1a showed a senescent-like phenotype and accumulation of senescence-associated heterochromatic foci (SAHF) which are typical in senescent cells, whereas overexpression of ING1b induced formation of nuclear apoptotic bodies (Soliman et al., in preparation). The mechanism by which cells respond differentially to ING1a and ING1b may be related to their preference in binding to various HAT/HDAC complexes and regulating gene transcription. In addition, ING1b interaction with PCNA also appears to be involved in the induction of apoptosis. Variants of ING1b containing point mutations within the PIP region induced apoptosis to a similar level as the control vector, consistent with their reduced efficiency in PCNA binding (Scott et al., 2001b). The ARF tumor suppressor has also been suggested to be involved in p33ING1b-induced apoptosis through interaction with the N-terminus of p33ING1b with amino acids 1-171 of p33ING1b being sufficient to bind ARF *in vivo*, while p33ING1b failed to affect the level of p21 in ARF-/- mouse embryonic fibroblasts (MEFs). ARF-/- MEFs became much less sensitive to p33ING1b overexpression and they retained a normal cell proliferation rate (Gonzalez et al., 2006). Recently ING1-knockout mice were generated. ING1-/- mice showed reduced body weight and size and were more sensitive to gamma irradiation. Loss of p37ING1 in MEFs significantly increased their proliferation rate (Kichina et al., 2006;Coles et al., 2007), consistent with previously identified roles of ING1 in negatively regulating cell proliferation (Garkavtsev et al., 1996).

ING proteins have also been directly implicated in transcriptional regulation. For example, antisense ING1 induced upregulation of cyclin B1, while adenovirus-mediated overexpression of p33ING1b inhibited the expression of cyclin B1 (Takahashi et al., 2002). It is not clear how ING1 proteins perform their roles in cell cycle regulation, and it may be linked to binding to AT-motif rich gene promoters, thus affecting gene transcription activities (Kataoka et al., 2003). It has been found that the gene expression of heat shock protein 70 (HSP70) is greatly increased by both p33ING1b and p32ING2 in a p53-independent mechanism (Feng et al., 2006). The family of heat shock proteins consists of more than ten identified members, and they serve as chaperones for assisting protein folding and translocation (Castelli et al., 2004). Through overexpression of various ING1b constructs, the first 70 amino acids of p33ING1b seemed to be responsible for the induction of HSP70 expression. By upregulating HSP70 level, p33ING1b sensitized cells to TNF-α induced apoptosis signaling, since HSP70 was thought to inhibit the NF-κB survival pathway (Feng et al., 2006).

A recent study suggested links of the ING proteins to transcriptional regulation via the Transforming Growth Factor-β (TGF-β) signaling pathway. The TGF-β pathway involves specific transmembrane serine/threonine kinase receptors and subsequent phosphorylation of R-Smad proteins (Massague, 1998). Similar to ING activities, the TGF-β pathway inhibits cell proliferation and displays tumor suppressive functions (Massague et al., 2005). ING2 was found to selectively upregulate TGF-β-dependent transcription through the PHD domain and facilitate TGF-β in inducing cell cycle arrest (Sarker et al., submitted 2007).

D) A novel conserved region in the ING family

Through previous comparative sequence analyses of ING proteins across different species, a highly conserved region which has a KIQI/KVQL motif labeled MDS00105 was identified by Kawaji and colleagues (Kawaji et al., 2002). In contrast to the PHD region, this region shows moderate sequence similarities among all ING family members, but it is well conserved within each subfamily in various species such as human, mouse, and fruitfly. The analysis divided it into three sub-motifs MDS00105.1-MDS00105.3 that distinguished ING1/ING2 (originally referred to as ING1L), an ING1-homolog, and ING3 subfamily members from each other (Kawaji et al., 2002). Their observations were subsequently independently extended by our group's bioinformatic searches. Our previous work indicated that the ING1/ING2 subfamily has the Q-E-L-G-D-[E/D]-K-[I/L/M]-Q-[I/L] sequence; the ING4/ING5 subfamily carries the K-E-[F/Y]-[S/G]-D-D-K-V-Q-L motif; and the ING3 subfamily is characterized by the L-E-D-A-D-E-K-V-Q-L motif (He et al., 2005). Though this region shows a relatively low degree of conservation among the ING protein family, it displays several highly conserved residues, suggesting a potentially significant role. Thus, while all of the previously described conserved regions of ING proteins have been determined to operate in specific biochemical pathways or in subcellular localization of INGs, this newly defined domain has not yet been functionally characterized and may thus serve to link the INGs to some of their major biological activities. Here my data suggests that this novel conserved region mediates the interaction of p33ING1b and nuclear A-type lamins and this interaction plays an important role in maintaining the genomic stability.

Section II. Nuclear lamins and laminopathies

Nuclear lamins are the principle components of the nuclear lamina, which is located underneath the inner nuclear membrane (INM). The nuclear envelope consists of a double-layer nuclear membrane, nuclear pore complexes, and the nuclear lamina (Broers et al., 2006). Lamins have been classified as type V intermediate filament (IF) proteins. IF proteins all share a well-defined conserved structure, including an N-terminal globular head domain, a central rod domain which is connected by three linker regions, and a C-terminal tail domain (McKeon et al., 1986). The rod domain of lamins is the most conserved region when compared with other IF proteins, whereas the two terminal domains are quite variable within different lamins (Parry et al., 1986). The rod domain is involved in the formation of a coiled-coil dimer between two lamin protein chains, the basic structure unit of lamin assembly (Stuurman et al., 1998). Similar to the ING family proteins, lamins also contain a nuclear localization signal sequence in their tail domains, in which mutations result in the assembly of cytoplasmic filaments (Loewinger and McKeon, 1988). Human genomes contain three lamin genes, LMNA, LMNB1, and LMNB2, and they encode at least seven different proteins that are classified as either A- or B-type lamins (Broers et al., 2006).

A) The lamin family and processing of the maturation of lamins

The LMNA gene can be alternatively spliced into four A-type lamins, lamin A, C, AΔ10, and C2, among which lamins A and C are the predominant products (McKeon et al., 1986;Goldman et al., 2002). A-type lamins are primarily expressed in differentiated cells,

and B-type lamins are expressed in all cells, suggesting lamins perform their functions through a cell-type specific manner (Rober et al., 1989;Furukawa and Hotta, 1993;Furukawa et al., 1994;Machiels et al., 1996). Mice lacking A-type lamins normally die within eight weeks after birth, and they were characterized by reduction in growth, lower weight and muscular dystrophy, a phenotype similar to the Emery-Dreifuss muscular dystrophy (EDMD) disease (Sullivan et al., 1999). Distinct from lamin C, lamin A is characterized by a tail region which has a CaaX motif (McKeon et al., 1986). The CaaX box is present in both lamin A and B-type lamins, and it consists of a cysteine, two aliphatic amino acids in the middle, and another C-terminal amino acid. The cleavage of this CaaX box is indispensable for the maturation of lamins (Broers et al., 2006). Lamin A is first synthesized as a pre-form with 18 extra amino acids. During the process of maturation of lamin A, it is farnesylated on the cysteine by farnesyltransferase. This is followed by methylation and proteolysis to release the -SIM (-AAX) of the CaaX motif. This cleavage is performed by the ZMSPTE-24 zinc metalloproteinase. Thus, lamin A is processed to a form referred to as pre-lamin A, and pre-lamin A is then able to translocate to the nuclear envelope. A final cleavage by ZMPSTE-24 subsequently takes place, which removes the 15 amino acids from the C-terminus of pre-lamin A, resulting in mature lamin A (Pendas et al., 2002;Broers et al., 2006).

B) Integral membrane proteins of the inner nuclear membrane

Lamins are essential for maintaining the mechanical strength of the nuclear structure, and to date, many nuclear envelope transmembrane proteins (NETs) have been reported to interact with lamins, including lamina-associated polypeptides (LAPs), emerin, lamin B

receptor (LBR), nesprins, and LEM2 (Broers et al., 2006). Integral membrane proteins are synthesized on the endoplasmic reticulum (ER) and proteins that are destined to remain in the ER or in the nuclear envelope contain specific signal sequences for targeting and retention. Models have been suggested for protein targeting to the inner nuclear membrane, and among those a so-called 'diffusion-retention' model is supported by several studies. In that model, diffusion of membrane proteins takes place in the interconnected membranes of the ER and the nuclear envelope, and subsequent binding to nuclear ligands such as lamins and chromatin prevents the membrane proteins from escaping (Holmer and Worman, 2001).

LAP1 and LAP2 were originally discovered through their associations with the nuclear envelope (Senior and Gerace, 1988;Foisner and Gerace, 1993). Six alternatively spliced isoforms of LAP2 have been identified. The membrane-associated LAP2 polypeptides preferably bind to B-type lamins as well as barrier-to-autointegration factor (BAF), DNA, and chromatin, and they are essential for cell survival (Yang et al., 1997;Furukawa et al., 1998;Furukawa, 1999;Gant et al., 1999). Lap2β interaction with lamins and chromatin is inhibited by mitotic phosphorylation (Foisner and Gerace, 1993). Lap2, emerin, and MAN1 all belong to the LEM-domain family of nuclear proteins, which share a 43-residue homologous domain, located at or near their N-termini (Lin et al., 2000). MAN1 is a protein with two transmembrane spanning domains and two terminal nucleoplasmic domains, and it binds to Smad transcription factors and regulates development and chromosome segregation (Liu et al., 2003). Emerin is characterized as a type II integral membrane protein with an N-terminal nucleoplasmic domain (Manilal et

al., 1996;Roux and Burke, 2007). It is very special among all binding partners of lamin A/C, since loss of emerin causes X-linked form of Emery-Dreifuss muscular dystrophy, the same as many dominant mutations within A-type lamins (Bione et al., 1994). In lamin A/C knockout mice, emerin partially mislocalizes to the ER, suggesting that A-type lamins serve a role for anchoring emerin on the inner nuclear membrane (Sullivan et al., 1999). In addition to emerin, a novel, ubiquitously expressed LEM domain protein, LEM2, has also been shown to interact with A-type lamins and proper localization of LEM2 requires A-type lamins at the nuclear envelope (Brachner et al., 2005). In $LMNA^{-/-}$ MEFs, the overexpressed LEM2 protein was distributed throughout the ER, and by restoring expression of GFP-lamin A LEM2 relocalized to the nuclear envelope.

The lamin B receptor (LBR) contains eight transmembrane spanning domains (Schuler et al., 1994). LBR binds to lamin B1 (Worman et al., 1988) and is essential for fetal development (Waterham et al., 2003). Studies using fluorescence recovery after photobleaching (FRAP) techniques demonstrated that GFP-LBR diffused rapidly within the ER membranes of interphase cells, and later diffusion of GFP-LBR from the ER to the nuclear envelope made the protein immobilized (Ellenberg et al., 1997). Nesprin-1α was the first nesprin found to bind directly to A-type lamins and emerin (Mislow et al., 2002). All nesprin family proteins (also known as Syne and NUANCE) are characterized by multiple spectrin repeat domains, and some alternatively spliced isoforms of nesprins are notable for their huge sizes (>800kDa) (Zhang et al., 2001;Zhang et al., 2002;Zhang et al., 2005). Functions of the nesprins are not clear yet, and many family members

possess an actin-binding domain. Nesprin-1 and Nesprin-2 can bind to actin and are influenced by the actin cytoskeleton (Zhang et al., 2002).

C) Dynamics of the nuclear envelope

Located most prominently on the peripheral nuclear lamina, lamins play a pivotal role in maintaining the shape and stability of the nuclear envelope. When lamins were immuno-depleted from cell-free extracts *in vitro* prior to the initiation of nuclear assembly, chromosome decondensation and nuclear pore assembly were inhibited in some cases, whereas in other studies, depletion failed to block the envelope assembly, but the resulting nuclei that lacked the lamina were very small and fragile (Burke and Gerace, 1986;Ulitzur et al., 1992;Ulitzur et al., 1997). The most dramatic change of the nuclear envelope occurs during cell division. Nuclear lamins are rapidly disassembled at the prophase/prometaphase transition in the process of cell cycle. It is thought that at the onset of mitosis, the disassembly of lamin filaments is initially driven by the phosphorylation of lamins by cdk1 (also known as cdc2), and upon phosphorylation, the head-to-tail interactions between lamin dimers are abolished (Heald and McKeon, 1990;Peter et al., 1990). However, another model suggests that the at the end of prophase microtubules bind and drag the membrane components away from the nucleus, thus disrupting the nuclear envelope and allowing kinases to function (Beaudouin et al., 2002). In mammalian cells, A-type and B-type lamins perform different stepwise functions in the dynamic process. The current view is that A-type lamins dissociate from the nuclear lamina at early prophase and during mitosis they occur in a soluble and non-membrane-associated state, and B-type lamins remain associated with some membrane structures (Broers et al., 2006). The depolymerized A-type lamins are released and

diffuse first into the nucleoplasm and subsequently break through the nuclear envelope and translocate into the cytoplasm (Georgatos et al., 1997).

At the completion of mitosis, the reassembly of nuclear lamins into a lamina and reformation of the nuclear envelope take place in which membrane targeting and proper localization of those integral membrane proteins are required. Lamin dephosphorylation is indispensable for nuclear lamina reassembly, and it has been found that type I protein phosphatase (PP1) is the major phosphatase responsible for dephosphorylating lamin B (Thompson et al., 1997). PP1 is a family of Ser/Thr phosphatases whose members are highly conserved among eukaryotes, and it is involved in many cellular processes, such as regulating retinoblastoma (Rb) phosphorylation status (Ludlow et al., 1993), histone H1 dephosphorylation (Paulson et al., 1996), and mitotic exit (Fernandez et al., 1992). Targeting PP1 to the nuclear envelope is performed by AKAP149, an A-kinase anchoring protein. AKAP149 contains a PP1-binding domain (PP1-BD), and overexpressing the PP1-BD peptide in Hela cells was shown to interfere with the recruitment of PP1 to the nuclear envelope and therefore disrupt the reassembly of B-type lamins at the end of mitosis. Those cells surprisingly displayed normal peri-nuclear staining of lamin A/C after two hours of transfection. Nevertheless, nuclear fragmentation followed by apoptosis was detected in almost all transfected cells after six hours from mitotic arrest, and LBR and lamins were extensively cleaved into fragments by proteolysis, suggesting a role in cell survival (Steen and Collas, 2001).

The regulation of various lamin structures formed during the reassembly of the nuclear envelope has been examined by interactions between lamins and other proteins.

Reassembly commences with the association of chromosome ends with LAP2α, BAF, and subsequently LBR and emerin (Haraguchi et al., 2000;Broers et al., 2006). When GFP-tagged A-type lamins were transfected into cells, vital imaging showed that lamina reassembly of lamin A/C did not initiate until after cytokinesis. When cytokinesis was completed, the majority of A-type lamins seemed to translocate towards the newly formed nucleus and associate with the chromatin very rapidly (Chaudhary and Courvalin, 1993;Broers et al., 1999).

D) Involvement of lamins in DNA replication

Recent studies suggest that during interphase, in addition to the nuclear periphery, lamins are also found in some nucleoplasmic areas. Those nucleoplasmic lamins aggregate as distinct foci or are organized into veil-like structures as shown by both immunofluorescence and live-cell imaging using GFP-tagged lamins (Liu et al., 2000;Moir et al., 2000b). However, distinct from the peri-nuclear lamins, the nucleoplasmic structures are much less resistant to detergent/high-salt extraction, suggesting the mediation of lamins in a variety of functions including assembly of the nuclear envelope, DNA replication, and gene transcription.

In mammalian cells, DNA synthesis occurring in S phase initiates in foci distributed throughout the nucleus (Nakamura et al., 1986;Ma et al., 1998) and subsequently the replication sites cluster into regions that contain heterochromatin (Nakayasu and Berezney, 1989). The first evidence that links nuclear lamins to DNA replication is that in *Xenopus laevis* egg extracts where lamins were functionally disrupted, the assembled

nuclei displayed defects in DNA synthesis (Newport et al., 1990;Meier et al., 1991;Spann et al., 1997;Ellis et al., 1997;Moir et al., 2000a). The mechanism by which lamins affect DNA replication remains contentious. In one study, BrdU-labeling in primary cells showed that DNA replication foci were located surrounding the nucleolus and colocalized with nucleoplasmic lamin A/C foci as well as members of the Rb protein family, whereas replication sites in immortalized cells were characterized by a more dispersed pattern. Moreover, both CAF-1 (p150) and PCNA were found in a limited number of these foci in G1 and early S phases of the cell cycle (Kennedy et al., 2000). However, another group suggested that the most obvious coalignment of lamin B with BrdU and PCNA occurred during mid-late S phase (Moir et al., 1994).

E) Nuclear lamins as regulators of transcription

Interactions between lamin A/C and Rb implicates the role of lamins in transcription, and the binding sites of lamins have been mapped to amino acids 247-355 in lamin A (Ozaki et al., 1994). Rb has been well established as both a tumor suppressor and transcriptional regulator, and it is absent or mutated in many human cancers (Nevins, 2001;Zhu, 2005). Rb can be modified by phosphorylation (Lee et al., 1987). The phosphorylation status of Rb is essential for performing its function in repressing gene transcription through interactions with E2F, and the nuclear anchorage of Rb is also regulated in a phosphorylation-dependent manner. During G1 phase, Rb is predominantly hypophosphorylated. This phosphorylation increases through the cell cycle and usually reaches the maximal level at late G1 or S phase (Mihara et al., 1989;Ludlow et al., 1990). It has been determined that during early G1 phase a significant portion of

hypophosphorylated Rb associates with the nuclear matrix that is capable of transcriptional repression (Mancini et al., 1994). The lamin A/C binding protein Lap2α was found to be indispensable for the nuclear anchorage of Rb. Lap2α and lamin A/C all bind to the pocket C of Rb which is located at the C-terminus. Rb is stabilized by this association (Markiewicz et al., 2002). Serum starvation and restimulation were used to regulate the level of Lap2α, since it is expressed in a growth-dependent manner in primary skin fibroblasts. When little or no Lap2α was detected in the nuclei of human diploid fibroblasts, Rb was no longer found after extraction of those non-anchored proteins. 18-24 hours following serum restimulation, Lap2α was expressed at a normal level and Rb could be detected throughout the nucleus following extraction (Markiewicz et al., 2002). Based on the knowledge that tethering of Rb in the nucleus is necessary for its functions (Hinds et al., 1992), this finding implicates potential important roles of both lamins and Lap2α in tumor suppression.

In addition to Rb, A-type lamins have also been reported to interact with other transcription regulators including SREBP1 (Lloyd et al., 2002), the Kruppel-like protein MOK2 (Dreuillet et al., 2002), and c-Fos (Ivorra et al., 2006). SREBP1 is a transcription factor belonging to the sterol regulatory element-binding protein family that may be involved in the transduction of the glucose effect (Ferre, 1999), and its interaction with lamins may be linked to the fat loss seen in laminopathies. The Fos family of AP-1 (Activating Protein-1) transcription factors consists of members such as c-Fos, FosB, and FosB2. They can form dimers with Jun proteins that bind to the regulatory sequences of their target genes. Lamin A/C and c-Fos interact with each other and colocalize at the

nuclear envelope, and overexpression of lamin A inhibits c-Fos functions through this interaction and suppresses the formation of heterodimers between Fos and Jun (Ivorra et al., 2006).

Further evidences for involvement of lamins in transcription have been provided by studies with B-type lamins and lamin-associated proteins. In embryonic cells and *Xenopus laevis* oocytes, B-type lamins can bind to RNA polymerase II (RNA pol II) which is involved in the process of RNA synthesis, and RNA pol II activity is inhibited by expressing dominant-negative lamin mutants (Spann et al., 2002). Lap2β and emerin interact with the germ cell-less (GCL) protein (Nili et al., 2001;Holaska et al., 2003). GCL is a transcriptional repressor which binds directly to the DP3 subunit of E2F-DP heterodimers and thereby represses E2F-DP-dependent gene transcription (de la et al., 1999). Interestingly, the E2F-DP-dependent genes are also E2F-responsive genes that are independently repressed by Rb (Harbour and Dean, 2000).

F) Lamins in aging and laminopathies

Laminopathies are a group of human diseases caused by mutations within the LMNA gene or defects in the processing of pre-lamin A. More than 200 mutations in the LMNA gene have already been identified in patients presenting laminopathies (Broers et al., 2004;Broers et al., 2006). Hutchinson-Gilford progeria syndrome (HGPS) is one of the most characterized disorders among the huge family of laminopathies and it was first reported by Hutchinson and Gilford a century ago. HGPS is a severe premature aging disease of children. Children with HGPS initially appear healthy at birth, but clinical

features start to appear within the first few years of life, including lower weight, delayed dentition, hair loss, skeletal abnormalities, etc. (DeBusk, 1972). Recently it was suggested that HGPS is most commonly caused by a *de novo* (not inherited) point mutation in the LMNA gene.

A single-base substitution $Gly^{608} \rightarrow Gly^{608}$ arising from the nucleotide $C^{1824} \rightarrow T^{1824}$ within exon 11 leads to a splicing defect, thus generating a truncated lamin A which lacks 50 amino acids near the C-terminus (Eriksson et al., 2003). It is thought that the presence of this LAΔ50 (progerin) may disrupt the maturation of pre-lamin A, thus causing severe changes in the nuclear envelope (Goldman et al., 2004). Fibroblasts from HGPS patients display deficiencies in both nuclear structure and function. Irregular nuclear shapes are frequently observed in HGPS fibroblasts, and these cells are also characterized by loss of peripheral heterochromatin and down-regulation of the LAP2 family of lamin A-associated proteins (Goldman et al., 2004;Scaffidi and Misteli, 2005).

Though it has not been determined whether lamin A plays a role in the normal physiological aging process, HGPS has long been proposed as a model for studying the underlying mechanisms involved in aging (DeBusk, 1972;Haithcock et al., 2005). Genomic instability has been analyzed in this premature aging syndrome using markers examining DNA damage, γ-H2AX and 53BP1. Elevated expression of both markers was observed in HGPS fibroblasts (Liu et al., 2005). Surprisingly, in another study in normal aging, which compares the skin fibroblast cell lines from both old (96 years) and young (3-11 years) individuals, more γ-H2AX foci were found in cells from old people than the

young ones (Scaffidi and Misteli, 2006), implicating HGPS in the study of normal aging process.

ZMPSTE-24 is a metalloproteinase essential in the post-translational processing of pre-lamin A, and deficiency in ZMPSTE-24 causes similar nuclear abnormalities as HGPS fibroblasts. Microarray analysis of genes in the liver of ZMPSTE-24-/- mice indicated that several downstream targets of the p53 tumor suppressor were significantly upregulated (>5 fold increase), including p21, Gadd45a, PA26, Btg2, Atf3, Rtp801, and Rgs16, with the level of p53 protein unchanged. Therefore, it was hypothesized that the failure in the pre-lamin A maturation might cause cells to undergo stress and activate the p53-signalling cascade (Varela et al., 2005).

Nowadays, a number of models have been suggested to link laminopathies to known functions of lamins and their associating proteins. Among these models, one hypothesis proposes that structural defects in lamins impair the mechanotransduction function of the nuclear lamina. LMNA-/- MEFs show less resistance to mechanical strain and an abrogated NF-κB-regulated response under mechanical stress (Lammerding et al., 2004;Lammerding and Lee, 2005). Disorganization of lamins gives rise to the weakness of the nuclear envelope and cells become less viable under mechanical stimulation. Recently another model suggests the accumulation of the partially processed pre-lamin A and LAΔ50 may be toxic to cells. Following farnesylation and carboxy-methylation, the pre-lamin A is already able to associate with the nuclear membrane. Effect of farnesyl transferase inhibitors (FTI) has been studied in treatments of laminopathies. FTI

treatment was shown to be able to improve the nuclear shape in ZMPSTE-24-/- MEFs as well as some restrictive dermopathy (RD) and HGPS fibroblasts (Toth et al., 2005;Rusinol and Sinensky, 2006). Blocking protein farnesylation is thought to attenuate the targeting of pre-lamin A and mutant lamin A to the nuclear envelope. FTI did not seem to have much effect in reducing the expression level of LAΔ50 by itself. However, when HGPS fibroblasts were treated by both FTI and a chromatin-modifying drug (e.g. HDAC inhibitor TSA), the accumulation of LAΔ50 was dramatically decreased, and nuclear shape and heterochromatin organization were greatly improved (Columbaro et al., 2005).

G) Epigenetic regulation in Hutchinson-Gilford progeria syndrome

Recent applications of antibodies highly specific for different degrees of methylation indicate histones H3K9me3 and H3K27me3 as markers for heterochromatin (Peters et al., 2003;Rice et al., 2003). Heterochromatin differs from euchromatin in its DNA base composition, replication timing, condensation state throughout the cell cycle, and the ability to silence 'euchromatic' genes placed adjacent to or within its territory (Dillon, 2004;Han et al., 2006). Heterochromatin protein 1 (HP1) initially identified in *Drosophila* was the first characterized heterochromatin-associated protein, and it is well conserved from yeast to human (James and Elgin, 1986). HP1 binds specifically to methylated histone H3K9, and the histone-fold domain of histone H3 has been identified as the binding region for the chromodomain of HP1 (Nielsen et al., 2001). In addition to the abnormalities seen in nuclear structure, alteration in epigenetic regulation has been correlated to HGPS. Both trimethylated histone H3K27 and H3K9 are reduced in HGPS

fibroblasts, whereas the trimethylation of histone H4K20 is upregulated. These changes in epigenetic control become more obvious during passage in culture (Columbaro et al., 2005;Shumaker et al., 2006). Moreover, Hela cells overexpressing GFP-LAΔ50 resulted in the similar alteration in these epigenetic markers (Columbaro et al., 2005;Shumaker et al., 2006).

In supporting HGPS as a model for normal aging, decreased expression of histone H3K9me3 was also detected in cells from old individuals, which was consistent with previous findings in the alteration in epigenetic control in HGPS firboblasts. Downregulation of HP1 was also found in these cells. (Shumaker et al., 2006;Scaffidi and Misteli, 2006). Furthermore, a recent study linked trimethylation of H3K9 to telomere length. Telomeres are located at the ends of linear chromosomes. In humans, telomeres consist of several kilobases of the TTAGGG duplex, followed by 200 to 300 nucleotides of single-stranded TTAGGG overhang, creating a telomeric DNA loop (t-loop) (Griffith et al., 1999). These repetitive sequences protect the ends of the chromosomes from damage by exonucleases and chromosome fusion. DNA is replicated by DNA polymerases that are unable to completely duplicate chromosome ends because of the end replication problem of linear chromosomes. As a result, chromosomes shorten by 50 to 100 bases per division at each end. Shortening telomeres does not measurably affect cell function until enough cell divisions have occurred that the telomeres become critically short (Han et al., 2006). Progressive loss of telomere length takes place when people get older. Benetti et al. showed that in MEFs of different generations the density of H3K9me3 heterochromatic mark at telomeric chromatin gradually decreased with

increasing mouse generations (Benetti et al., 2007). These common hallmarks strongly implicate HGPS in the study of normal aging process.

CHAPTER TWO: MATERIALS AND METHODS

A) Bioinformatics searches

Bioinformatic analysis of the Lamin-Interacting-Domain (LID) in both ING proteins and in the whole genome was conducted following a similar strategy to that primarily employed by our group (He et al., 2005). Extensive protein-protein BLAST (Basic Local Alignment Search Tool) searches for the LID region of ING1 were performed at the NCBI website (http://www.ncbi.nlm.nih.gov/BLAST/) using the default settings on all databases available by March 2007 (Altschul et al., 1997;Schaffer et al., 2001). Multiple sequence alignments of the LID sequences in ING1-5 proteins used in this study were conducted by the T_coffee program (Notredame et al., 2000) and subsequently visualized by the GENEDOC program.

B) DNA constructs and mutagenesis

p33ING1b expression construct containing full-length ING1b cDNA was subcloned into pCI vector (Promega) (Garkavtsev et al., 1996). The deletion construct of the LID region was made by dividing the ING1b cDNA into two fragments and then ligating them together into pcDNA3.1 vector (Invitrogen). The two fragments were generated by PCR reactions using primers 5'-CACGAATTCTATGTTGAGTCCTG, 5'-TGAACTCGAGCATCCGCCGCTTCTG, 5'-ATCACTCGAGGGCAAGGCTGG, and 5'-GGTGCTCTAGACTCTACCTGTTG. The LID+NLS construct was made using primers 5'-AGGAATTCATGTGGCACTGTGTG and 5'-GTGCTCTAGACTCCGCCTTGG and cloned into pcDNA4/TO/myc-HisA vector

(Invitrogen). The NLS fragment was also cloned into the same vector by the same reverse primer as the LID+NLS construct and the forward primer used was 5'-AGGAATTCATGGACAAGCCCAACA. Primers used for constructing the multimer of the LID (ING1b-TriLID+NLS) included 5'-ATCACTCGAGGCTGCACTGTGTG, 5'-GTGCTCTAGACTCCGCCTTGG, 5'-AGGAATTCATGTGGCACTGTGTG, 5'-TGAACTCGAGTCGCTGTTGCCC, 5'-ATCGAAGCTTGAGACAGACGG, and 5'-CTGGAATTCGCTGTTGCCC.

For all PCR reactions, 100 ng plasmid DNA was mixed with primers (10 pmol each) and 0.25mM dNTP and Taq DNA polymerase (New England Biolabs) was used for elongation. 1% agarose gels were made to separate DNA products and DNA was purified from gels with a QIAquick gel extraction kit (QIAGEN). All constructs had been checked by DNA sequencing and the sequencing primers were the pCI T7 sequencing primer (5'-TAATACGACTCACTATAGG) and the pcDNA4/TO/myc-HisA CMV sequencing primer (5'-CGCAAATGGGCGGTAGGCGTG).

Myc-tagged full length LMNA and 415-664 constructs in pcDNA3.1 were gifts from Brian Burke (University of Florida), and myc-tagged LMNA 1-406 in pcDNA3 and 1-447 in pCEP4 were gifts from Eileen White (Rutgers University). Vector expressing green fluorescent protein (GFP) (Clontech) was used for co-transfection. Small-scale and large-scale DNA preparations were performed with DNA miniprep or maxiprep purification kits following the manufacturer's protocol (Qiagen). Oligonucleotide

synthesis and DNA sequencing were conducted by the University Core DNA Services at the University of Calgary.

C) Model cell systems and transfection

Cell culture procedures

Human primary diploid fibroblasts HS68 (ATCC CRL-1635), human embryonic kidney epithelial cell line HEK293 (ATCC CRL-1573), skin fibroblasts from Hutchinson-Gilford progeria syndrome (HGPS) patients (Coriell AG11513, AG00989), murine LMNA+/+ and LMNA-/- mouse embryonic fibroblasts (Sullivan et al., 1999) (gifts from Brian Burke), and mouse embryonic stem cells R1 (Nagy et al., 1993) were used in this study. Cells were grown in Dulbecco's modified Eagle's medium (DMEM) supplemented with penicillin/streptomycin and 10% fetal bovine serum (FBS) and incubated at 37°C (with 5% CO2). Cells were maintained as monolayers and split with trypsin-EDTA (Gibco BRL). The split ratios for HS68 and HGPS fibroblasts were 1:2; for HEK293 1:2 or 1:4; for mouse embryonic fibroblasts 1:8; for R1 mouse embryonic stem cells 1:6.

For embryonic stem cells, tissue culture plates were first covered with 0.1% gelaton and air dried for 5 min. After trypsinization, 5 ml medium was added to cells and cells were transferred to a new tube and centrifuged for 5 minutes at 600 x g. Supernatant was removed and cell pellets were resuspended in 10ml fresh medium.

Unless otherwise specified, the mean population doubling (MPD) levels for HS68 cells used in this study were between 35-38. The AG11513 HGPS fibroblasts were at passages 18-20; the AG00989 fibroblasts were at passages 25-28; and the mouse embryonic fibroblasts were at passages 19-20.

Transfection of HEK293 cells

For transfection studies, HEK293 cells were seeded onto 10-cm dishes 24 hours prior to transfection and they were transfected at 70-80% confluence by the traditional calcium phosphate method. First, 10 µl of 2M $CaCl_2$ was mixed with 338 µl filter-sterilized (FS) H_2O. In a separate tube, 15 µg plasmid DNA was added to FS H_2O to make 100 µl of DNA solution. The DNA solution was added dropwise to the $CaCl_2$ solution and mixed by pipetting. 52 µl of 2M $CaCl_2$ was subsequently added to the mixture gently. Finally, the $CaCl_2$+DNA solution was added to 500µl 2 x HEPES buffer (8g NaCl, 0.2g $Na_2HPO4{\cdot}7H_2O$, and 6.5g HEPES in 500ml distilled water, pH 7.0) dropwise and very slowly (1 sec/drop), and in the meantime air bubbles were introduced into the HEPES solution. This mixture was incubated at room temperature for 30 minutes with vortexing every 10 minutes and then it was spreaded onto cells gently. For co-immunoprecipitation studies, cells were harvested at 24 hours after transfection, otherwise cell harvest was performed at 48 hours following transfection.

D) β-galactosidase staining and apoptosis assay

β-galactosidase assay

Young (MPD 29) and old (MPD 95) HS68 fibroblasts, AG11513 (passage 29) HGPS fibroblasts, and transfected HEK293 cells were used in this study. Cells to be stained for β-galactosidase activity were cultured in 6-cm tissue culture dishes prior to staining. For HEK293 cells transfected with GFP or LID+NLS, staining was performed 48 hours after transfection. Cells were washed with PBS (pH 7.2) and then fixed with 2% para-formaldehyde for 5 minutes at room temperature. After removing the fixation solution and washing cells three times with PBS (pH 7.2), cells were stained for 20 hours at 37°C (without CO_2) in a freshly made X-galactoside solution (1mg/ml X-gal solution, 5mM potassium ferricyanide, 5mM potassium ferrocyanide, 2mM $MgCl_2$, 0.15M NaCl, and 1 x PBS, pH 6.0). 1ml of the staining solution was added to each 6-cm dish. The next day, cells were washed with PBS (pH 6.0) and digitally photographed with phase-contrast microscopy.

Flow cytometry

For the analysis of apoptosis, HEK293 cells were co-transfected with GFP and various ING1b constructs and harvested at 48 hours. Cells were trypsinized for 2 minutes, washed twice with ice-cold PBS, and transferred to plastic FACS tubes (Falcon 35/2054). Following centrifugation at 1000 x g for 5 minutes, the pelleted cells were resuspended in 500µl PBS and fixed in 500µl ice-cold 2% para-formaldehyde at 4°C for one hour. After fixation, cell pellets were spun down, washed, and resuspended in 500µl PBS. Permeabilization was carried out by adding 1.5ml ice-cold 95% ethanol to the cells while

vortexing. Ethanol was added dropwise to cells. Samples were kept at -20°C for two days. Before analysis, cells were centrifuged and washed once in PBS. Pellets were treated with 1mg/ml RNaseA in PBS for 30 minutes at room temperature and subsequently 2.5µg propidium iodide (PI) was added to the samples to stain DNA. Cell cycle analysis was performed using a Becton-Dickinson FACScan flow cytometer at the University of Calgary Flow Cytometry Core Facility after samples were incubated for 15 minutes in dark at room temperature.

E) Purification of His-tagged protein complexes

His-tagged construct encoding tandem repeat of the LID region along with the NLS was tranfected into HEK293 cells. The pcDNA4/TO/myc-HisA vector was used as a negative control in parallel. 24 hours after transfection, cells were lysed under non-denaturing condition in 800µl lysis buffer (pH 8.0) containing 20mM Tris (pH 7.4), 300mM NaCl, 10mM KCl, 0.2mM EDTA, 0.5% DOC, 0.5% Tween-20, 1% NP-40, and 10mM imidazole. Cell lysates were then loaded onto Ni-NTA spin columns (Qiagen) which were already equilibrated with lysis buffer. Columns were centrifuged at 2,000 rpm for 3 minutes at 4°C and washed three times with 600µl wash buffer (pH 8.0) (50mM Na_2HPO4, 300mM NaCl, 15mM imidazole, and 0.2% Tween-20). All flow-through was collected to test the efficiency of His-tag purification. Elution buffer (pH 8.0) (50mM Na_2HPO4, 300mM NaCl, 250mM imidazole, and 0.1% Tween-20) was subsequently used to elute proteins off the columns.

Before submitting the samples for liquid chromatography-mass spectrometry (LC/MS/MS), buffer was changed to 50mM NaCl using Microcon columns (Millipore). The LC/MS/MS analysis was done by Southern Alberta Mass Spectrometry (SAMS) Facility at the University of Calgary and the database search engine Mascot was used to identify potential binding partners (http://www.matrixscience.com/home.html).

F) Co-immunoprecipitation and western blotting assays

Co-immunoprecipitation procedures

Cells were lysed in 1ml RIPA buffer (10mM Tris PH7.4, 150mM NaCl, 10mM KCl, 1mM EDTA, 0.5% DOC, 0.5% Tween-20, 0.5% NP-40, and 5µg/mL DNaseI). Protease inhibitor cocktail tablets (Roche) were added to RIPA buffer (1 tablet/8 ml buffer). Sonication was carried out at setting #4 on a Mandel Scientific Sonicator (Model XL2020) and samples were sonicated for 6 x 15 seconds on ice. After sonication, cell lysates were clarified by centrifugation at maximum speed for 2 minutes at 4°C and supernatants were transferred to new tubes. 30 µl of whole cell lysates were aliquoted to test expression levels of proteins.

For immunoprecipitations with antibodies from hybridoma supernatants (anti-ING1 and anti-myc), beads saturated with antibodies were added to cell lysates in RIPA buffer and incubated for 4 hours at 4°C on a rocker. Mixture of four mouse monoclonal ING1 antibody hybridoma supernatants (CAb1-4) (Boland et al., 2000) were used for ING1 co-immunoprecipitations (co-IPs) and 2.5ml mixed supernatants were used for each co-IP. Hybridoma supernatants were preincubated with Protein G-Sepharose beads (GE

Healthcare) overnight at 4°C and beads were rinsed a couple of times before adding to lysates. For immunoprecipitations with lamin A/C antibody (Santa Cruz sc-7292), 2 µg antibody was used for each sample. Lamin A/C antibody was incubated with cell lysates for 3.5 hours at 4°C, and after that Protein G-Sepharose beads were added for another 30 minutes. Following incubation, beads were precipitated and washed with RIPA buffer for three times. 20 µl of 2 x Laemmli sample buffer (0.1M Tris-HCl pH 6.8, 4% SDS, 20% glycerol, 10% β-mercaptoethanol, 0.1% bromophenol blue) was subsequently added to the beads. The mouse anti-flag antibody M2 (Sigma) was used as a non-specific IgG control.

Western blotting

For whole cell protein extracts without immunoprecipitations, the harvested cell pellets were washed twice in ice-cold PBS and 250µl of 2 x Laemmli sample buffer was added. Before loading on the SDS-PAGE gel, all samples were boiled for 3 minutes at 100°C. 15% (for proteins <60kDa) and 8% (for proteins >60kDa) poly-acrylamide gels were used to separate proteins of different molecular weights. Following electrophoresis at 100-150V for 1-2 hours, proteins were transferred to pure nitrocellulose membrane (Pall) or immobilon transfer PVDF (Millipore). Membranes were blocked in PBS-Tween (0.1% Tween-20) with 5% skim milk at room temperature for 2 hours and followed by incubation with primary antibodies overnight at 4°C. Anti-lamin A/C (Santa Cruz sc-7292), anti-lamin A (Santa Cruz sc-20680), anti-actin (Santa Cruz sc-32251), anti-histone H2B (Cell Signaling 2722), and anti-His-tag (Abcam ab1206) were diluted in PBS-Tween with 3% skim milk and their dilutions used in this study were 1:300, 1:500, 1:200,

1:500, and 1:3000 respectively. The next day membranes were washed three times for 10 minutes each in PBS-Tween and then incubated with goat-anti-mouse or goat-anti-rabbit horseradish peroxidase (HRP)-conjugated secondary antibodies (Chemicon) using dilutions 1:5000 for one hour at room temperature. The ExactaCruz (Santa Cruz sc-45042) secondary antibody was used in the immunoprecipitation-western experiment that identified the binding regions in lamins. Further washes were performed exactly in the same way as those following incubation with primary antibodies. Equal amounts of the two solutions of Immobilon western chemiluminescent HRP substrate (Millipore) were mixed and then added to the membranes. Membranes were finally exposed and developed to film using a Kodak X-OMAT 2000 processor. For stripping and reblotting membranes, membranes were incubated in stripping buffer for 1 hour and followed by regular blocking and blotting steps.

Coomassie Brilliant Blue staining

For Coomassie Brilliant Blue staining used to test equal loading of samples, after completion of electrophoresis, gels were stained with a staining solution at room temperature for 30 minutes followed by washing with sufficient destaining solution overnight. Gels were finally dried on Whatman 3MM paper at 80°C for one hour.

G) Cell Fractionation

Cell pellets were collected on ice. 250µl 0.5% NP-40 in ice-cold PBS was added to pellets and incubated for 20 minutes at 4°C. An 18-G needle (PrecisionGlide) was used to extract cytoplasmic components of cells. Following extraction, samples were

centrifuged at maximum speed for 5 min at 4°C. Supernatant was subsequently transferred to a new tube and collected as cytoplasmic proteins. To minimize cytoplasm contaminations, the remaining pellets were extracted again with another 200µl 0.5% NP-40 buffer and followed by centrifugation for 5 minutes. Finally pellets were lysed with 150µl 2 x Laemmli sample buffer to generate nuclear fractions.

H) Far Western Blotting

To perform far western blotting (protein overlay assay), cell lysates were electrophoresed on denaturing SDS-PAGE gel and transferred to nitrocellulose as described. For the protein composition analysis of samples, an identical gel was stained with Coomassie Brilliant Blue. After membrane transfer, membranes were washed twice with PBS to remove SDS and followed by a quick rinse in binding buffer (10% glycerol, 0.1M NaCl, 0.02M Tris pH 7.6, 1mM EDTA, and 0.1% Tween-20). Blocking was performed with 2% skim milk in binding buffer overnight at 4°C. Membranes were subsequently incubated with Ni-NTA purified His-tagged-LID+NLS protein (10µg/ml) in binding buffer with 2% skim milk for 1 hour at room temperature and washed with PBS-Tween for 4 x 5 minutes. The anti-myc-tag antibody 9E10 and the goat-anti-mouse HRP-conjugated secondary antibody were used to detect bound protein.

I) Fluorescence Microscopy and Image Processing

Indirect immunofluorescence

Cells were plated and cultured onto glass coverslips. If desired, transfections by calcium phosphate method were performed two days before fixation. At approximately 70-80%

confluence, cells were washed twice with ice-cold PBS. Cells were fixed with 3.5% para-formaldehyde in PBS (pH 7.2) at room temperature for 10 minutes and followed by washes for three times in PBS. Fresh 0.5% Triton X-100 (Sigma) in PBS was used to permeabilize cells, and the time for permeabilization was 5 minutes. Further washes were done as described. The blocking step was carried out by 3.5% bovine serum albumin (BSA) in PBS for one hour at room temperature. Human and mouse ING1 proteins were visualized by mouse monoclonal antibody Cab1 and lamin A was labeled with a rabbit polyclonal antibody (Santa Cruz sc-20680) at a 1:200 dilution. Primary antibodies were incubated at 37°C for one hour in a moisture chamber. Cells were washed again with PBS-Tween (0.02% Tween-20) for 4 x 5 minutes. Secondary antibodies used in this study were goat anti-rabbit Alexa Fluor 488 and goat anti-mouse Alexa Fluor 568 (Invitrogen) (1:1000 dilution) and cells were incubated with them for 40 minutes at room temperature. After rinsing, samples were mounted in 30µl aqueous mounting medium with anti-fading agents (Biomeda) with the DNA-specific dye DAPI (1µg/ml) onto slides.

Image processing

Staining was visualized using a Zeiss Axiovert 200 microscope with a motorized stage and a condenser with a numerical aperture of 0.55 for Differential Interference Contrast (DIC) observations. AxioVision v4.5 software was used to take pictures and digital deconvolution was subsequently performed with VayTek Microtome software. Images were imported into Adobe Photoshop v7.0 and false colors were added under the indexed

color mode. For superimposition, one image was first converted to a RGB mode and then pasted to a second one. The "screen" function was used to blend two colors together.

J) Electron microscopy

For transmission electron microscopy (TEM), cells were grown in 35mm tissue culture dishes. The monolayer cultures were then fixed with a solution of 2% glutaraldehyde in 0.2M NaCacodylate buffer for 30 minutes. The samples were then washed twice in Cacodylate buffer and post-fixed for 1 hour with 2% osmium tetroxide in Cacodylate buffer, dehydrated in ethanol, and embedded in Polybed 812 resin (J.B. EM Services Ltd.). Thin cross sections were cut with a diamond knife on a Reichert ultramicrotome. Sections were stained with uranyl acetate and lead citrate and examined on a Hitachi H-7000 TEM microscope at the Microscopy and Imaging Facility of the University of Calgary.

CHAPTER THREE: RESULTS

Section I. Bioinformatics analysis of the lamin interacting domain of ING1

Previous studies indicated the existence of a novel region containing KIQI/KVQL residues upstream of the NLS region (Kawaji et al., 2002), and comprehensive phylogenetic analysis by our group identified additional adjacent conserved sequences among all ING family members (He et al., 2005). In order to characterize this motif, the first aim was to determine if it defined a new protein domain and whether this domain was ING protein-specific. The sequences of the novel region in different isoforms of ING1 are exactly the same. Multiple sequence alignments of the Lamin Interacting Domain (LID) sequences of ING1-5 were performed using the program T_COFFEE (Notredame et al., 2000) with default settings. The alignments were subsequently adjusted and shaded using the multiple sequence alignment editor GENEDOC. Consistent with previous reports, this region showed a relatively low degree of conservation in all ING family members and could be grouped into three subfamilies including ING1/2, ING4/5, and ING3 (Fig. 3). The Lamin Interacting Domain of ING1 consists of 53 amino acids, from amino acids 74 to 126 in p33ING1b (217 to 269 in p47ING1a, 5 to 57 in p24ING1c, and 30 to 82 in p27ING1d).

The Basic Local Alignment Search Tool (BLAST) is frequently used for calculating similarities of sequences. BLAST searches were performed at the NCBI website on all databases available in March 2007 (Altschul et al., 1997) with default settings. In order to

get more information for analyzing the function of the Lamin Interacting Domain, four amino acids at each side of the LID of ING1 were extended, so that the query peptide was 61 residues. 140 matches of the query sequence were obtained (Fig. 4), among which most were members of the ING family in human and mouse, their distant orthologs in *Xenopus* and *Drosophila melanogaster*, and several unnamed predicted proteins whose functions are not clear at this point. The top 20 matches are listed in Table 1. It was noticed that some ING family proteins appeared several times in the whole list under different names and accession numbers, and this was probably due to redundant entries in this database.

This study was initially driven by a discovery-based hypothesis prior to using mass spectrometry to identify proteins. We first suspected this domain as a region involved in chromatin remodeling based on current knowledge of ING proteins. Therefore, sequence alignments of the LID were performed with proteins already identified as chromatin remodeling proteins, such as p300, CBP, ACF1 (ATP-dependent chromatin assembly factor large subunit CG1966-PA), NURF301 (nucleosome remodeling factor large subunit), and WSTF (Williams syndrome transcription factor). All these proteins are characterized by variants of the PHD zinc finger motif present in ING family members (Bienz, 2006). However, the alignments indicated no significantly conserved residues among any of these sequences (data not shown). Based on these searches on current databases, the Lamin Interacting Domain was found to be surprisingly unique to the ING protein family.

Since interactions of ING and lamins were also tested in mouse embryonic fibroblasts in this study, sequence alignments of ING and lamin A with their mouse orthologs were conducted. Similar to the ING1 gene in human, the murine ING1 can also be alternatively spliced into several isoforms. p37ING1 is the mouse ortholog of p33ING1b (Zeremski et al., 1999), and their sequence alignment was shown in Fig. 5a. p37ING1 is of the same length as p33ING1b, and they share extremely conserved domains, including the LID region. Moreover, the sequence alignments of lamin A in mouse and human also displayed conserved sequence patterns between these two proteins (Fig. 5b). As a result, these alignments strongly suggested that their mouse orthologs might perform similar functions in protein-protein interactions.

Section II. Identification of binding partners through Liquid Chromatography–Mass Spectrometry (LC/MS/MS)

A) Purification of the His-tagged protein complex and application of LC/MS/MS

In order to begin characterizing the function of this novel conserved region, I designed a His-tagged construct encoding a triple-repeat of the LID region and a single NLS domain. With the NLS domain, upon overexpression in HEK293 cells it would be targeted to the nucleus. For a negative control, an empty vector was transfected and run in parallel, so that it would identify the proteins that bound non-specifically to the Ni-NTA columns. Binding of the 6 x His tag to Ni-NTA does not depend on the 3-dimensional structure of the protein. Untagged proteins that have histidine residues in close proximity on their surface can also bind to Ni-NTA, but in most cases this

interaction is much weaker than the binding of the 6×His tag. Since there is a higher potential for binding background contaminants under native conditions than under denaturing conditions, low concentrations of imidazole in both lysis and wash buffers were used (Fig. 6a). The imidazole ring is part of the structure of the histidine residue. The imidazole rings in the histidine residues of the 6 x His tag bind to the nickel ions immobilized by the NTA groups on the matrix. Imidazole itself can also bind to the nickel ions and disrupt the binding of dispersed histidine residues in non-tagged background proteins. At low imidazole concentrations, non-specific, low-affinity binding of proteins is prevented, while 6 x His-tagged proteins still bind strongly to the Ni-NTA matrix. Therefore, adding imidazole to the lysis buffer leads to greater purity in fewer steps. In the elution step of the pull down assay, whereas all elution methods (imidazole, pH, and EDTA) are equally effective, imidazole is the mildest and is recommended under native conditions. In this study, 250mM imidazole was added to the elution buffer, and at this concentration imidazole normally saturates the Ni-NTA matrix and results in nearly complete elution of native proteins. In contrast, proteins can be damaged by a reduction in pH and the presence of metal ions in the eluate may have an adverse effect on the protein structure or on the effectiveness of subsequent Mass Spectrometry analyses (Janknecht et al., 1991).

Following purification of the His-tagged protein complex, salt concentration of the buffer was decreased by buffer exchange through columns, which was recommended for analysis by liquid chromatography-mass spectrometry (LC/MS/MS). In this case, the

LC/MS/MS started with rapid digestion of the protein complex with immobilized trypsin on a liquid chromatography column. Following elution from the column, the digested protein mixture was directly passed to a tandem mass spectrometer for mass analyses and amino acid sequencing of proteolytic fragments. Sequence fragments were then compared with a database of theoretical fragment sequences based on relative sizes of proteins and the protease used to digest proteins. The reason for choosing LC/MS/MS is that it is both cost-effective and useful for high-throughput analyses.

To date, various algorithms (e.g. SEQUEST, Mascot, MSTag) are used for database searches. In this study, the Mascot search engine was applied to identify peptides and proteins which best matched the data generated from the LC/MS/MS analysis (Helsens et al., 2007). Mascot features probability-based scoring, and its basic functions are to calculate the probability that matches generated from the experimental data and the database is random. In other words, a lower probability means a better match and a higher likelihood that the data are not random. In order to make it more convenient for researchers to read those numbers for probabilities (usually in scientific notation), an ion score is generated for each match. The reported ion score represents $-10\text{Log}_{10}(P)$, where P is the probability for being a random event. This permutation means that the best match is the one with the highest score. The significance threshold of the probability was 0.05 (1 in 20 chance to be false-positive), and as a result, a score threshold indicating identity or extensive homology was calculated from the total number of peptides that fell within the mass tolerance window (Perkins et al., 1999). The ion score cut-off in this study associated with this modality was 48 as calculated by the Mascot program. In addition to

individual ion scores, protein scores are generated by the Mascot program. Weighting factors along with peptide scores are used to generate protein scores. Though all the protein hits are listed in the order of their protein scores, these scores are not always desirable to be used to compare the significance of hits, especially if a great number of peptides with relatively low ion scores are assigned to a single large protein (Chepanoske et al., 2005). As a result, one of the acknowledged guidelines for interpreting protein identification data is that proteins showing two or more peptides with ion scores higher than the threshold have reasonable chances of being "real" matches (Carr et al., 2004).

B) Potential interacting proteins identified by LC/MS/MS

Using a significance threshold of $p<0.05$, 110 protein hits were obtained from the His-tagged protein complexes, and 105 hits in the negative control. Approximately one fourth of the total hits showed two or more peptides with acceptable ion scores (>48 in this study). Some of them were of the same protein families, since those peptides used for searching were conserved among them. The acceptable hits from the experimental sample were subsequently compared with those in the negative control, and nine of them were found to be unique to the His-tagged protein complexes (Table 2). Three of the nine proteins were members of nuclear lamins, including lamin A/C isoform 2, lamin A/C isoform 3, and lamin B1. According to the NCBI protein database, lamin A/C isoform 2 and 3 are referred to lamin C and lamin AΔ10 respectively, and both are A-type lamins that are alternatively spliced from the LMNA gene. Most of the matching peptides from these two A-type lamins were the same, and all these peptides were also present in lamin A. Actually, lamin A itself did not show up in the results, and this might be due to the

algorithms applied by the Mascot program. There were four peptides with ion scores >48 in lamin C and three in lamin AΔ10, indicating A-type lamins as potential binding partners of the novel conserved region in ING1 proteins.

To confirm the LC/MS/MS results, western blotting with lamin A/C antibody was done using the eluated protein solution of the negative control and the experimental sample, and both lamins A and C were shown in the LID-recovered complexes (Fig. 6b). Lamin C was also presented in the negative control, but perhaps the level was too low for LC/MS/MS to detect. Since lamin C contains four neighboring histidines at its C-terminus, it is likely to appear as a background binding protein especially when the Ni-NTA matrix can not be saturated by His-tagged proteins in the negative control. In the sample transfected with the His-tagged construct, the eluate contained significantly more lamins A and C, suggesting that they are specific interacting proteins.

In addition to lamins, six other proteins have been identified by LC/MS/MS as shown in Table 2. The T-complex protein 1 Beta subunit (TCP-1-BETA) belongs to the TCP-1 chaperonin family, which is involved in productive folding of proteins. It is a small protein with two matching peptides that have high ion scores, so there is a relatively good chance for it being a real match. However, since this protein was identified through genome-wide analysis (Loftus et al., 1999), currently no additional details are recorded on the NCBI website.

The splicing factor 3B subunit (SF3B) 2 (SAP145) is a spliceosome-associated protein, and it contains a SAP domain which has been characterized as a putative DNA-binding domain (Aravind and Koonin, 2000). The SF3B complex is required for the assembly of the spliceosomal complex A, which functions in U2 snRNP binding in the process of pre-mRNA splicing (Gozani et al., 1996;Das et al., 2000).

Among the rest of protein hits, the SWI/SNF complex 170 KDa subunit (BAF170) is associated with chromatin remodeling function. Mammalian SWI/SNF complex is a multi-protein complex and serves as an ATP-dependent nucleosome remodeling factor. It consists of at least 10 subunits and all subunits are well conserved from yeast to human. The core subunit of the SWI/SNF complex is either BRG1 or BRM (Simone, 2006), thus dividing it into two subfamilies. Subunits of the complex regulate various cellular processes, and they play critical roles in cell cycle control, gene transcription, apoptosis, differentiation and development, etc. (Martens and Winston, 2003).

The NF45 (Nuclear Factor-45) protein with a protein score of 74 is a protein involved in DNA and RNA binding, and it belongs to the same family as NF90. Both proteins are known to regulate interleukin-2 (IL-2) gene transcription through binding specifically to a sequence of an antigen receptor response element (ARRE) in the IL-2 promoter (Ting et al., 1998;Langland et al., 1999). NF90 has been identified as a substrate of the double-stranded RNA dependent kinase (PKR) (Langland et al., 1999), while NF45 and NF90 can interact with and be phosphorylated by the DNA-dependent protein kinase (DNA-PK) (Ting et al., 1998).

Section III. Physical interactions between ING1 and lamin A/C

A) ING1 binds to lamins through the lamin interacting domain

To further confirm the LC/MS/MS results that A-type lamins might be binding partners of the novel identified region of ING1, we made use of immunoprecipitation-western (IP-western) assays to analyze the interactions. IP-western of overexpressed proteins was first carried out, since it would be able to give an idea of the interaction and regions involved. Various ING1b constructs were made by PCR mediated method, including a deletion mutant lacking the LID region (ING1bΔLID), a LID+NLS construct, a Tri-LID+NLS construct (previously used for LC/MS/MS), and a NLS construct (Fig. 7).

HEK293 cells were used for overexpression studies, since they are easy to transfect, and the transfection efficiency was always between 80-90% using the calcium phosphate method in this study. Wild-type ING1b, ING1bΔLID, LID+NLS, NLS, and empty expression vector (indicated as V) were transfected into HEK293 cells and co-immunoprecipitations were preformed using a mixture of ING1 antibodies Cab1-4 which recognized a region within the NLS motif. DNaseI was added to the lysis buffer and relatively longer sonication times were used to shear the DNA and break the lamin filaments. An anti-flag antibody was used for the non-specific IgG control and the samples in these controls were all transfected with wild-type ING1b. As shown in Fig. 8, while the input of the lysates showed similar levels of lamin A/C in all samples, lamin A/C could only be pulled down by the overexpressed ING1b and the LID+NLS proteins, but not the ING1bΔLID and the NLS proteins. Similar results were obtained from

reciprocal IP-western where lamin A/C antibody was used, and the wild-type p33ING1b and the LID+NLS proteins avidly bound to endogenous lamin A/C whereas the LID deletion mutant and the NLS fragment did not (Fig. 9). The expression levels of proteins were also shown in both figures, in order to make sure that the variances in the binding capacity were not due to unequal protein levels.

B) Mapping the binding sites of lamin A/C

The next aim was to determine which region of lamin A/C was involved in the interaction with p33ING1b. ING1b and fragments of lamin A (LMNA, 1-406, 1-447, 415-664) were co-transfected into HEK293 cells. Since all of these lamin A constructs contained myc-tags at either N- or C- terminus, we used an anti-myc antibody to immunoprecipitate the lamin complexes from lysates. However, all fragments seemed to associate with p33ING1b (Fig. 10). This may be due to both lamins and p33ING1b binding to chromatin, with chromatin acting as a linker for these proteins or due to the formation of lamin-ING multimers. Chromatin binding sites have been identified in both the α-helical rod domain and the 411-553 amino acids of lamin A (Glass et al., 1993;Stierle et al., 2003). To exclude the former possibility, the LID+NLS protein was used instead of the intact p33ING1b to be overexpressed in HEK293 cells. The LID+NLS fragment was also cloned in a myc-tagged vector, so the immunoprecipitation of protein complexes was performed by the ING antibodies Cab1-4. Since some of the lamin fragments have molecular weights close to that of the heavy chains of antibodies, a unique secondary antibody that could not recognize the heavy and light chains was used in this assay. As shown in Fig. 11, with similar overexpression levels of the LID+NLS

protein, full length lamin A could be pulled down. In addition to lamin A, both the 1-406 and 1-447 fragments were also co-immunoprecipitated with the LID+NLS protein, but the carboxyl tail of lamin A could not be detected in the recovered protein complexes. These results suggest that the N-terminus of lamin A is necessary for mediating the interaction with ING1 and that the terminal 406-664 amino acids are not required.

C) Different binding capacities between endogenous ING1 and lamins in various cell strains

Since a robust physical interaction between the overexpressed ING1b and lamins had been shown and the LID region was involved in this interaction, we asked if the mutant lamin A (progerin) found in HGPS fibroblasts could also bind to ING1 proteins. We chose three different cell lines to perform this experiment, including HS68 human diploid fibroblasts and two lines of fibroblasts from HGPS patients (AG11513, AG00989). AG11513 carries the more typical $Gly^{608}\rightarrow Gly^{608}$ mutation that affects splicing and AG00989 has a missense mutation ($Arg^{644}\rightarrow Cys^{644}$) in lamin A, resulting in defects in the putative cleavage recognition sequence by ZMPSTE-24, the endoprotease essential for pre-lamin A processing (Pendas et al., 2002;Broers et al., 2006). The HGPS fibroblasts grew much more slowly than the normal HS68 even at low passages. They took around 5-7 days to duplicate and cells became larger in size, indicating that they were already entering senescence. As shown in Fig. 12, progerin (LAΔ50) was already detected in AG11513 at passages 18-20. When co-immunoprecipitation assays were conducted, ING1 proteins were able to pull down lamin A/C in HS68 as well as pre-

lamin A and lamin C in AG00989. However, in HGPS fibroblasts AG11513, only a very low amount of lamin A/C were shown to associate with ING1, as compared with the protein levels from the other two cell lines. The input indicated that though AG11513 displayed expression of progerin, the levels of wild-type lamin A/C were not significantly different than in HS68. The expression levels of p33ING1b were also tested after immunoprecipitation, and AG11513 showed a higher level of ING1.

D) Far western blotting analysis for *in vitro* interaction of ING1 and lamins

The next question addressed was whether the LID+NLS protein and lamins directly bind each other, and for this purpose far western blotting assays were applied. Cell lysates from HS68 fibroblasts, HGPS cell lines AG11513 and AG00989, and wild-type and LMNA-/- mouse embryonic fibroblasts were used. The LID+NLS protein served as bait protein, and it was overexpressed in HEK293 cells and purified through Ni-NTA spin columns. With one hour of incubation at room temperature, the LID+NLS protein could be readily detected on the membrane, though noise in addition to specific signals was shown (Fig. 13a). Bait protein and antibodies were stripped off the membrane, and a lamin A antibody was subsequently used for blotting since the lamin A/C antibody failed to recognize lamins from MEFs. The expression level of lamin A in different cell lines is shown in Fig. 13b. It was clear that the LID+NLS protein could bind intact lamin A, but not the LAΔ50 mutant *in vitro*. It seemed that lamin C did not directly interact with the LID+NLS protein, suggesting that lamin A might be the main protein that binds ING1, consistent with the lack of ING1b-progerin binding. Fig. 13c shows the Commassie Brilliant Blue staining of the same samples which demonstrates nearly equal loading.

E) Co-localization studies of ING1 and lamin A

Based on the data from the endogenous IP-western assay, interactions between ING1 and lamin A were further tested by co-localization studies through immunofluorescence. I first used those three cell lines previously chosen for IP-western. 24 hours after plating onto glass coverslips, cells were fixed by para-formaldehyde and stained for ING1 (red), lamin A (green), and DNA (blue). Cab1 antibody was used for ING1 staining in this assay. Deconvolution microscopy was used to visualize the samples. For all experimental samples, the exposure time was between 20-80ms, depending on the strengths of signals. A negative control with secondary antibodies only was performed with exposure time 100ms, and staining was not detected (data not shown).

In normal HS68 fibroblasts, ING1 was predominantly in the nucleus, with a significant portion on the nuclear envelope that co-localized with lamin A. The AG00989 HGPS fibroblasts displayed mainly nuclear, with some cytoplasmic staining of ING1. In contrast, in the AG11513 cell strain where a very weak interaction was shown by the IP-western biochemical method, ING1 proteins were largely absent from the nucleus, and this finding raised the possibility that lamins might be necessary for the nuclear anchorage of ING1 (Fig. 14). Cells with misshapen nuclei were found in a small proportion of both cell lines of HGPS fibroblasts. DAPI staining for DNA did not show chromatin condensation in HGPS fibroblasts, suggesting apoptosis does not have a major role in their observed cellular defects. In addition, co-localization of ING1 and lamin A at different stages of the cell cycle were also studied. During mitosis, ING1 showed preferences in binding to lamin A but not chromatin (Fig. 15).

To determine whether lamin A serves to anchor ING1 in the nucleus as it does for some interacting proteins such as Rb, emerin, and LEM2, we subsequently studied the subcellular localization of ING1 in the LMNA-/- MEFs to see if it would be mislocalized as well. Since it has been well established that A-type lamins only express in differentiated cells, the R1 embryonic stem (ES) cells were also tested for ING1 localization. For ES cell culture, cells were plated on gelatin-coated coverslips 18 hours before fixation at a lower density than usual, so that they could be separated as individual cells under microscope. The sequence homology searches in Fig. 5 indicated that both ING1 and lamin A are quite conserved from human to mouse. At the same exposure time which was used previously for HS68 (80ms), no obvious staining of lamin A could be detected in LMNA-/- MEFs and ES cells, consistent with the fact that they do not express A-type lamins. The nuclei of LMNA-/- MEFs were often elongated comparing with the round ones of wild-type. In wild-type MEFs, ING1 preferentially localized in the nucleus and a significant co-localization between ING1 and lamin A was observed. However, in both LMNA-/- MEFs and ES cells, ING1 was distributed throughout the whole cell and only a very small proportion remained in the nucleus (Fig. 16).

F) Nuclear fractionation of mouse embryonic fibroblasts

Following identification of the staining patterns of ING1 in wild-type and LMNA knockout MEFs, biochemical assays were performed to address questions of subcellular localization using an independent method. The cytoplasmic fraction of MEFs was extracted using NP-40 buffer, and the nuclear pellet was dissolved with SDS sample buffer. ING1 levels in different components were tested by western blotting using Cab1

antibody. In wild-type fibroblasts, ING1 proteins were mainly detected in the nuclear fraction, with a very small proportion in the cytoplasmic extract. This observation has been previously seen in many other cell lines including HS68, since ING1 localization changes in a similar manner as lamins. During mitosis both lamin A/C and ING1 are located in the cytoplasm. Since the LMNA-/- MEFs have no lamin A, we can not distinguish cytoplasmic and nuclear fractions by lamin A expression, so a histone H2B antibody was used as a nuclear marker. In the LMNA knockout MEFs, ING1 protein could not be detected in the nuclear fraction, and the cytoplasmic extract showed a much higher level of ING1 than the wild-type MEFs (Fig. 17). No histones were present in any cytoplasmic components, indicating that there was no significant contamination of nuclear proteins in this fraction. Considering results from both subcellular localization and western blotting assays, we suggest that lamin A may be required for retention of ING1 in the nucleus.

Section IV. Biological effects of the interaction between ING1 and lamins

A) Overexpression of the LID induces apoptosis through binding to lamins

Since these data suggested an interaction between ING1 and lamin A/C through the LID region, I asked what the physiological effects of this interaction might be. Ectopic upregulation of p33ING1b, but not p47ING1a, has been shown to induce apoptosis (Scott et al., 2001;Vieyra et al., 2002). Therefore, it was tested if the association of ING1 with lamins would play any role in regulating apoptosis. The degree of apoptosis was evaluated in HEK293 cells transfected with GFP, ING1b, ING1bΔLID, and LID+NLS 48 hours following transfection. The viability of cells, as well as degree of apoptosis, was

analyzed by propidium iodide (PI) staining, which is the most commonly used dye to quantitatively assess DNA content. Apoptosis is a major form of programmed cell death. Apoptotic cells are characterized by DNA fragmentation and they often end up with a deficit in DNA content. Propidium iodide is capable of binding and labeling DNA, so when cells are stained with this DNA-specific fluorochrome they can be recognized by flow cytometry as cells having less DNA than G1 cells and forming a so-called "sub-G1" peak (Tounekti et al., 1995).

The apoptosis assay was done three times. As shown in Fig. 18, ING1b induced a significant increase (~5 fold) in the percentage of apoptotic cells comparing to the basal level (Fig. 18a-b), while the ING1bΔLID did not seem to have much effect on inducing apoptosis (Fig. 18c). Surprisingly, the LID+NLS protein could induce apoptosis by itself (Fig. 18d). Although the degree of apoptosis was slightly less than that seen in cells transfected with wild-type ING1b, it was far more than the control and ING1bΔLID constructs in this aspect, suggesting that the interaction with lamins is necessary for p33ING1b in regulating apoptosis. Previous studies using primary diploid fibroblasts to analyze apoptosis by p33ING1b showed a smaller percentage of apoptotic cells (around 10-15%) (Scott et al., 2001;Vieyra et al., 2002), and the reason might be that different cells may display various sensitivity to p33ING1b.

In addition to their effects on apoptosis, expression of both the LID+NLS and ING1bΔLID resulted in more cells in the S phase and fewer in the G2 phase of the cell cycle. For the control sample, 5.24% of cells were in G2 and 29.97% of cells were at the

S phase. The overexpression of ING1b did not affect this distribution too much (4.55% in G2 and 28.93% in S). In the ING1bΔLID transfected sample, only 1.69% of cells were found in G2, while 37.24% of cells were in the S phase. Loss of cells in the G2 phase was more evident in the LID+NLS sample, and no cells were shown to arrest at the G2 phase. The G2/M checkpoint seemed to become less efficient after transfection with the LID+NLS and ING1bΔLID. Since the G2/M checkpoint is responsible for maintaining genomic stability and cells with damaged DNA will be arrested for entering mitosis, we next asked if overexpression would affect nuclear morphology.

B) Effects on nuclear morphology

The effects of p33ING1b and the LID on nuclear architecture were investigated 48 hours following transfection. Surprisingly, overexpression of the LID+NLS protein induced a remarkable increase of cells with irregular nuclear shapes or multi-lobulated nuclei, and both phenotypes were similar to late-passage HGPS fibroblasts (Goldman et al., 2004). For most multi-nucleated cells, their nuclei were also misshapen and it frequently looked like normal nuclei were "taken apart" by some mechanical means. For some multi-nucleated cells in the LID+NLS and ING1bΔLID transfected samples, several nuclei at similar sizes indicated possible defects in mitosis, suggesting that the G2/M checkpoint might indeed be affected to some extent. In HEK293 cells, 57% of the LID transfected cells showed thickening of the nuclear lamina, irregular nuclear shapes, and multiple nuclei, compared to the 9% transfected with a control vector. Fig. 19 shows the nuclear changes in cells co-transfected with the GFP vector. Though not as efficient as the LID, ING1bΔLID induced a bit more misshapen nuclei than ING1b. In contrast,

overexpression of the intact p33ING1b protein has been well established to induce an apoptotic nuclear phenotype (Scott et al., 2001). Cells with abnormal nuclei and multiple nuclei, as a subgroup, were counted and shown in Fig. 20. Our criteria here for classifying abnormal nuclei was either irregular nuclear shapes or multiple nuclei.

To examine the effects of the LID on nuclear morphology at a higher degree of resolution, we studied the status of the nuclear lamina and chromatin of the transfected cells by electron microscopy (EM). EM is an essential tool to visualize ultrastructual components such as chromatin, mitochondria, ER, and nuclei. Using heavy metals for staining, cellular structures display either electron-dense (high affinity) or electron-lucent (low affinity) due to their different affinities for metals. For example, the heterochromatin area shows electron-dense, whereas the euchromatin is electron-lucent, since their chromatin is at different stages of condensation.

HS68, the two HGPS fibroblast cell lines, as well as MEFs were also visualized by EM. The EM was carried out using a blind experimental protocol, and cells shown in Fig. 21 represented the most frequently observed phenotypes. No significant changes in nuclear shapes were detected in AG00989, while misshapen nuclei were found in AG11513 where ING1 was largely mislocalized. As shown in Fig. 21e-f, the LID+NLS and ING1bΔLID induced a marked alteration in the nuclear shape, either misshapen or with multiple nuclei, as previously shown by light microscopy. The structure and distribution of peripheral heterochromatin in cells expressing the LID or ING1bΔLID were compared at a higher magnification (Fig. 22), where frequent discontinuities in the peripheral

heterochromatin in both LID (b) and ING1bΔLID (c) transfected cells were found, which was similar to the architecture seen in some HGPS fibroblasts (Goldman et al., 2004). The control GFP-transfected cells (a) displayed an evenly distributed pattern of heterochromatin. In addition, in a number of cells overexpressing these constructs, different degrees of distension of the outer nuclear membrane was noted, which is highlighted by the horizontal arrow in Fig. 22c. Fig. 23 shows the phenotypes of LMNA+/+ and LMNA-/- MEFs, and loss of peripheral heterochromatin was observed in LMNA-/- MEFs as described in previous reports (Sullivan et al., 1999).

C) Senescence-associated β-Galactosidase expression in cells overexpressing the LID region

Based on the observation that overexpression of the LID induced changes in peripheral heterochromatin and the nuclear envelope reminiscent of HGPS fibroblasts, senescence-associated β-galactosidase (β-gal) activity was tested in young and old HS68, HGPS fibroblasts, and LID-transfected HEK293 cells. Though the underlying mechanisms by which β-gal staining as a biomarker for replicative senescence remains unclear, β-gal activity is normally seen in senescent cells. Young, healthy HS68 fibroblasts (MPD 29) (Fig. 24a) showed no β-gal staining. In contrast, when replicative senescence approached in HS68 fibroblasts *in vitro* (MPD 95), cells gradually become flattening and more than 80% of cells displayed β-gal expression (Fig. 24b). The AG11513 HGPS fibroblasts were also tested for β-gal activity. In a previous report regarding the β-gal staining on HGPS fibroblasts, cells were at late population doublings (MPD 55) (McClintock et al., 2006). The HGPS cells used here in this assay were at a relatively low passage number (MPD

29), since they took a long time to duplicate. With similar passage level as normal HS68 fibroblasts, ~14% of AG11513 fibroblasts showed dark blue β-gal staining (Fig. 24c), suggesting they already started to enter senescence. To study the role of the LID in senescence, HEK293 cells were transfected with a GFP control vector or the LID+NLS construct. No obvious β-gal staining was seen in the GFP-transfected cells. However, with a very high transfection efficiency (~90%), a significant increase in β-gal activity was observed and dark blue was present in almost all LID-transfected cells (Fig. 24e), suggesting that the disrupted lamin-ING1 interactions might be involved in the premature aging defects associated with HGPS.

CHAPTER FOUR: DISCUSSION

Section I. Proteins that may associate with the novel conserved region (lamin interacting domain)

The aim of this project was to identify binding partners of the novel conserved region within all ING family members and if any, characterize the physiological functions of the interaction. We chose the His-tagged protein, since proteins containing one or more 6 x His affinity tags, located at either the amino and/or carboxyl terminus of the protein, can bind to Ni-NTA groups on the matrix with an affinity far greater than that of antibody-antigen or enzyme-substrate interactions (according to the supplier's handbook). Recently, mass spectrometry has become a central analytical technique for protein identifications and studies for post-translational modifications in proteins. Like mass fingerprinting to identify proteins, LC/MS/MS analysis identifies proteins based on the comparison of experimental data with theoretical proteolytic digestion data. Distinct from mass fingerprinting, LC/MS/MS analysis allows proteins to be identified by matching primary structures (sequences), rather than just comparing a spectral pattern, thus generating a less ambiguous identification than that resulting from the mass fingerprinting method (Sterner and Berger, 2000).

The LC/MS/MS results indicated several potential binding partners of this region, and we initially considered lamin A/C as strong interactors based on their ion scores for LC/MS/MS, their known functions, and their similar dynamic subcellular localizations during the cell cycle (Nigg, 1992;Moir and Goldman, 1993). In this study the association

between ING1 and lamin A/C has been tested by biochemical methods and it turns out to be a bona fide robust interaction. Another member of nuclear lamins, lamin B, was also present in the LC/MS/MS result but at present we believe that this may be an indirect interaction. The far western blotting data indicated that the LID+NLS protein binds to lamin A directly *in vitro*. Lamins form structures containing intermediate filaments at the nuclear envelope, so that under non-denaturing His-tag purification, the conditions may not be stringent enough to break all lamin filaments.

In addition to lamin A/C, the BAF170 component and other components of the SWI/SNF complex are strong candidates for potential interactions as well. Actually a previous report has indicated a possible linkage between p33ING1b and the SWI/SNF complex. BAF250, BRG1, BAF170, BAF53, and BAF47 were all found in both anti-SAP30 and anti-p33ING1b immunoprecipitates, and it was suggested that ING1b was linked to these proteins by SAP30 (Kuzmichev et al., 2002). Consistent with these data, the N-terminal 125 amino acids of p33ING1b have been identified to be involved in binding SAP30, and the lamin interacting domain (74-126) is located within this region. Since both ING1 and the SWI/SNF complex have been linked to functions involved in chromatin remodeling and ING1 proteins have been thought to perform these functions through binding HAT or HDAC complexes (Vieyra et al., 2002a), one of the future directions would be to study the interactions between ING1 and the SWI/SNF complex. Another protein that we are interested for further analysis is the SAP145 subunit that associates with protein splicing function. Since ING1 has been shown to be alternatively spliced into at least three isoforms and different isoforms seem to have distinct roles in regulating cellular

processes, this SAP145 subunit may be involved in the assembly of the spliceosomal complex (Aravind and Koonin, 2000) that performs the splicing of ING1 mRNA.

Section II. A role for lamin A in the subcellular localization of ING1 proteins

This study demonstrates that ING1 and lamin A/C bind each other *in vivo* in normal primary fibroblasts, human embryonic kidney epithelial cells, fibroblasts from Hutchinson-Gilford progeria syndrome patients, and mouse embryonic fibroblasts. Using overexpression assays, we identified the binding regions within ING1 and lamins, the amino acids 74-126 in p33ING1b and 1-406 in lamin A/C. Though lamin C appeared to bind ING1 *in vivo*, it was not present in the *in vitro* far western blotting assay. This might be caused by an indirect interaction bridged by lamin A or lamin C was not completely renatured in the far western blotting. In the AG11513 progeria cell line, the truncated lamin A product failed to interact with ING1b, as shown by both endogenous IP-Western and far western blotting assays. Interestingly, this LAΔ50 lacks the 50 amino acids encoded by the exon 11 in its C-terminus (Eriksson et al., 2003) and actually contains an intact ING1 interacting region. While consistent with our data, the reason why progerin, which lacks the 50 aa does not bind ING1 while lamin C, which differs from lamin A in the last 97 aa (567-664 in lamin A) does *in vivo*, is not obvious given that interaction was mapped to the N-terminus of lamin A. This suggests that the tail region of lamins has profound effects upon the ability of the rod domain to interact with ING1, and suggests the possibility that ING proteins may bind dimers or multimers, rather than monomers of lamin *in vivo*, although interaction with monomers is possible *in vitro* based upon far western analyses.

Moreover, the loss of these 50 amino acids may cause a significant conformational change in its structure which interferes with its folding status and thereby protein-protein interactions, and this may further convey a dominant gain-of-function property on wild-type lamins, since the wild-type lamins in this AG11513 cell line displayed reduced level of interaction with ING1. However, the premature aging of HGPS patients with the common $Gly^{608}\rightarrow Gly^{608}$ mutation may not be related to the aberrant association between ING1 and lamin A, since defects in ING1b by downregulation or knockout have been shown to facilitate cell proliferation in a p53-independent manner (Garkavtsev and Riabowol, 1997;Coles et al., 2007).

The other HGPS cell line, AG00989, analyzed here has defects in pre-lamin A processing by ZMPSTE-24 proteinase (Pendas et al., 2002;Broers et al., 2006). As a result, accumulation of pre-lamin A and absence of mature lamin A are characteristics of these fibroblasts. This mutation in the LMNA gene was first described as "atypical progeria", since the patient attained an age that was greater than the median age of mortality for regular HGPS ($Gly^{608}\rightarrow Gly^{608}$ mutation) patients, and they had an unspecified type of dwarfism (Csoka et al., 2004). Though it is not clear if it exactly resembles cells deficient in ZMPSTE-24, ZMPSTE-24-/- mice show accelerated aging similar to those seen in HGPS patients and upregulation of p53 target genes (Bergo et al., 2002;Varela et al., 2005).

At the same passage level that severe changes in nuclear architecture were observed in around 35% of the AG11513 fibroblasts, less defect was found in this AG00989

fibroblast cell line (20% abnormal cells), which was consistent with previous findings that this mutation in the LMNA gene affected nuclear morphology at a lower extent compared to other identified LMNA mutations (Csoka et al., 2004). Most cells have regular nuclear shapes and the peripheral heterochromatin is evenly distributed underneath the nuclear lamina as visualized by the EM analyses. Since ING1 proteins retain their interactions with lamin A/C in AG00989 and are mainly located in the nucleus, while in AG11513, ING1 is largely mislocalized to the cytoplasm, it is reasonable to speculate that ING1 proteins perform a role in maintaining the integrity of the nucleus.

Subsequent ING1 localization studies in the LMNA+/+ and LMNA-/- MEFs as well as the nuclear fractionation of LMNA-/- MEFs indicate that the subcellular localization of ING1 proteins is dependent on A-type lamins. To further address the role of lamin A, it should be possible to see if ING1 could be brought back to the nucleus by rescuing the expression of lamin A in LMNA-/- MEFs. With a large portion of cells showing minor defects in their nuclei, the LMNA-/- MEFs remain growing normally. It is presently unknown how the mislocalization of ING1 affects cellular activities, and restoring of ING1 expression in the nucleus without introducing lamin A should allow to study the role of ING1 proteins.

Section III. ING1-induced apoptosis and changes in nuclear morphology by interacting with lamins

Ectopic overexpression of p33ING1b induces apoptosis, and binding to PCNA has been shown to be able to regulate this ability (Scott et al., 2001b). Since the PIP domain that interacts with PCNA is only present in p33ING1b, it is thought that the distinct N-terminus of ING1 isoforms is involved in the function of inducing apoptosis. Here it is demonstrated that in addition to PCNA, association with nuclear lamins is also necessary for p33ING1b to perform this function, and the ING1bΔLID that could not bind lamins failed to promote apoptosis effectively. We also observed a significant proportion of apoptotic cells by overexpressing the LID+NLS protein. Based on the idea that the ING1-lamin interaction may be essential, a very informative study will be to test the ability of p33ING1b to induce apoptosis in the AG11513 HGPS cell line.

The details of the mechanisms by which the LID+NLS protein affects apoptosis and how proteolysis of lamins contributes to apoptosis are presently obscure. It is thought that degradation of the nuclear lamina is an important step in apoptosis. Apoptosis is characterized by a variety of biochemical and morphological changes, including key alterations in the nucleus. Nuclear changes in apoptosis consist of proteolytic cleavage of the nuclear lamina, chromatin condensation, nuclear fragmentation, and clustering of nuclear pore complexes (Martelli et al., 2001). Consistent with playing an active role, an uncleavable mutant of lamin A resulted in delayed apoptosis (Rao et al., 1996). Failure of the assembly of B-type lamins by overexpressing the AKAP149 PP1-binding domain (PP1-BD) has also been shown to induce apoptosis (Steen et al., 2000;Steen et al., 2003).

Both A- and B-type lamins are degraded in the process of apoptosis in several cell types (Gruenbaum et al., 2000). Caspases, a family of cysteine-aspartate proteases, are essential regulators of apoptosis, and caspase-6 has been identified as the one that is specifically responsible for the cleavage of lamins (Rao et al., 1996;Slee et al., 2001;Lee et al., 2006). Lamin A/C are cleaved at their conserved 227-230 regions that are found to bind chromatin and involved in the formation of the lamina (Broers et al., 2006).

One of our hypotheses is that the LID+NLS protein would avidly bind to lamin A/C and thus affect the associations of lamins with other molecules such as LAP, LBR, and even chromatin. Many lamin binding partners have already been implicated in cell proliferation through transcriptional regulation. Though we have not yet completed high resolution mapping of the region of lamin A that interacts with ING1, we show that lamin A binds ING1 through its first 406 amino acids, and this region contains the chromatin binding sites as well as the cleavage sites recognized by caspase 6. ING1 proteins may perform a role as a bridge between lamins and histones, and overexpression of the LID+NLS protein would possess a dominant-negative function on endogenous ING1, thus resulting in loss of chromatin-binding activity of lamins. Failure of chromatin anchoring on the envelope may further trigger the initiation of apoptosis signaling.

Another hypothesis relates lamins to the role of ING1b-PCNA interaction in apoptosis. Interaction with PCNA seems to perform an important role in regulating apoptosis, since an ING1b PIP mutant that does not bind PCNA protects cells from apoptosis (Scott et al., 2001b). Lamin A/C has been linked to DNA replication by co-localization with PCNA

(Spann et al., 1997;Kennedy et al., 2000). As a result, although lacking the PIP region, the LID+NLS protein may be indirectly involved in association with PCNA and therefore regulate apoptosis in this manner. PCNA is a factor required for the elongation step of replication, and localization of PCNA and RFC (another factor required for elongation) was altered in cells overexpressing a mutant lamin lacking the N-terminus. Presence of this mutant protein caused redistribution of lamins and resulted in nucleoplasmic aggregates containing endogenous and mutant lamins, PCNA, and RFC, and these aggregates failed to associate with chromatin (Spann et al., 1997). Since we demonstrate that the N-terminus of lamins is necessary to interact with ING1, it raises the possibility that ING1 may be able to link lamins to chromatin.

In addition to a role in apoptosis, expression of the LID induced a significant increase in senescence-associated β-galactosidase activity, similar to staining observed in the HGPS strain AG11513, consistent with this fragment inducing an HGPS-like phenotype. We also observed significantly more cells (>2 fold) with abnormal nuclei in the LID+NLS transfected cells than in the ING1b transfected ones. This might be due to the decrease in the mechanical strength of the nuclear envelope previously noted for HGPS fibroblasts. Nuclear lamina perform an essential role in maintaining nuclear shape and physical interaction with the overexpressed LID+NLS protein may cause the nuclear lamina to become more "vulnerable". Though the ING1bΔLID was not able to promote apoptosis effectively, a relatively great amount of cells also displayed a similar phenotype. Since the ING1b protein that lacks the LID region can not interact with lamins, upon overexpression it would not stick to the nuclear periphery and would cause less dramatic

effects than the LID+NLS itself. However, it would still interfere with the interactions between endogenous p33ING1b and lamins to some extent, since it contains the PHD region that binds histones H3K4me2 and H3K4me3.

Section IV. Epigenetic controls related to ING-lamin interactions

Results from electron microscopy indicated the loss of peripheral heterochromatin in most LID+NLS and some ING1bΔLID transfected cells. It has been suggested that ING2 could stabilize the mSin3A-HDAC complex through recognition by H3K4me3 (Shi et al., 2006). The trimethylated histone H3K4 primarily occurs with gene activation (Santos-Rosa et al., 2002;Shi et al., 2006), whereas dimethylated forms of H3K4 are enriched in both active and silenced chromatin (Vakoc et al., 2006). For the first time this finding suggested a role for H3K4me3 in negative regulation of gene transcription. Moreover, the heterochromatin marker H3K9me3 has recently been implicated in gene activation (Vakoc et al., 2005). As a result, proteins that read and interpret the histone codes in both positive and negative ways are thought of as more equally important in transcriptional regulation.

In addition to ING2, ING1 is another component of the HDAC1 complex, and it may be involved in keeping the transcriptional sites inactivated in a similar manner as ING2. The p33ING1b-Sin3A/HDAC complex has been suggested to be required to maintain specific status of histone modification, such as methylation of histone H3K9, and knockdown of ING1 by siRNA results in decreased H3K9me2 and H3K9me3. Furthermore, p33ING1b associates with pericentric heterochromatin in late S phase (Xin et al., 2004). Considering

our result regarding the effect of disrupted ING1 activity on peripheral heterochromatin, it is possible that normal expression of ING1 may be necessary for the formation of peripheral heterochromatin.

ING1 proteins may perform various functions in chromatin remodeling since they associate with both HAT and HDAC complexes and thus contribute to post-translational modifications of histones (Vieyra et al., 2002a). Binding to H3K4me3 suggests an important role for ING1 in reading these histone codes. The subcellular localization of ING1 proteins may also determine their preferences in regulating histone modifications. Peri-nuclear and centromeric chromatin is primarily involved in gene silencing, and ING1 that located in these areas may have a preference on HDACs, whereas the remaining nucleoplasmic ING1 proteins associate with more HATs than HDACs. Fig. 25 shows a model that is proposed for the roles of ING1 proteins in chromatin remodeling by associating with partners.

CHAPTER FIVE: CONCLUSIONS

The aim of this project was to unravel the details of ING functions in pathways involved in epigenetic regulation, senescence, and apoptosis, specifically by determining what the function of a domain unique to the ING proteins was. Both *in vivo* and *in vitro* approaches indicated a robust interaction between p33ING1b and lamin A. The newly-defined lamin interacting domain is a domain specific to ING family members and further analyses of interactions of other ING family members with lamins will be performed. Disruption of the nuclear anchoring function of lamin A for ING1 proteins implicates ING1 functions in laminopathies such as Hutchinson-Gilford progeria syndrome and many cellular activities including apoptosis and senescence. Further determination of the biological importance of the ING1-lamin interactions will significantly help to clarify the biochemical mechanisms used by the ING1 class II tumor suppressor in regulating these processes. This better understanding will contribute to our long-term goal of exploiting knowledge of these pathways in cancer therapy.

Table 1. Top 20 BLAST hits on the sequence of the Lamin Interacting Domain. BLAST searches of the LID sequence were performed on the NCBI website. The top 20 hits included ING family members from human, mouse, rat, *Xenopus*, etc. and predicted proteins that were similar to INGs. An unnamed protein product and a hypothetical protein were also shown on the list, and their functions are not clear yet.

Identifier	Description	Organism
gi|38201661	Inhibitor of growth family, member 1 isoform D	Homo sapiens
gi|38201663	Inhibitor of growth family, member 1 isoform C	Homo sapiens
gi|38201665	Inhibitor of growth family, member 1 isoform B	Homo sapiens
gi|38201667	Inhibitor of growth family, member 1 isoform A	Homo sapiens
gi|9944281	Growth inhibitory protein ING1	Homo sapiens
gi|27263169	ING1 isoform	Homo sapiens
gi|7158369	ING1 tumor suppressor, variant C	Homo sapiens
gi|7158367	ING1 tumor suppressor, variant B	Homo sapiens
gi|7158365	ING1 tumor suppressor, variant A	Homo sapiens
gi|57103416	PREDICTED: similar to inhibitor of growth family, member 1 isoform 1	Canis familiaris
gi|50730550	PREDICTED: similar to ING1 protein	Gallus gallus
gi|6456562	p33ING1 protein	Mus musculus
gi|16741522	Inhibitor of growth family, member 1	Mus musculus
gi|94384581	PREDICTED: similar to inhibitor of growth family, member 1	Mus musculus
gi|57547050	p33ING1b variant 5	Xenopus laevis
gi|61817915	PREDICTED: similar to inhibitor of growth family, member 1	Bos taurus
gi|84370364	Inhibitor of growth family, member 1	Rattus norvegicus
gi|57547048	p33ING1b variant 4	Xenopus laevis
gi|47226952	Unnamed protein product	Tetraodon nigroviridis
gi|94536655	Hypothetical protein LOC678608	Danio rerio

Table 2. List of the proteins identified by Liquid Chromatography-Mass Spectrometry (LC/MS/MS) that may interact with the LID. The criteria for choosing proteins is that they show at least two peptides with individual ions scores >48 as calculated by the Mascot program, which indicate identity or extensive homology. Scores of proteins are derived from ions scores as a non-probabilistic way for ranking protein hits. Ions score is calculated by -10*Log(P), where P represents the probability that the observed match is a random event. Lamins constituted three of the total nine hits. Lamin A/C isoform 2 had the highest score of all.

GenBank Accession Number	Protein	Mass	Score	Peptides Matched
5031875	**Lamin A/C isoform 2**	65096	187	R.SGAQASSTPLSPTR.I (Ions score 41) K.EDLQELNDR.L (Ions score 48) R.AQHEDQVEQYK.K (Ions score 34) R.NSNLVGAAHEELQQSR.I (Ions score 68) R.VAVEEVDEEGKFVR.L (Ions score 81) K.SNEDQSMGNWQIK.R (Ions score 36) K.SNEDQSMGNWQIK.R Oxidation (M) (Ions score 15) R.SVTVVEDDEDEDGDDLLHHHHVSGSR.R (Ions score 94)
1871210	T-complex protein 1 Beta subunit (TCP-1-BETA)	22924	150	R.VQDDEVGDGTTSVTVLAAELLR.E (Ions score 96) R.EALLSSAVDHGSDEV.K (Ions score 108)
2498883	Splicing factor 3B subunit 2 (Spliceosome-associated protein 145) (SAP 145)	97596	129	K.LAQQQAALLMQQEER.A (Ions score 48) R.QEEMNSQQEEEEMETDAR.S (Ions score 75) R.SSLGQSASETEEDTVSVSK.K (Ions score 69) R.GSDSPAADVEIEYVTEEPEIYEPNFIFFK.R (Ions score 29) K.EEQKTMK.S (Ions score 14) R.KGPAPELQGVEVALAPEELELDPMAMTQK.Y Oxidation (M) (Ions score 18)
27436948	**Lamin A/C isoform 3**	70618	128	R.SGAQASSTPLSPTR.I (Ions score 41) K.EDLQELNDR.L (Ions score 48) R.AQHEDQVEQYK.K (Ions score 34) R.NSNLVGAAHEELQQSR.I (Ions score 68)

				R.VAVEEVDEEGKFVR.L (Ions score 81) K.SNEDQSMGNWQIK.R (Ions score 36) K.SNEDQSMGNWQIK.R Oxidation (M) (Ions score 15) R.TALINSTGEGSHCSSSGDPAEYNLR.S (Ions score 6)
1549241	SWI/SNF complex 170 KDa subunit	132650	91	K.DMDEPSPVPNVEEVTLPK.T (Ions score 54) K.ADPAFGLESSGIAGTTSDEPERIEESGNDEAR.V (Ions score 67) R.DIGEGNLSTAAAAALAAAAVK.A (Ions score 18)
15126742	**Lamin B1**	66367	83	K.SLEGDLEDLKDQIAQLEASLAAAK.K (Ions score 55) K.TTIPEEEEEEEEAAGVVVEEELFHQQGTPR.A (Ions score 61)
9910280	UDP-glucose ceramide glucosyltransferase-like 1 isoform 1	177078	88	K.WFSTPLLLEASEFLAEDSQEK.F (Ions score 53) R.IIGPLEDSELFNQDDFHLLENIILK.T (Ions score 88) R.YVLEPEISFTSDNSFAK.G (Ions score 20)
532313	NF45 protein	44669	74	R.NQDLAPNSAEQASILSLVTK.I (Ions score 74) K.INNVIDNLIVAPGTFEVQIEEVR.Q (Ions score 53) R.KILGQEGDASYLASEISTWDGVIVTPSEK.A (Ions score 25)
42541350	TPA: TPA_exp: cytoplasmic activation/proliferation-associated protein 1	76814	69	K.SSGPPPPSGSSGSEAAAGAGAAAPASQHPATGTGAVQTEAMK.Q (Ions score 48) K.QGLNGVPILSEEELSLLDEFYK.L (Ions score 56)

Figure 1. Structural features and binding partners of p33ING1b. p33ING1b consists of 279 amino acids and possesses several functional domains including a nuclear localization sequence (NLS) and a plant homeodomain (PHD) motif. ING1b interacts with PCNA, Sap30, 14-3-3, ARF, histone H3K4me3, karyopherins, and specific phosphoinositide (PIs) in the binding regions indicated. In this study, we mapped a novel conserved domain located upstream of the NLS that interacts with lamin A/C. PIP = PCNA-interacting protein motif; PB = partial bromodomain; LID = lamin interacting domain; NLS = nuclear localization signal; PHD = plant homeodomain; PBR = polybasic region.

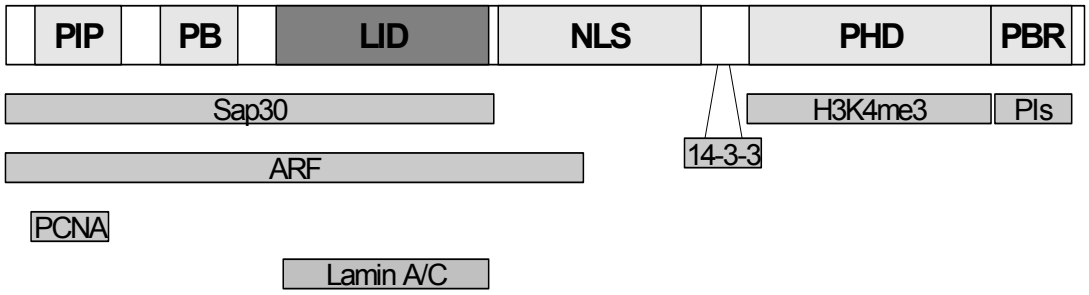
PIP
PB
LID
NLS
PHD
PBR
Sap30
H3K4me3
PIs
14-3-3
ARF
PCNA
Lamin A/C

Figure 2. Proposed model of tumor suppressors regulating chromatin structure. In this model it is proposed that internal (telomere erosion, oxidative damage) and external (ionizing radiation, ultraviolet, chemical agents) stresses initiate a damage signal that is transduced via PI3 kinase family members to protein complexes containing polycomb group proteins. These complexes, which may be regulated by PML complex proteins, contain enzymes that modify histones to tip the balance of activity toward modifications that favor the formation of heterochromatin. The Rb, p53, and ING tumor suppressors, like the polycomb proteins Bmi1 and CBX7, may serve to target HDAC and other activities to regions of the genome where the formation of heterochromatin helps to impose and maintain a senescence-specific configuration and pattern of gene expression.

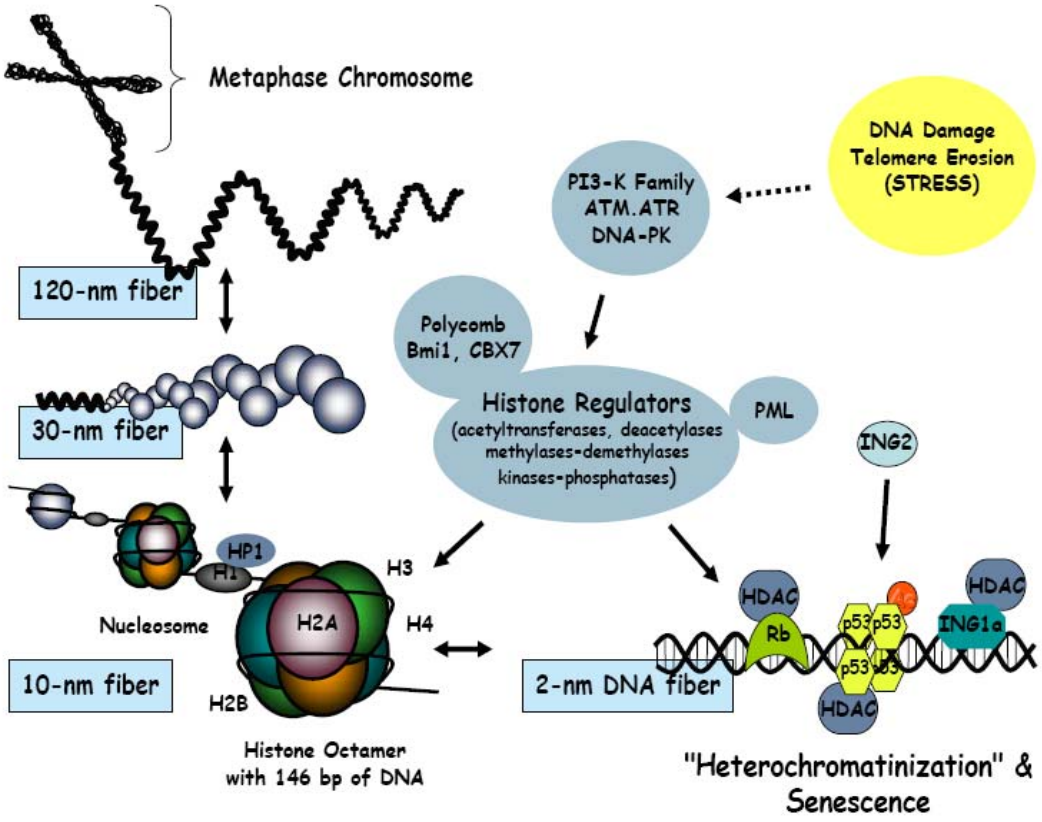
Metaphase Chromosome
DNA Damage
Telomere Erosion
(STRESS)
PI3-K Family
ATM.ATR
DNA-PK
120-nm fiber
Polycomb
Bmi1, CBX7
Histone Regulators
(acetyltransferases, deacetylases
methylases-demethylases
kinases-phosphatases)
PML
ING2
30-nm fiber
HP1
H1
H3
H4
H2A
H2B
Nucleosome
10-nm fiber
Histone Octamer
with 146 bp of DNA
HDAC
Rb
p53
p53
p53
p53
HDAC
ING1a
HDAC
2-nm DNA fiber
"Heterochromatinization" &
Senescence

Figure 3. Multiple sequence alignments of the Lamin Interacting Domain (LID). The sequences of the LID in ING1-5 were analyzed by T_coffee and visualized by the GENEDOC program. The LID regions in ING1-5 are approximately 50 amino acids. Based on multiple sequence comparison, the sequences of the LID can be subdivided in three subfamilies, ING1/2, ING4/5, and ING3. The LID region of ING1 is from amino acids 74 to 126. Residues shaded in black indicate high conservation in the whole family, and those shaded in grey are less conserved ones.

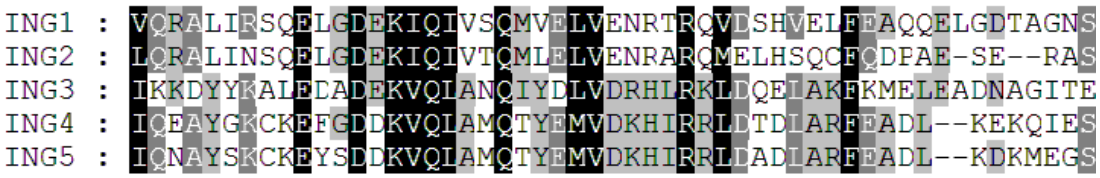
ING1 : VQRALIRSQELGDEKIQIVSQMVELVENRTRQVDSHVELFEAQQELGDTAGNS
ING2 : LQRALINSQELGDEKIQIVTQMLELVENRARQMELHSQCFQDPAE-SE--RAS
ING3 : IKKDYYKALELADEKVQLANQIYDLVDRHLRKLDQELAKFKMELEADNAGITE
ING4 : IQEAYGKCKEFGDDKVQLAMQTYEMVDKHIRRLDTDLARFEADL--KEKQIES
ING5 : IQNAYSKCKEYSDDKVQLAMQTYEMVDKHIRRLDADLARFEADL--KDKMEGS

Figure 4. Distribution of the 140 BLAST hits on the sequence of the LID. BLAST was conducted on the NCBI website. Each protein was given a score in different colors representing various sequence similarity. The hit score gives an indication of how good the alignment is; the higher the score, the better the alignment. In general terms, this score is calculated from a formula that takes into account the alignment of similar or identical residues, as well as any gaps introduced to align the sequences. Among the 140 blast hits, most were members of ING family in human and mouse, their distant orthologs in *Xenopus* and *Drosophila melanogaster*, and a few predicted proteins whose functions have not been clarified.

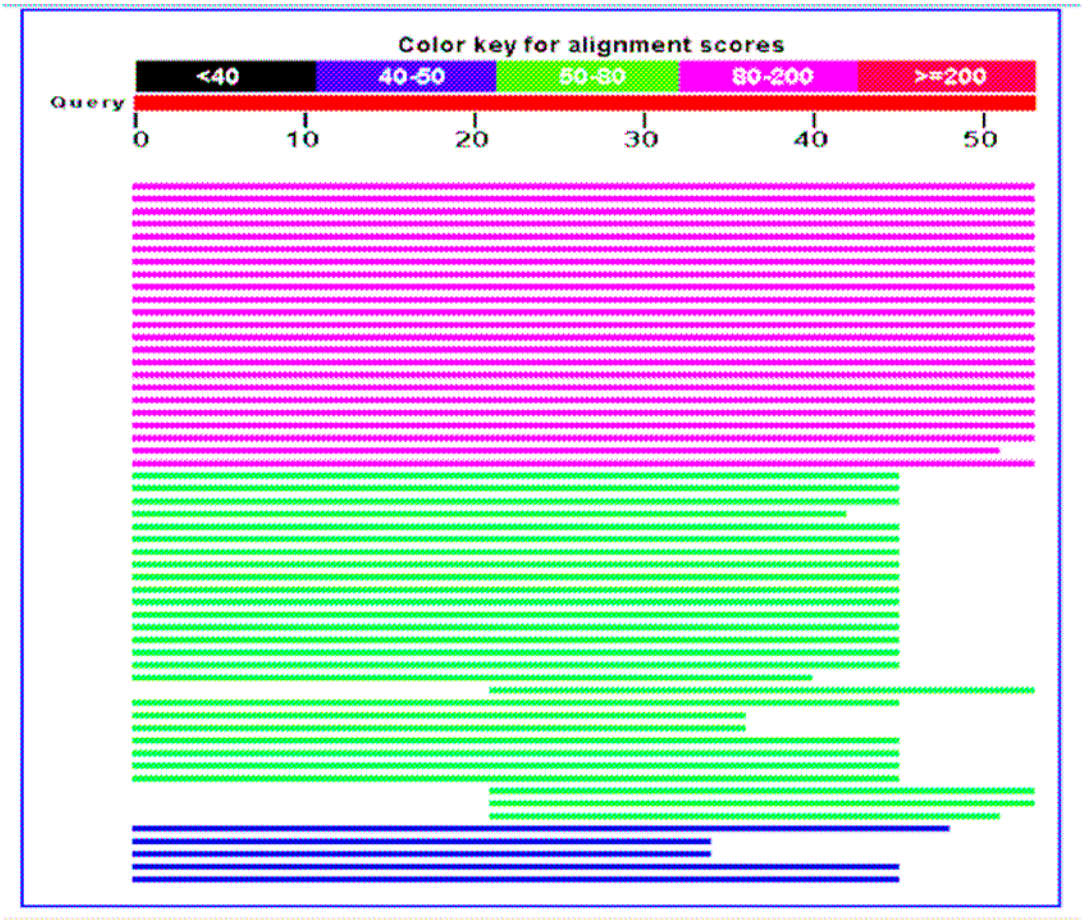
Color key for alignment scores
<40
40-50
50-80
80-200
>=200
Query
0
10
20
30
40
50

Figure 5. Multiple sequence alignments of ING1 and lamin A in human and mouse. Since ING1-lamin interactions were also analyzed in mouse embryonic fibroblasts in this study, sequence alignments of proteins from these two origins were performed. Using the same method as the sequence alignments for the LID region, p33ING1b (human) and p37ING1 (mouse) (panel a) as well as lamin A in human and mouse (panel b) were analyzed.

(a)

```
p33ING1b : MLSPANGEQLHLVNYVEDYLDSIESLPFDLQRNVSLMREICAKYQEILKELDECYERFSRETDGAQKRRM :  70
p37ING1  : MLSPANGEQIHLVNYVEDYLDSIESLPFDLQRNVSLMREICAKYQEILKELDDYYEKFKRETDGTQKRRV :  70

p33ING1b : LHCVQRALIRSQELGDEKIQIVSQMVELVENRTRQVDSHVELFEAQQELGDTAGNSGKAGADRPKGEAAA : 140
p37ING1  : LHCIQRALIRSQELGDEKIQIVSQMVELVENRSRQVDSHVELFEAHQDISDGTGGSGKAGQDKSKSEAIT : 140

p33ING1b : QADKPNSKRSRRQRNNENRENASSNHDHDDGASGTPKEKKAKTSKKKKRSKAKAEREASPADLPIDPNEP : 210
p37ING1  : QADKPNNKRSRRQRNNENRENASNNHDHDDITSGTPKEKKAKTSKKKKRSKAKAEREASPADLPIDPNEP : 210

p33ING1b : TYCLCNQVSYGEMIGCDNDECPIEWFHFSCVGLNHKPKGKWYCPKCRGENEKTMDKALEKSKKERAYNR : 279
p37ING1  : TYCLCNQVSYGEMIGCDNDECPIEWFHFSCVGLNHKPKGKWYCPKCRGESEKTMDKALEKSKKERAYNR : 279
```

(b)

```
LA-human : METPSQRRATRSGAQASSTPLSPTRITRLQEKEDLQELNDRLAVYIDRVRSLETENAGLRLRITESEEVVSREVSGIKAAYEAELGD :  87
LA-mouse : METPSQRRATRSGAQASSTPLSPTRITRLQEKEDLQELNDRLAVYIDRVRSLETENAGLRLRITESEEVVSREVSGIKAAYEAELGD :  87

LA-human : ARKTLDSVAKERARLQLELSKVREEFKELKARNTKKEGDLIAAQARLKDLEALLNSKEAALSTALSEKRTLEGELHDLRGQVAKLEA : 174
LA-mouse : ARKTLDSVAKERARLQLELSKVREEFKELKARNTKKEGDLIAAQARLKDLEALLNSKEAALSTALSEKRTLEGELHDLRGQVAKLEA : 174

LA-human : ALGEAKKQLQDEMLRRVDAENRLQTMKEELDFQKNIYSEELRETKRRHETRLVEIDNGKQREFESRLADALQELRAQHEDQVEQYKK : 261
LA-mouse : ALGEAKKQLQDEMLRRVDAENRLQTLKEELDFQKNIYSEELRETKRRHETRLVEIDNGKQREFESRLADALQELRAQHEDQVEQYKK : 261

LA-human : ELEKTYSAKLDNARQSAERNSNLVGAAHEELQQSRIRIDSLSAQLSQLQKQLAAKEAKLRDLEDSLARERDTSRRLLAEKEREMAEM : 348
LA-mouse : ELEKTYSAKLDNARQSAERNSNLVGAAHEELQQSRIRIDSLSAQLSQLQKQLAAKEAKLRDLEDSLARERDTSRRLLAEKEREMAEM : 348

LA-human : RARMQQQLDEYQELLDIKLALDMEIHAYRKLLEGEEERLRLSPSPTSQRSRGRASSHSSQTQGGGSVTKKRKLESTESRSSFSQHAR : 435
LA-mouse : RARMQQQLDEYQELLDIKLALDMEIHAYRKLLEGEEERLRLSPSPTSQRSRGRASSHSSQSQGGGSVTKKRKLESSESRSSFSQHAR : 435

LA-human : TSGRVAVEEVDEEGKFVRLRNKSNEDQSMGNWQIKRQNGDDPLLTYRFPPKFTLKAGQVVTIWAAGAGATHSPPTDLVWKAQNTWGC : 522
LA-mouse : TSGRVAVEEVDEEGKFVRLRNKSNEDQSMGNWQIRRQNGDDPLMTYRFPPKFTLKAGQVVTIWASGAGATHSPPTDLVWKAQNTWGC : 522

LA-human : GNSLRTALINSTGEEVAMRKLVRSVTVVED--DEDEDGDDLLHHEHGSHCSSSGDPAEYNLRSRTVLCGTCGQPADKASASGSGAQV : 607
LA-mouse : GSSLRTALINSTGEEVAMRKLVRSLTMVEDNEDDDEDGEELLHHEFGSHCSGSGDPAEYNLRSRTVLCGTCGQPADKA-AGGAGAQV : 608

LA-human : GGPISSGSSASSVTVTRSYRSVGGSGGGSFGDNLVTRSYLLGNSSPRTQSPQNCSIM : 664
LA-mouse : GGSISSGSSASSVTVTRSFRSVGGSGGGSFGDNLVTRSYLLGNSSPRSQSSQNCSIM : 665
```

Figure 6. Purification of His-tag protein complexes by Ni-NTA columns and lamin A/C protein levels in the complexes. (A) HEK293 cells were transfected with the His-tagged Tri-LID+NLS construct or the empty vector as a negative control. Trasfection was performed using calcium phosphate method. Cells were harvested at 24 hours following transfection and cell lysis was performed under native condition. Lysates were subsequently loaded to the Ni-NTA columns and washed three times with low concentration of imidazole (15mM). Elution buffer with high concentration of imidazole (250mM) was used to elute the proteins. (B) Based on the LC/MS/MS results that A-type lamins might be binding partners of the novel conserved region of ING1, equal amounts from the Ni-NTA column-eluted protein complexes were tested for lamin A/C expression. A little amount of lamin C and no lamin A were detected in the negative control (V), whereas significant more lamins A and C were present in the experimental sample. This further confirms the potential interactions between ING1 and lamins.

(A)

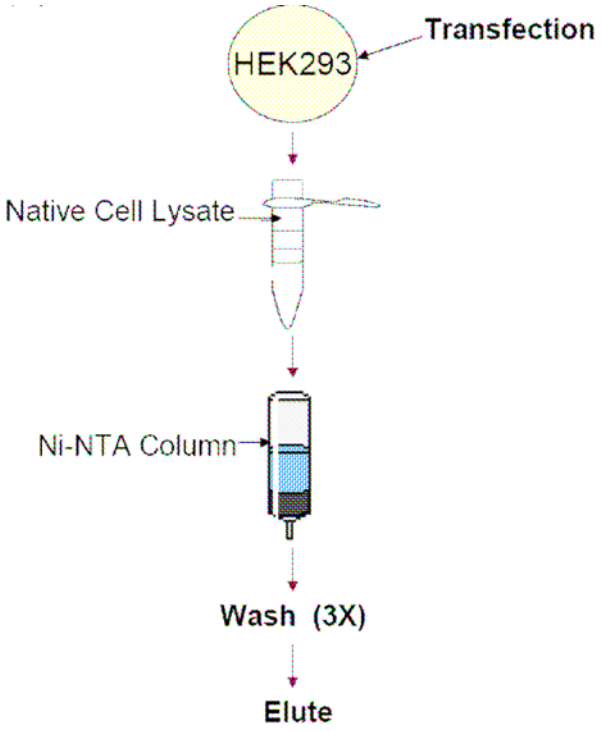
HEK293
Transfection
Native Cell Lysate
Ni-NTA Column
Wash (3X)
Elute

(B)

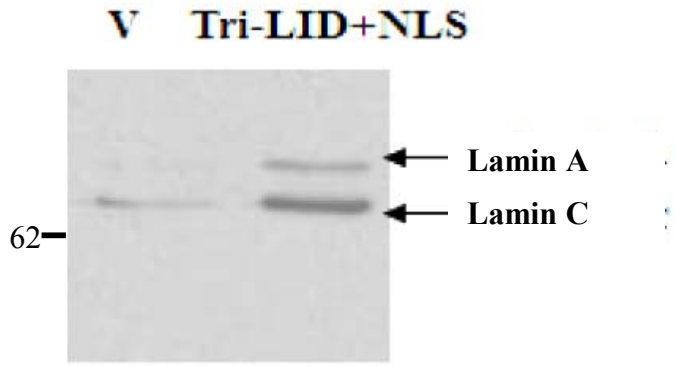
V
Tri-LID+NLS
Lamin A
Lamin C
62

Figure 7. Schematic representation of the ING1b constructs used in the study. Various ING1b constructs were made to analyze the interactions with lamin A/C, including ING1bΔLID, LID+NLS, NLS, and Tri-LID+NLS (for LC/MS/MS). All fragments were constructed with PCR mediated method. The positions of amino acids in the molecule are shown.

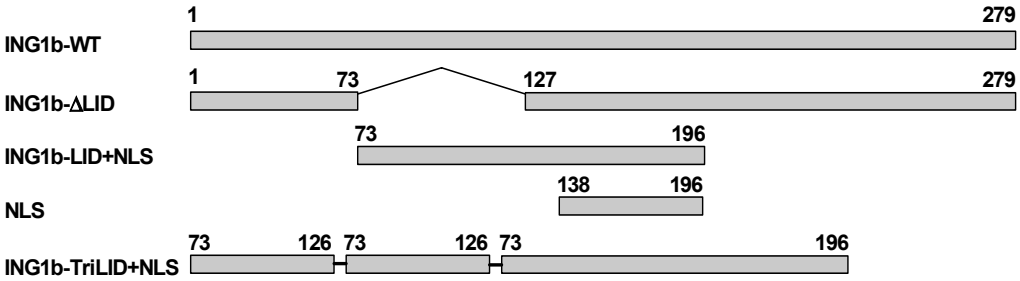
1
279
ING1b-WT
1
73
127
279
ING1b-ΔLID
73
196
ING1b-LID+NLS
138
196
NLS
73
126
73
126
73
196
ING1b-TriLID+NLS

Figure 8. ING1b binds to lamin A/C through the LID region. Various ING1b constructs showed different binding capacities to lamin A/C. 24 hours following transfection in HEK293 cells, both the ING1b and the LID+NLS proteins were able to co-immunoprecipitate with lamin A/C, while the deletion mutant and the NLS region could not. The non-specific IgG control was performed using an anti-Flag antibody. The lower two panels indicate expression levels of overexpressed proteins and endogenous lamins tested by the input lysates.

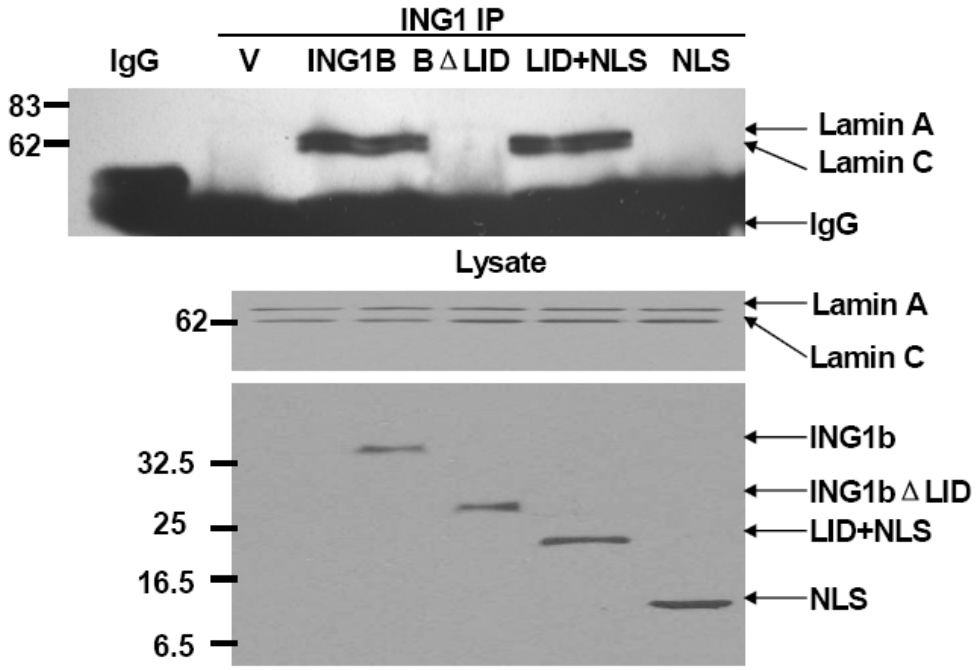
ING1 IP
IgG
V
ING1B
B Δ LID
LID+NLS
NLS
83
62
Lamin A
Lamin C
IgG
Lysate
62
Lamin A
Lamin C
32.5
25
16.5
6.5
ING1b
ING1b Δ LID
LID+NLS
NLS

Figure 9. Reciprocal co-immunoprecipitations performed with a lamin A/C antibody. Protein complexes were immunoprecipitated using lamin A/C antibody and probed with a mixture of ING1 antibodies Cab1-4. When ING1b constructs were overexpressed at similar levels in HEK293 cells (bottom panel), lamin A/C could only pull down p33ING1b and the LID+NLS fragment.

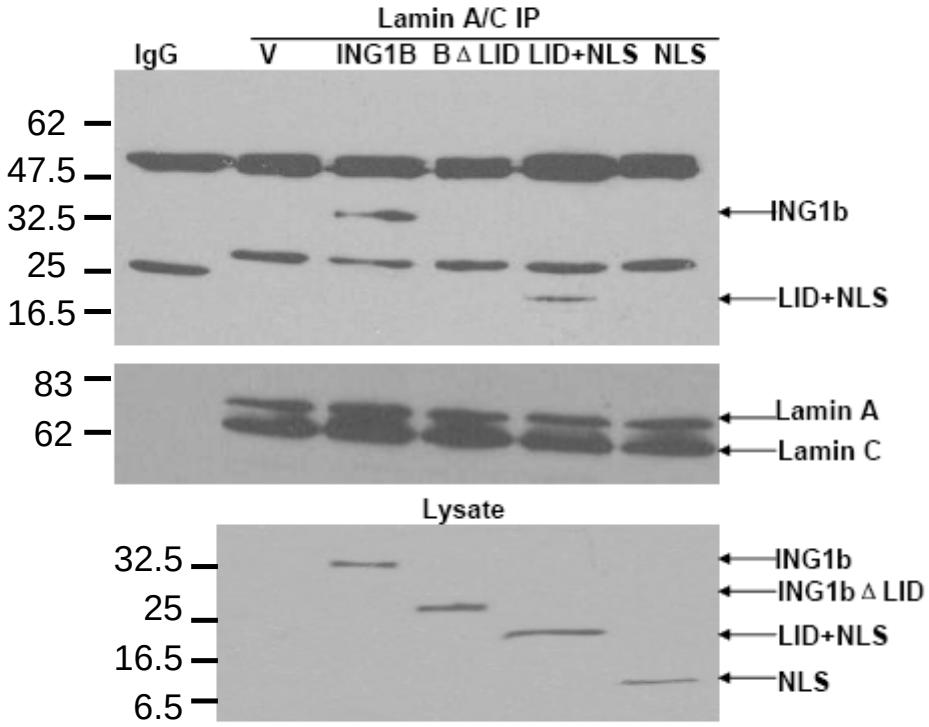
Lamin A/C IP
IgG
V
ING1B
BΔLID
LID+NLS
NLS
62
47.5
32.5
25
16.5
ING1b
LID+NLS
83
62
Lamin A
Lamin C
Lysate
32.5
25
16.5
6.5
ING1b
ING1bΔLID
LID+NLS
NLS

Figure 10. All fragments of lamin A bind to p33ING1b. In order to map the binding region in lamin A that mediates the interaction with ING1b, full length lamin A and two myc-tagged fragments of lamin A (1-447 and 415-664) were co-transfected into HEK293 cells with wild-type p33ING1b. Myc-tagged protein complexes were pulled down by the anti-myc antibody 9E10, and p33ING1b was detected in all samples suggesting that there might be a third bridge protein between them. The heavy chains of the IgG indicated nearly equal amounts of antibodies used.

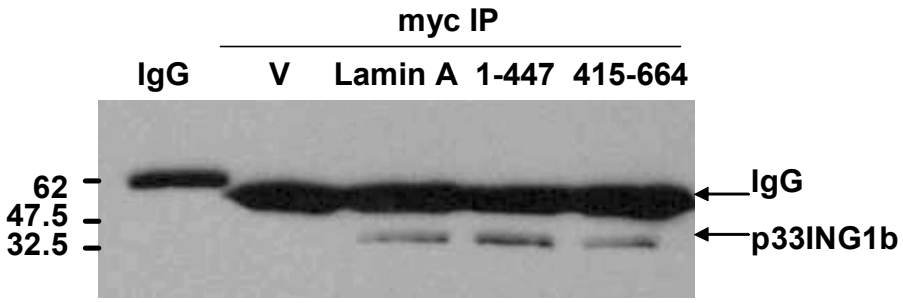
myc IP
IgG
V
Lamin A
1-447
415-664
62
47.5
32.5
IgG
p33ING1b

Figure 11. The N-terminus of lamin A is involved in the association with ING1. To exclude the possibility of the existence of a linker protein mediating the lamin-ING1 interaction, the LID+NLS construct instead of the wild-type ING1b was co-transfected into HEK293 cells with myc-tagged constructs encoding fragments of lamin A (lamin A, 1-406, 1-447, 415-664). Using the ExactaCruz secondary antibody that does not recognize denatured IgG bands, we identified that the N-terminal 1-406 amino acids of lamin A were sufficient for binding to ING1. Levels of the LID+NLS protein were tested after immunoprecipitation (middle panel). Overexpression of different lamin fragments in the lysates was indicated in the bottom panel.

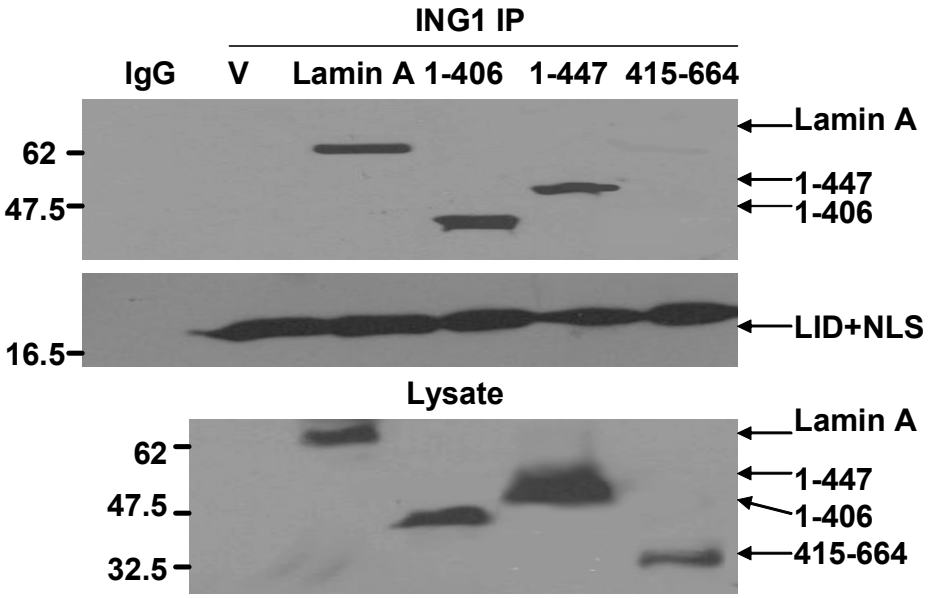
ING1 IP
IgG
V
Lamin A 1-406
1-447
415-664
62
47.5
Lamin A
1-447
1-406
16.5
LID+NLS
Lysate
62
47.5
32.5
Lamin A
1-447
1-406
415-664

Figure 12. Associations between endogenous ING1 and lamin A in normal HS68 human fibroblasts and Hutchinson-Gilford progeria syndrome (HGPS) fibroblasts. AG11513, an HGPS cell line carrying the typical $G^{608} \rightarrow G^{608}$ mutation, showed very weak associations between ING1 and lamins and ING1 failed to interact with the truncated lamin AΔ50 (progerin). Another HGPS cell line AG00989, which has a missense mutation $Arg^{644} \rightarrow Cys^{644}$ in LMNA, displayed the similar level of interactions as HS68. The passage of AG11513 used here was around 20, and at this passage the LAΔ50 could already be detected. The ING1b protein showed a higher level in AG11513 than HS68 and AG00989. Actin expression was tested to confirm that nearly equal amounts of lysates were loaded.

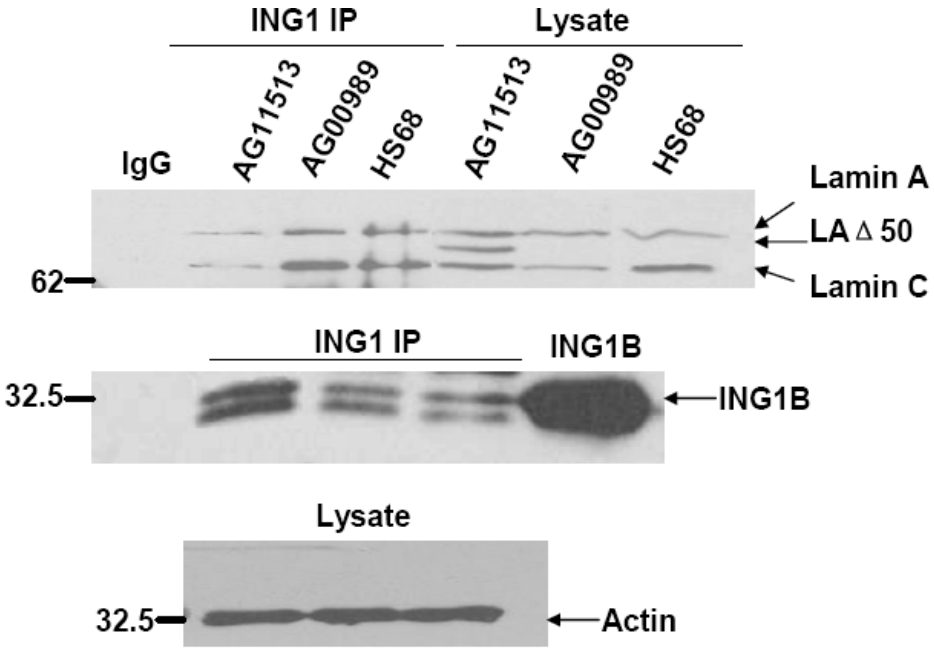
ING1 IP
Lysate
IgG
AG11513
AG00989
HS68
AG11513
AG00989
HS68
Lamin A
LA Δ 50
Lamin C
62
ING1 IP
ING1B
32.5
ING1B
Lysate
32.5
Actin

Figure 13. The LID+NLS polypeptide binds lamin A but not progerin in vitro. Associations of ING1 and lamin A were tested by far western (protein overlay) assay. Equal amounts of lysates from LMNA+/+ MEFs, LMNA-/- MEFs, HS68, AG11513, and AG00989 cells were electrophoresed on SDS-PAGE gel, transferred, and renatured as described in methods. The His-tag purified LID+NLS protein was used to probe the membranes. The LID+NLS protein was shown to bind lamin A *in vitro* (a). Equal loading of cell lysates were indicated by Commassie Brilliant Blue staining in panel c. The levels of lamin A in cell lysates were detected by a rabbit anti-lamin A antibody that could recognize mouse lamins (b).

(a)

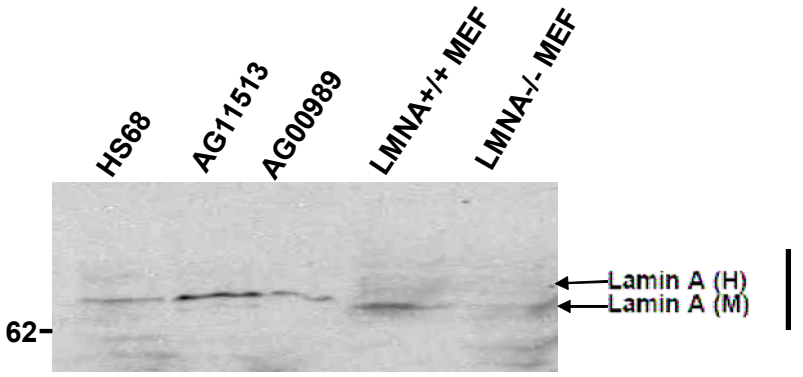
HS68
AG11513
AG00989
LMNA+/+ MEF
LMNA-/- MEF
62
Lamin A (H)
Lamin A (M)

(b)

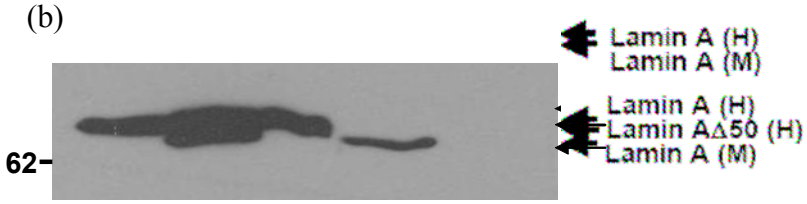
Lamin A (H)
Lamin A (M)
62
Lamin A (H)
Lamin AΔ50 (H)
Lamin A (M)

(c)

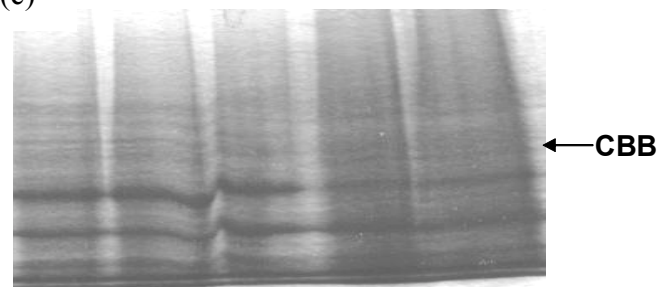
CBB

Figure 14. Co-localization study of ING1 and lamin A. Immunofluorescence staining on ING1 (red) and lamin A (green) and their localization were studied by with deconvolution microscopy. Para-formaldehyde was used to fix cells. ING1 was predominantly in the nucleus in HS68 and AG00989 cell lines, with some cytoplasmic staining in AG00989. However, in AG11513 HGPS fibroblasts, ING1 was largely mislocalized to the cytoplasm. DNA was visualized with DAPI staining (blue). Localization of ING1 and lamin A was merged with Adobe photoshop.

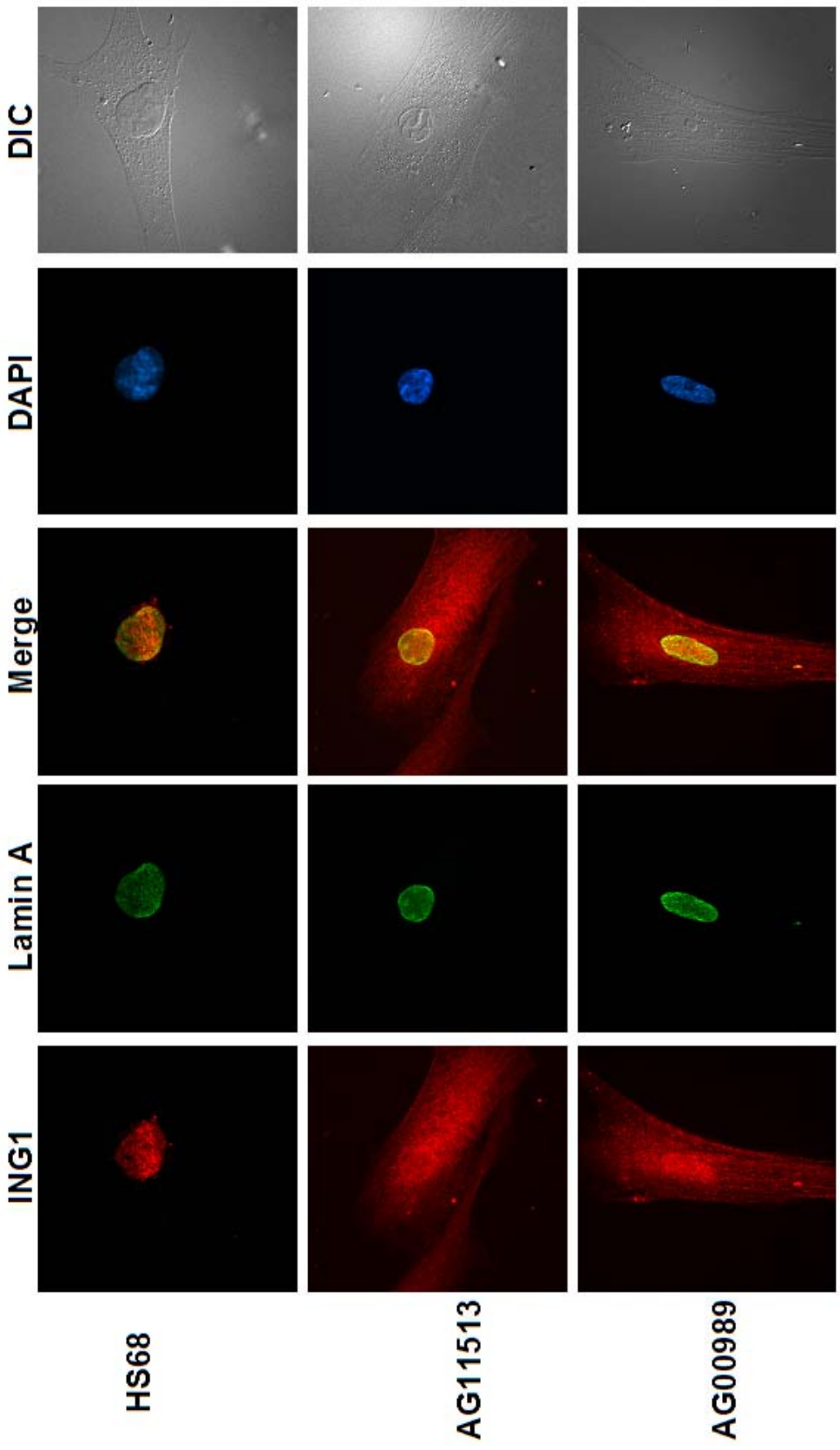
DIC
DAPI
Merge
Lamin A
ING1
HS68
AG11513
AG00989

Figure 15. Co-localization of ING1 and lamin A at different stages of the cell cycle. HS68 fibroblasts were fixed at a relative low confluence and stained for ING1, lamin A, and DNA. Their localization at interphase and different stages of mitosis (prophase, metaphase, early telophase, and telophase) are shown. ING1 seemed to have a higher affinity to lamin A than to chromatin, especially in metaphase and telophase.

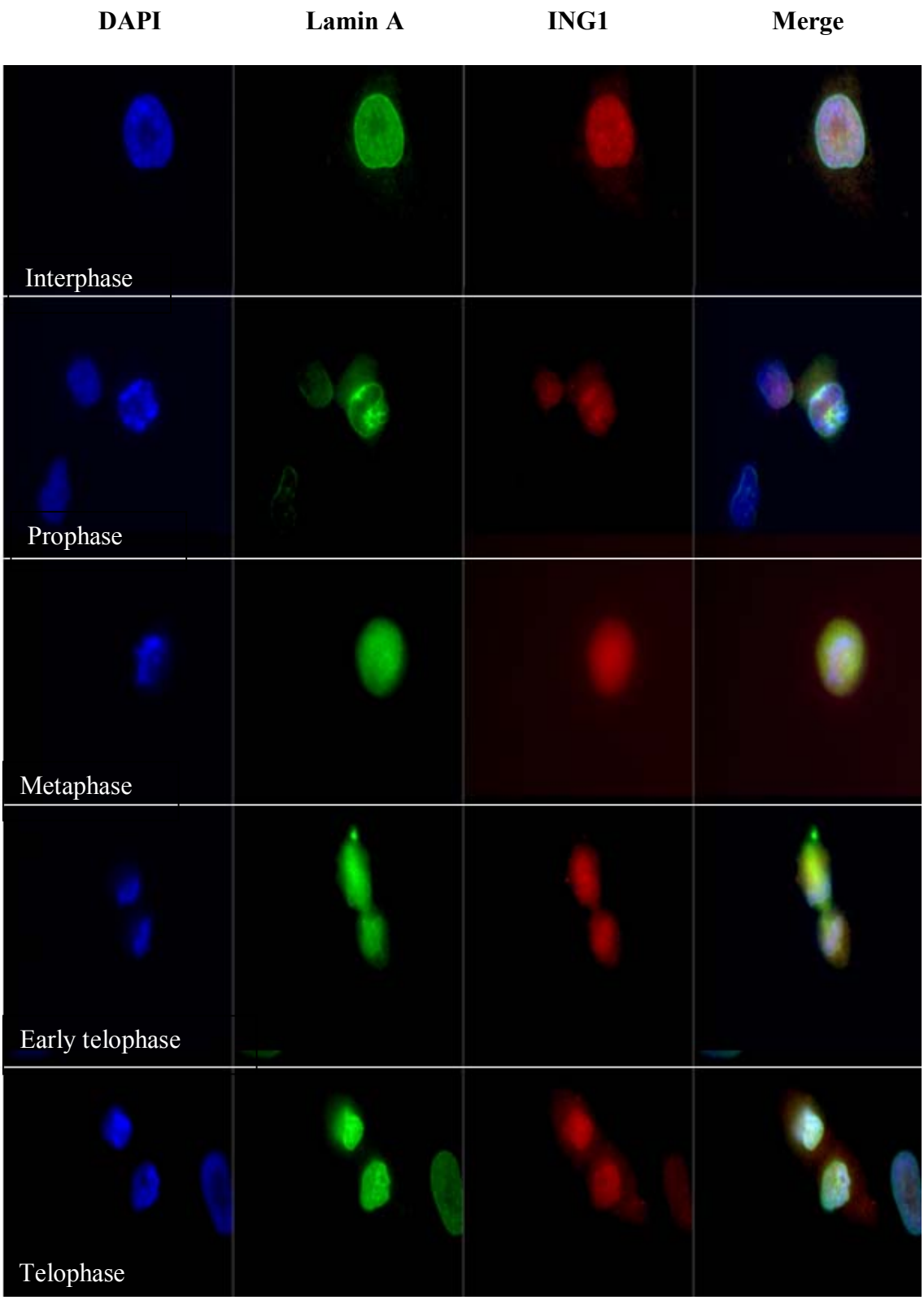
DAPI
Lamin A
ING1
Merge
Interphase
Prophase
Metaphase
Early telophase
Telophase

Figure 16. Localization of ING1 in wild-type and LMNA-/- MEFs and ES cells. Similar to human ING1, mouse ING1 was mainly in the nucleus in wild-type MEFs. In LMNA-/- MEFs and ES cells that do not express lamin A, ING1 seemed to be excluded from the nucleus, suggesting a role for A-type lamins in nuclear anchorage of ING1. The LMNA-/- MEFs frequently displayed elongated nuclei shapes as shown by the DAPI staining. For ES cells, cells were fixed at a relative low confluence, so that individual cells could be studied.

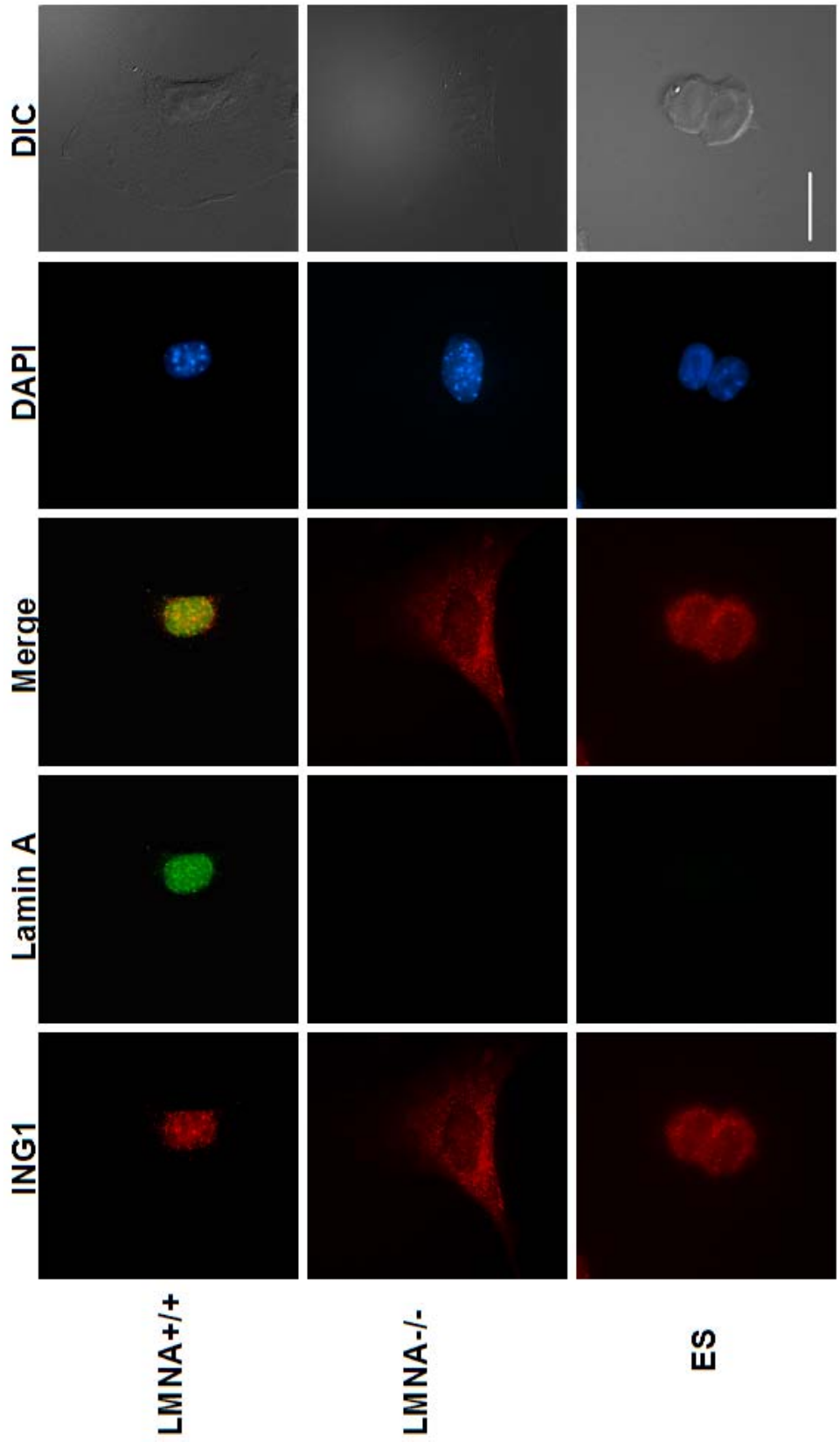
DIC
DAPI
Merge
Lamin A
ING1
LMNA+/+
LMNA-/-
ES

Figure 17. ING1 levels in nuclear fractionations of MEFs. NP-40 buffer was used to perform nuclear fractionations as described in methods. ING1 levels in total (T), cytoplasmic (C), and nuclear (N) fractions of syngeneic wild-type (LMNA+/+) and LMNA-/- murine fibroblasts. Blotting for lamin A and histone H2B confirmed the knockout status of LMNA-/- MEFs and the purity of cytoplasmic and nuclear fractions. Commassie Blue Staining showed total protein in samples. Consistent with previous immunofluorescence data, ING1 was almost absent in the nucleus in LMNA-/- MEFs.

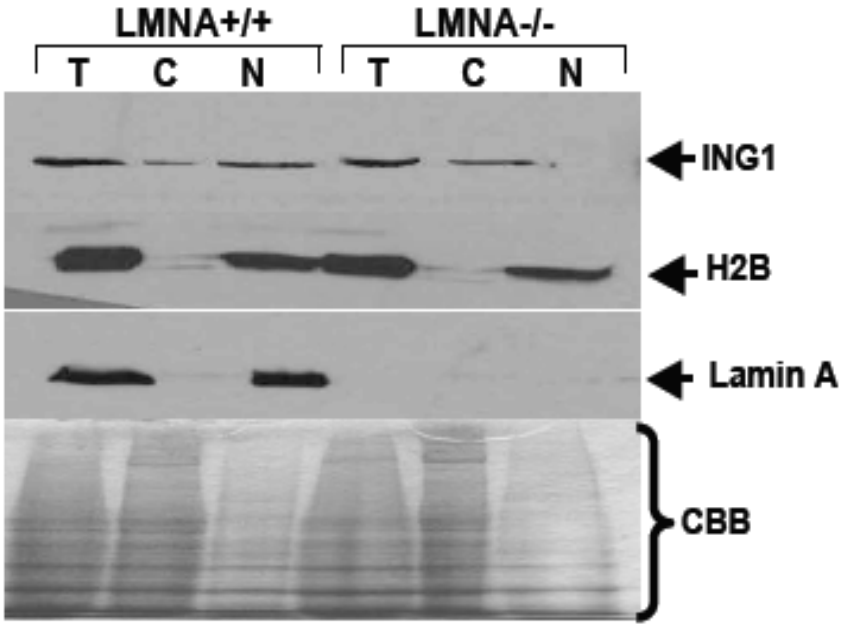
LMNA+/+
LMNA-/-
T
C
N
T
C
N
ING1
H2B
Lamin A
CBB

Figure 18. Interactions with lamins regulates ING1 induction of apoptosis. GFP and ING1b constructs were transfected into HEK293 cells. Cells were harvested at 48 hours following transfection and stained with propidium iodide (PI). Cells with a sub-G1 DNA content as a measure of apoptosis are highlighted by the arrows. The LID induced apoptosis by itself at a similar level to wild type ING1b, while the ING1bΔLID failed to promote apoptosis effectively. Values presented are the average of three independent assays.

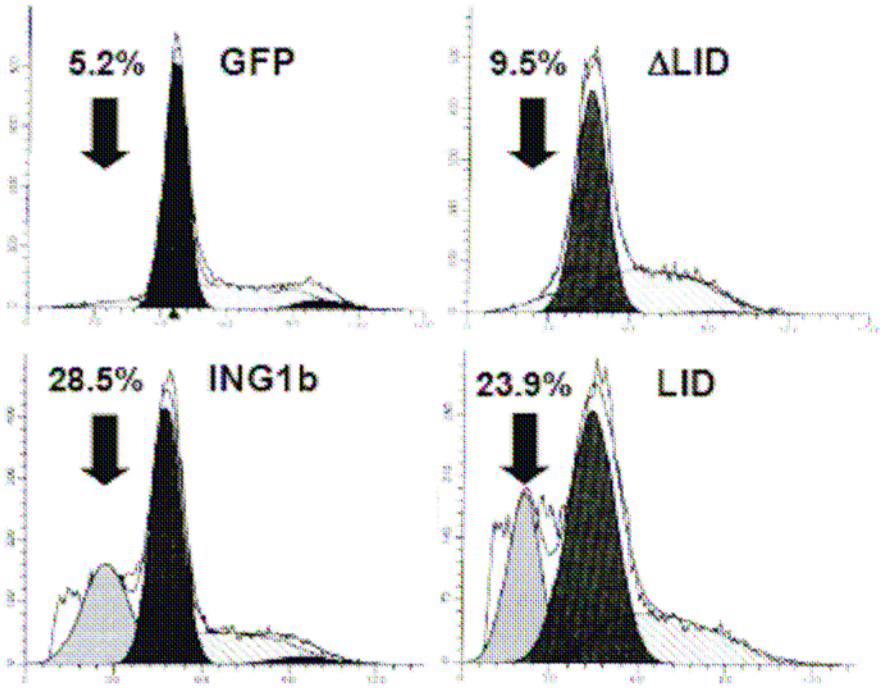
5.2%
GFP
9.5%
ΔLID
28.5%
ING1b
23.9%
LID

Figure 19. Overexpression of ING constructs affects nuclear morphology. ING1b constructs were co-transfected with GFP into HEK293 cells and morphology of GFP-positive cells was examined 48 hours later. DNA was stained with DAPI. Transfection with intact ING1b initially induced a flattened cell morphology as seen in the DIC image and in formation of pycnotic nuclei and other features typical of apoptosis as highlighted by the arrow in the expanded panel to the right and previously reported by many groups. Transfection with the ING1bΔLID construct resulted in abnormal nuclear morphology including multi-nucleated cells but little indication of highly condensed regions of chromatin as seen for ING1b. The LID by itself induced more significant changes in morphology than the ING1bΔLID did.

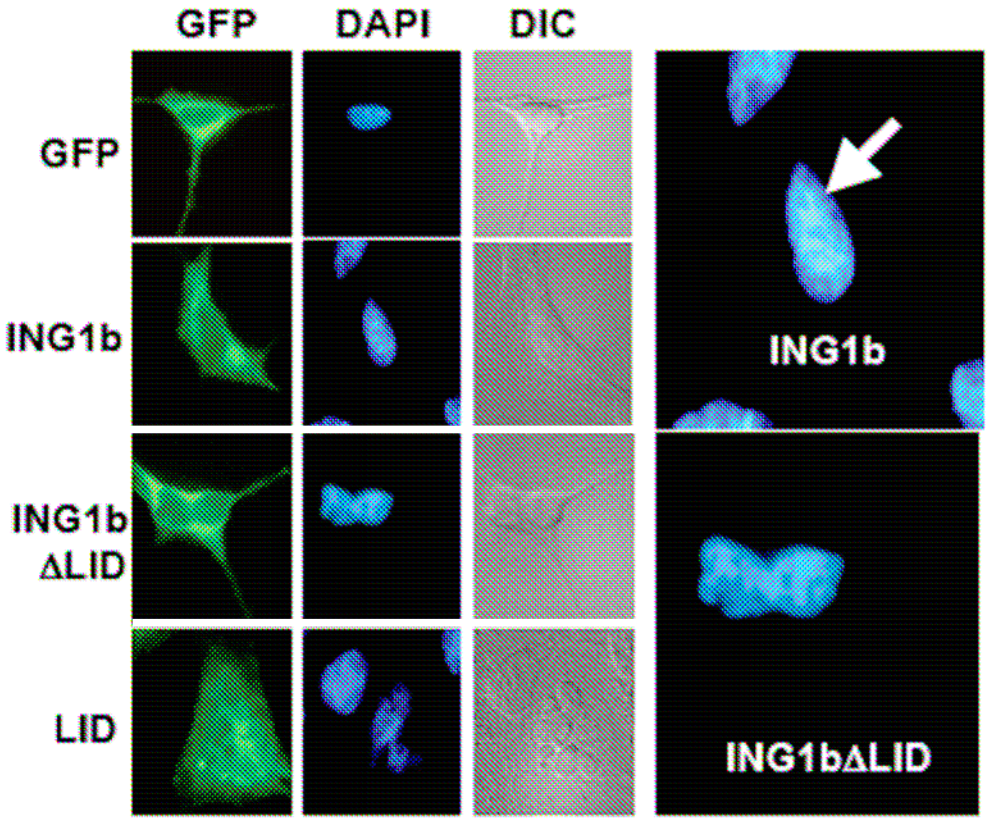
GFP
DAPI
DIC
GFP
ING1b
ING1b
ΔLID
LID
ING1b
ING1bΔLID

Figure 20. Quantitation of effects in nuclear morphology in transfected cells. The percentages were estimated by visual inspection 48 hours after transfection of HEK293 cells with constructs encoding GFP (1), ING1b (2), ING1bΔLID (3), or the LID (4). Abnormal nuclei (a) were defined as those having irregular shapes with multi-lobulation or multiple nuclei (b) and did not include cells with condensed chromatin alone as shown for ING1b transfection. More cells with multi-nuclei (3-4 fold) were observed in the sample transfected with the LID fragment than wild-type ING1b and the ING1bΔLID. p is calculated from t-tests. Error bars represent ± standard deviation.

(a)

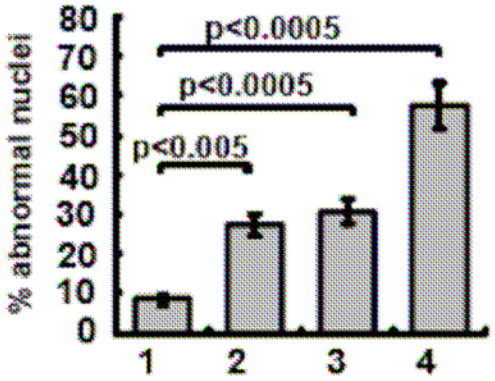
% abnormal nuclei
80
70
60
50
40
30
20
10
0
p<0.0005
p<0.0005
p<0.005
1
2
3
4

(b)

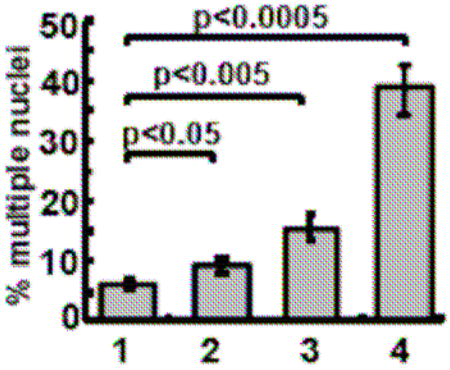
% multiple nuclei
50
40
30
20
10
0
p<0.0005
p<0.005
p<0.05
1
2
3
4

Figure 21. Electron microscopic analysis of HS68, HGPS fibroblasts, and ING1b-transfected cells. Compared to HS68 (a) and AG00989 (b), lobulation and involutions highlighted by the arrows were frequently observed on the nuclear envelope of AG11513 fibroblasts (c) as previously described for HGPS cells. Magnifications used in panels a-f are the same and the bar equals 2µm. d-f, HEK293 cells transfected with GFP (d), the LID (e), or ING1bΔLID (f) were fixed and stained 48 hours after transfection. In contrast to the GFP control which showed morphology similar to untransfected cells (compare panels a & d), both the LID and LID deletion ING1 constructs frequently showed nuclear membrane invaginations, lobulation, or multiple nuclei. Some transfected cells showed discontinuities in the nuclear membrane as highlighted by the arrow in panel f.

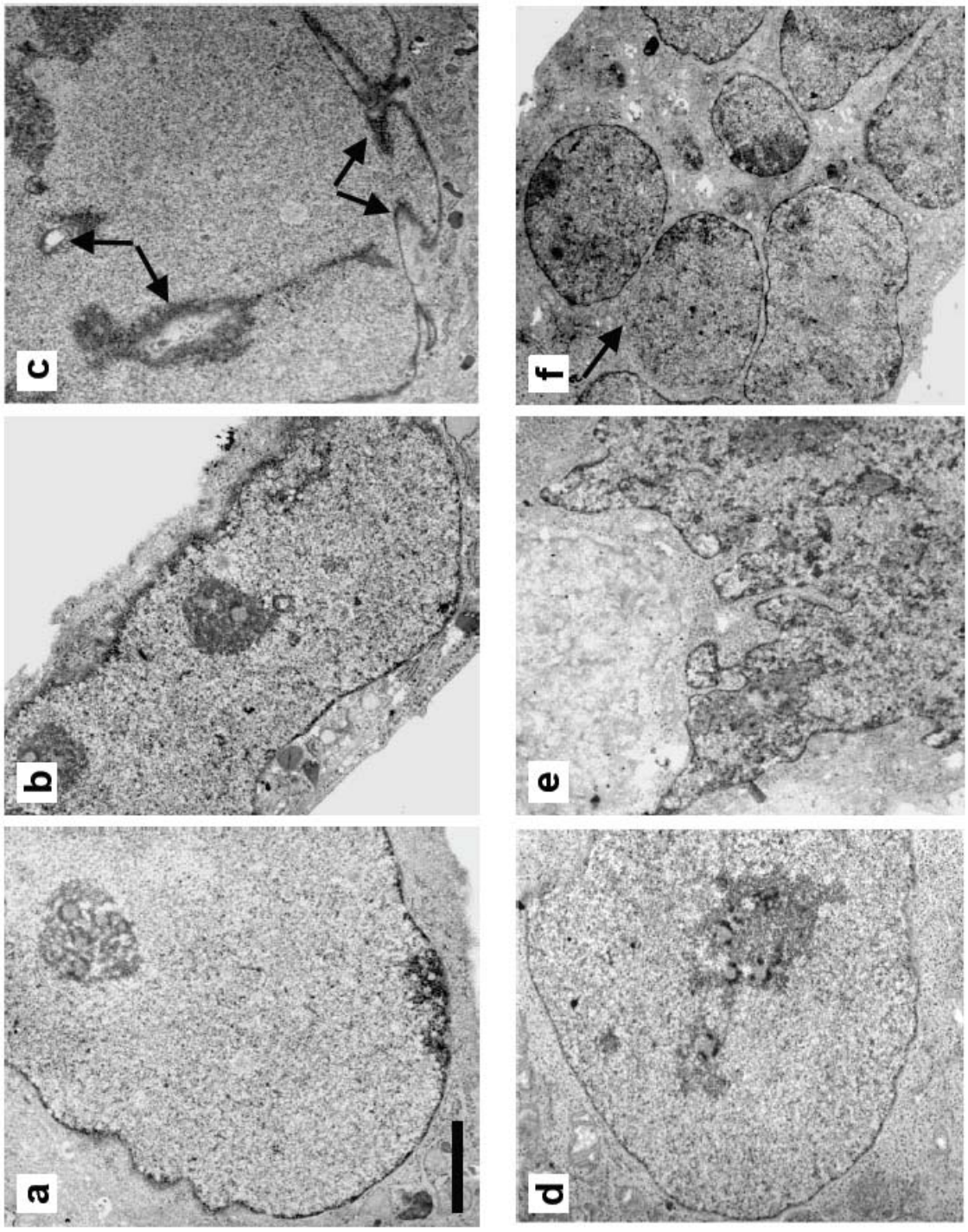
a
b
c
d
e
f

Figure 22. Visualization of peripheral heterochromatin in ING1-transfected cells. The GFP control (a) showed a largely continuous layer of peripheral heterochromatin. Panels b-c are higher magnification micrographs of LID (b) and ING1bΔLID (c) transfected cells that highlight discontinuities in the peripheral heterochromatin (arrowheads) that have been reported in both HGPS and lamin A/C knockout cells. The horizontal arrow in panel c shows distention of the outer nuclear membrane. The bar indicates 0.3mm.

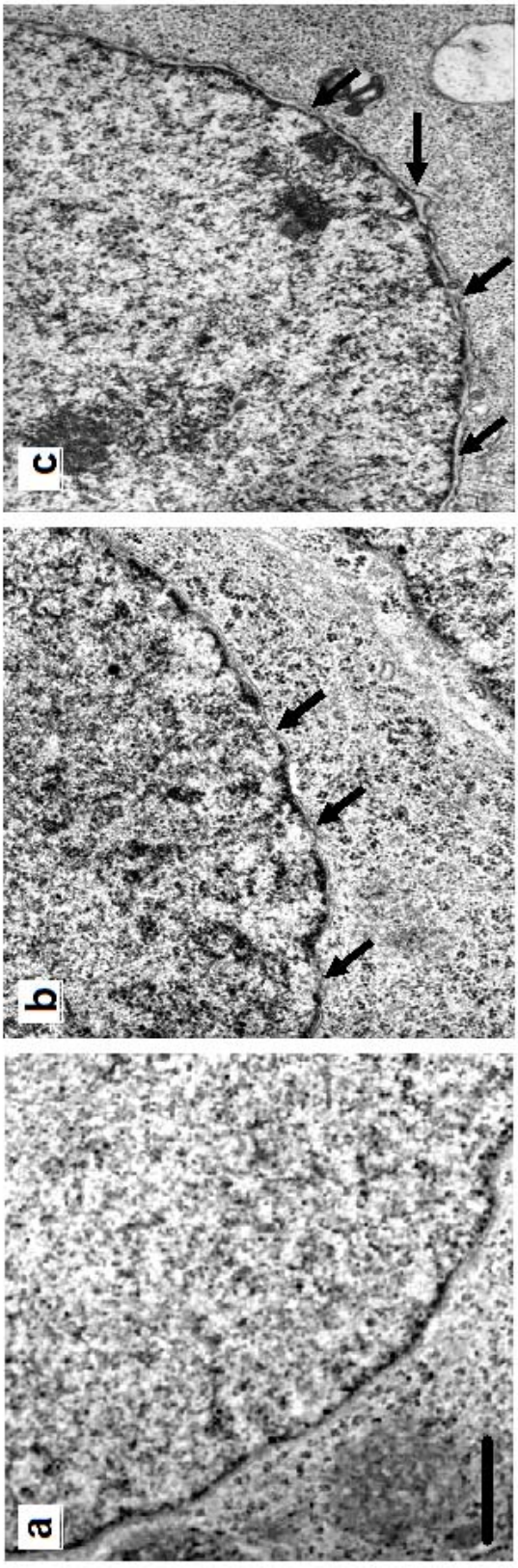
c
b
a

Figure 23. Nuclear morphology of wild-type and LMNA-/- MEFs analyzed by EM. Using the same staining method, wild-type (a) and LMNA-/- (b) MEFs were studied by EM. A great amount of LMNA-/- MEFs were characterized by elongated nuclei, and their nucleoli appeared to become larger than those of wild-type MEFs. Loss of peripheral heterochromatin was also observed in some areas of LMNA-/- MEFs.

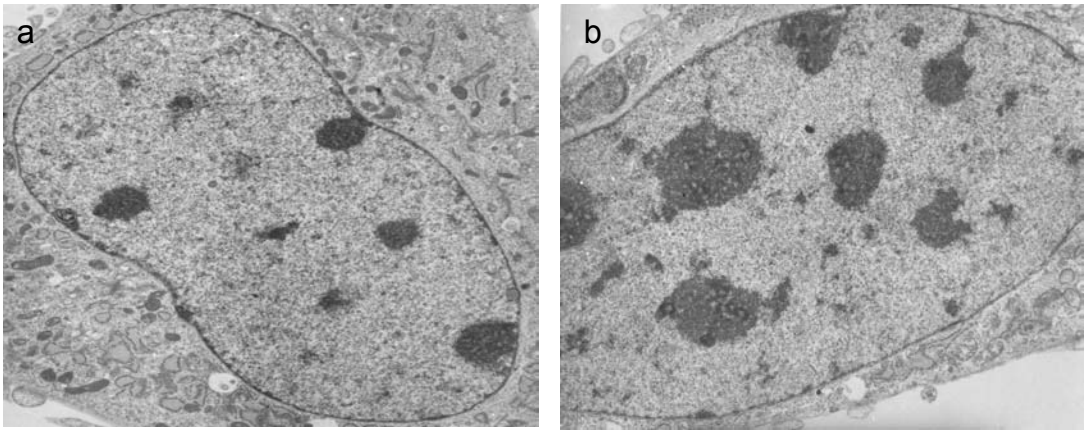
a
b

Figure 24. Overexpression of the LID induced senescence-associated β-galactosidase staining. Senescence-associated β-galactosidase activity was analyzed in young (MPD 29) and old (MPD 95) HS68, AG11513 HGPS fibroblasts (passage 29), and LID-transfected HEK293 cells. Senescent HS68 cells showed a high level of β-galactosidase expression, whereas no obvious staining was observed in young HS68 cells. Even at low passages, the HGPS fibroblasts displayed ~14% β-gal-positive cells, suggesting the initiation of replication senescence. Overexpression of the GFP control vector did not have any effect on β-gal expression (d). Consistent with a role of the LID in inducing HGPS-like phenotype, almost all LID-transfected cells (e) showed dark blue staining.

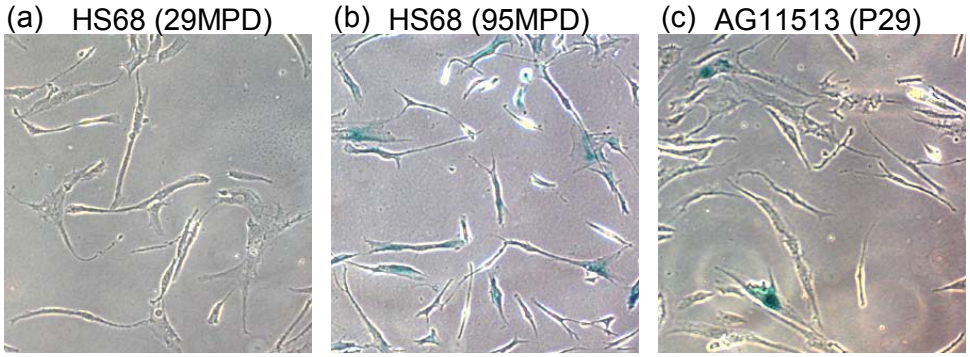
(a) HS68 (29MPD)
(b) HS68 (95MPD)
(c) AG11513 (P29)

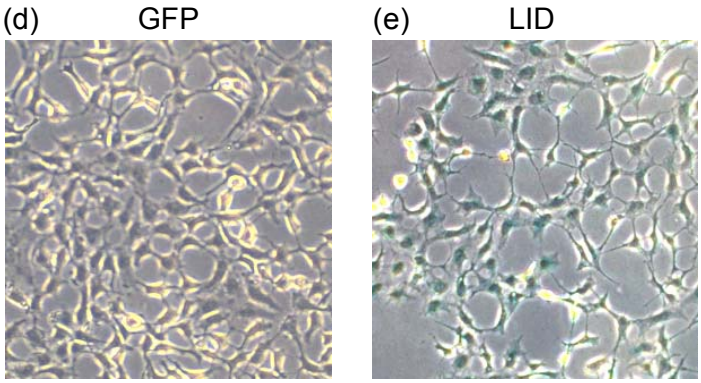
(d) GFP
(e) LID

Figure 25. Model of mechanisms by which ING1 regulates chromatin remodeling through interaction with lamins. ING1 proteins may perform various functions in chromatin remodeling through interactions with both HAT and HDAC complexes. Binding to trimethylated histone H3K4 suggests an important role for ING1 in reading histone codes. Subcellular localization of ING1 may also determine their preferences in regulating histone modifications. Peri-nuclear ING1 associated with lamins may have a preference on HDACs, whereas nucleoplasmic ING1 proteins may bind to more HATs than HDACs, thus contributing to gene transcription. Phosphorylation of ING1b mediates its interaction with 14-3-3 and this interaction is involved in directing ING1b to the cytoplasm.

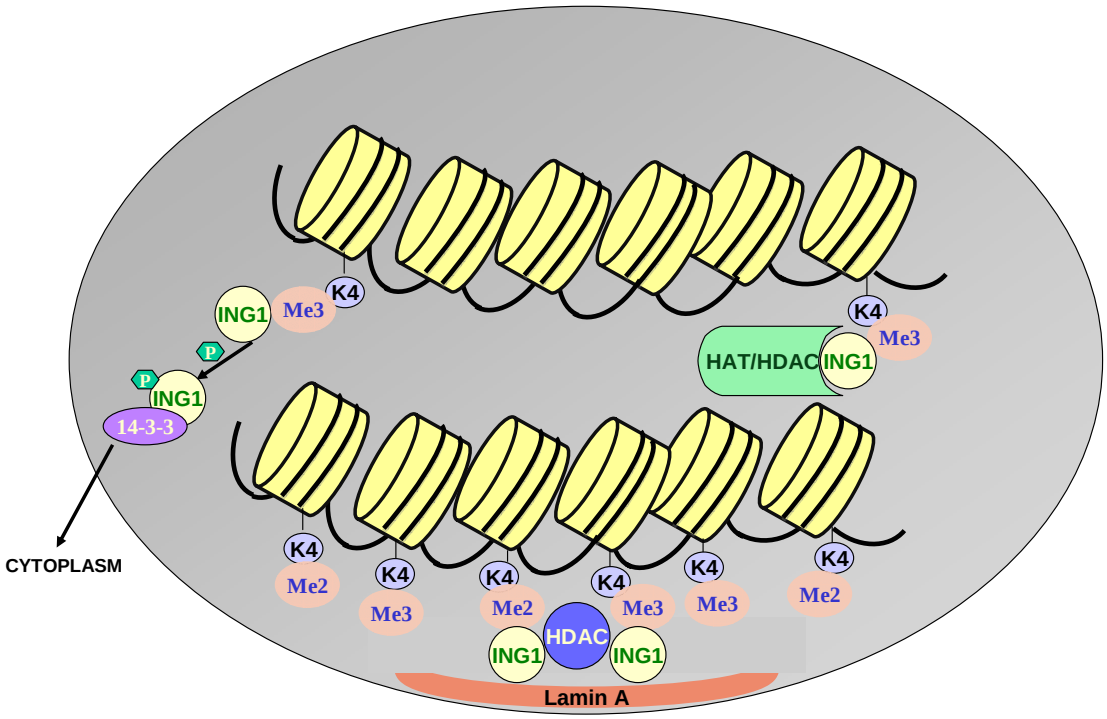
ING1
Me3
K4
P
P
ING1
14-3-3
CYTOPLASM
HAT/HDAC
ING1
K4
Me3
K4
Me2
K4
Me3
K4
Me2
K4
Me3
K4
Me3
K4
Me2
HDAC
ING1
ING1
Lamin A

CHAPTER SIX: BIBLIOGRAPHY

1. Allard,S., R.T.Utley, J.Savard, A.Clarke, P.Grant, C.J.Brandl, L.Pillus, J.L.Workman, and J.Cote. 1999. NuA4, an essential transcription adaptor/histone H4 acetyltransferase complex containing Esa1p and the ATM-related cofactor Tra1p. *EMBO J.* **18**: 5108-5119.

2. Altschul,S.F., T.L.Madden, A.A.Schaffer, J.Zhang, Z.Zhang, W.Miller, and D.J.Lipman. 1997. Gapped BLAST and PSI-BLAST: a new generation of protein database search programs. *Nucleic Acids Res.* **25**: 3389-3402.

3. Aravind,L. and E.V.Koonin. 2000. *Trends Biochem. Sci.* **25**: 112-114.

4. Bannister,A.J. and T.Kouzarides. 2005. Reversing histone methylation. *Nature* **436**: 1103-1106.

5. Beaudouin,J., D.Gerlich, N.Daigle, R.Eils, and J.Ellenberg. 2002. Nuclear envelope breakdown proceeds by microtubule-induced tearing of the lamina. *Cell* **108**: 83-96.

6. Benetti,R., M.Garcia-Cao, and M.A.Blasco. 2007. Telomere length regulates the epigenetic status of mammalian telomeres and subtelomeres. *Nat. Genet.* **39**: 243-250.

7. Berardi,P., M.Russell, A.El-Osta, and K.Riabowol. 2004. Functional links between transcription, DNA repair and apoptosis. *Cell Mol. Life Sci.* **61**: 2173-2180.

8. Bergo,M.O., B.Gavino, J.Ross, W.K.Schmidt, C.Hong, L.V.Kendall, A.Mohr, M.Meta, H.Genant, Y.Jiang, E.R.Wisner, B.N.Van, R.A.Carano, S.Michaelis, S.M.Griffey, and S.G.Young. 2002. Zmpste24 deficiency in mice causes spontaneous bone fractures, muscle weakness, and a prelamin A processing defect. *Proc. Natl. Acad. Sci. U. S. A* **99**: 13049-13054.

9. Bienz,M. 2006. The PHD finger, a nuclear protein-interaction domain. *Trends Biochem. Sci.* **31**: 35-40.

10. Bione,S., E.Maestrini, S.Rivella, M.Mancini, S.Regis, G.Romeo, and D.Toniolo. 1994. Identification of a novel X-linked gene responsible for Emery-Dreifuss muscular dystrophy. *Nat. Genet.* **8**: 323-327.

11. Boland,D., V.Olineck, P.Bonnefin, D.Vieyra, E.Parr, and K.Riabowol. 2000. A panel of CAb antibodies recognize endogenous and ectopically expressed ING1 protein. *Hybridoma* **19**: 161-165.

12. Brachner,A., S.Reipert, R.Foisner, and J.Gotzmann. 2005. LEM2 is a novel MAN1-related inner nuclear membrane protein associated with A-type lamins. *J. Cell Sci.* **118**: 5797-5810.

13. Broers,J.L., C.J.Hutchison, and F.C.Ramaekers. 2004. Laminopathies. *J. Pathol.* **204**: 478-488.

14. Broers,J.L., B.M.Machiels, G.J.van Eys, H.J.Kuijpers, E.M.Manders, D.R.van, and F.C.Ramaekers. 1999. Dynamics of the nuclear lamina as monitored by GFP-tagged A-type lamins. *J. Cell Sci.* **112 (Pt 20)**: 3463-3475.

15. Broers,J.L., F.C.Ramaekers, G.Bonne, R.B.Yaou, and C.J.Hutchison. 2006. Nuclear lamins: laminopathies and their role in premature ageing. *Physiol Rev.* **86**: 967-1008.

16. Burke,B. and L.Gerace. 1986. A cell free system to study reassembly of the nuclear envelope at the end of mitosis. *Cell* **44**: 639-652.

17. Cao,R., L.Wang, H.Wang, L.Xia, H.Erdjument-Bromage, P.Tempst, R.S.Jones, and Y.Zhang. 2002. Role of histone H3 lysine 27 methylation in Polycomb-group silencing. *Science* **298**: 1039-1043.

18. Carr,S., R.Aebersold, M.Baldwin, A.Burlingame, K.Clauser, and A.Nesvizhskii. 2004. The need for guidelines in publication of peptide and protein identification data: Working Group on Publication Guidelines for Peptide and Protein Identification Data. *Mol. Cell Proteomics.* **3**: 531-533.

19. Castelli,C., L.Rivoltini, F.Rini, F.Belli, A.Testori, M.Maio, V.Mazzaferro, J.Coppa, P.K.Srivastava, and G.Parmiani. 2004. Heat shock proteins: biological functions and clinical application as personalized vaccines for human cancer. *Cancer Immunol. Immunother.* **53**: 227-233.

20. Chaudhary,N. and J.C.Courvalin. 1993. Stepwise reassembly of the nuclear envelope at the end of mitosis. *J. Cell Biol.* **122**: 295-306.

21. Chepanoske,C.L., B.E.Richardson, R.M.von, and J.M.Peltier. 2005. Average peptide score: a useful parameter for identification of proteins derived from database searches of liquid chromatography/tandem mass spectrometry data. *Rapid Commun. Mass Spectrom.* **19**: 9-14.

22. Choy,J.S., B.T.Tobe, J.H.Huh, and S.J.Kron. 2001. Yng2p-dependent NuA4 histone H4 acetylation activity is required for mitotic and meiotic progression. *J. Biol. Chem.* **276**: 43653-43662.

23. Coles,A.H., H.Liang, Z.Zhu, C.G.Marfella, J.Kang, A.N.Imbalzano, and S.N.Jones. 2007. Deletion of p37Ing1 in mice reveals a p53-independent role

for Ing1 in the suppression of cell proliferation, apoptosis, and tumorigenesis. *Cancer Res.* **67**: 2054-2061.

24. Columbaro,M., C.Capanni, E.Mattioli, G.Novelli, V.K.Parnaik, S.Squarzoni, N.M.Maraldi, and G.Lattanzi. 2005. Rescue of heterochromatin organization in Hutchinson-Gilford progeria by drug treatment. *Cell Mol. Life Sci.* **62**: 2669-2678.

25. Csoka,A.B., H.Cao, P.J.Sammak, D.Constantinescu, G.P.Schatten, and R.A.Hegele. 2004. Novel lamin A/C gene (LMNA) mutations in atypical progeroid syndromes. *J. Med. Genet.* **41**: 304-308.

26. Das,R., Z.Zhou, and R.Reed. 2000. Functional association of U2 snRNP with the ATP-independent spliceosomal complex E. *Mol. Cell* **5**: 779-787.

27. de la,L.S., K.E.Allen, S.L.Mason, and N.B.La Thangue. 1999. Integration of a growth-suppressing BTB/POZ domain protein with the DP component of the E2F transcription factor. *EMBO J.* **18**: 212-228.

28. DeBusk,F.L. 1972. The Hutchinson-Gilford progeria syndrome. Report of 4 cases and review of the literature. *J. Pediatr.* **80**: 697-724.

29. Dillon,N. 2004. Heterochromatin structure and function. *Biol. Cell* **96**: 631-637.

30. Doyon,Y., C.Cayrou, M.Ullah, A.J.Landry, V.Cote, W.Selleck, W.S.Lane, S.Tan, X.J.Yang, and J.Cote. 2006. ING tumor suppressor proteins are critical regulators of chromatin acetylation required for genome expression and perpetuation. *Mol. Cell* **21**: 51-64.

31. Dreuillet,C., J.Tillit, M.Kress, and M.Ernoult-Lange. 2002. In vivo and in vitro interaction between human transcription factor MOK2 and nuclear lamin A/C. *Nucleic Acids Res.* **30**: 4634-4642.

32. Ellenberg,J., E.D.Siggia, J.E.Moreira, C.L.Smith, J.F.Presley, H.J.Worman, and J.Lippincott-Schwartz. 1997. Nuclear membrane dynamics and reassembly in living cells: targeting of an inner nuclear membrane protein in interphase and mitosis. *J. Cell Biol.* **138**: 1193-1206.

33. Ellis,D.J., H.Jenkins, W.G.Whitfield, and C.J.Hutchison. 1997. GST-lamin fusion proteins act as dominant negative mutants in Xenopus egg extract and reveal the function of the lamina in DNA replication. *J. Cell Sci.* **110 (Pt 20)**: 2507-2518.

34. Eriksson,M., W.T.Brown, L.B.Gordon, M.W.Glynn, J.Singer, L.Scott, M.R.Erdos, C.M.Robbins, T.Y.Moses, P.Berglund, A.Dutra, E.Pak, S.Durkin, A.B.Csoka, M.Boehnke, T.W.Glover, and F.S.Collins. 2003. Recurrent de novo

point mutations in lamin A cause Hutchinson-Gilford progeria syndrome. *Nature* **423**: 293-298.

35. Feng,X., S.Bonni, and K.Riabowol. 2006. HSP70 induction by ING proteins sensitizes cells to tumor necrosis factor alpha receptor-mediated apoptosis. *Mol. Cell Biol.* **26**: 9244-9255.

36. Feng,X., Y.Hara, and K.Riabowol. 2002. Different HATS of the ING1 gene family. *Trends Cell Biol.* **12**: 532-538.

37. Fernandez,A., D.L.Brautigan, and N.J.Lamb. 1992. Protein phosphatase type 1 in mammalian cell mitosis: chromosomal localization and involvement in mitotic exit. *J. Cell Biol.* **116**: 1421-1430.

38. Ferre,P. 1999. Regulation of gene expression by glucose. *Proc. Nutr. Soc.* **58**: 621-623.

39. Foisner,R. and L.Gerace. 1993. Integral membrane proteins of the nuclear envelope interact with lamins and chromosomes, and binding is modulated by mitotic phosphorylation. *Cell* **73**: 1267-1279.

40. Furukawa,K. 1999. LAP2 binding protein 1 (L2BP1/BAF) is a candidate mediator of LAP2-chromatin interaction. *J. Cell Sci.* **112 (Pt 15)**: 2485-2492.

41. Furukawa,K., C.E.Fritze, and L.Gerace. 1998. The major nuclear envelope targeting domain of LAP2 coincides with its lamin binding region but is distinct from its chromatin interaction domain. *J. Biol. Chem.* **273**: 4213-4219.

42. Furukawa,K. and Y.Hotta. 1993. cDNA cloning of a germ cell specific lamin B3 from mouse spermatocytes and analysis of its function by ectopic expression in somatic cells. *EMBO J.* **12**: 97-106.

43. Furukawa,K., H.Inagaki, and Y.Hotta. 1994. Identification and cloning of an mRNA coding for a germ cell-specific A-type lamin in mice. *Exp. Cell Res.* **212**: 426-430.

44. Gant,T.M., C.A.Harris, and K.L.Wilson. 1999. Roles of LAP2 proteins in nuclear assembly and DNA replication: truncated LAP2beta proteins alter lamina assembly, envelope formation, nuclear size, and DNA replication efficiency in Xenopus laevis extracts. *J. Cell Biol.* **144**: 1083-1096.

45. Garkavtsev,I., I.A.Grigorian, V.S.Ossovskaya, M.V.Chernov, P.M.Chumakov, and A.V.Gudkov. 1998a. The candidate tumour suppressor p33ING1 cooperates with p53 in cell growth control. *Nature* **391**: 295-298.

46. Garkavtsev,I., C.Hull, and K.Riabowol. 1998b. Molecular aspects of the relationship between cancer and aging: tumor suppressor activity during cellular senescence. *Exp. Gerontol.* **33**: 81-94.

47. Garkavtsev,I., A.Kazarov, A.Gudkov, and K.Riabowol. 1996. Suppression of the novel growth inhibitor p33ING1 promotes neoplastic transformation. *Nat. Genet.* **14**: 415-420.

48. Garkavtsev,I. and K.Riabowol. 1997. Extension of the replicative life span of human diploid fibroblasts by inhibition of the p33ING1 candidate tumor suppressor. *Mol. Cell Biol.* **17**: 2014-2019.

49. Georgatos,S.D., A.Pyrpasopoulou, and P.A.Theodoropoulos. 1997. Nuclear envelope breakdown in mammalian cells involves stepwise lamina disassembly and microtubule-drive deformation of the nuclear membrane. *J. Cell Sci.* **110 (Pt 17)**: 2129-2140.

50. Glass,C.A., J.R.Glass, H.Taniura, K.W.Hasel, J.M.Blevitt, and L.Gerace. 1993. The alpha-helical rod domain of human lamins A and C contains a chromatin binding site. *EMBO J.* **12**: 4413-4424.

51. Goldman,R.D., Y.Gruenbaum, R.D.Moir, D.K.Shumaker, and T.P.Spann. 2002. Nuclear lamins: building blocks of nuclear architecture. *Genes Dev.* **16**: 533-547.

52. Goldman,R.D., D.K.Shumaker, M.R.Erdos, M.Eriksson, A.E.Goldman, L.B.Gordon, Y.Gruenbaum, S.Khuon, M.Mendez, R.Varga, and F.S.Collins. 2004. Accumulation of mutant lamin A causes progressive changes in nuclear architecture in Hutchinson-Gilford progeria syndrome. *Proc. Natl. Acad. Sci. U. S. A* **101**: 8963-8968.

53. Gong,W., M.Russell, K.Suzuki, and K.Riabowol. 2006. Subcellular targeting of p33ING1b by phosphorylation-dependent 14-3-3 binding regulates p21WAF1 expression. *Mol. Cell Biol.* **26**: 2947-2954.

54. Gong,W., K.Suzuki, M.Russell, and K.Riabowol. 2005. Function of the ING family of PHD proteins in cancer. *Int. J. Biochem. Cell Biol.* **37**: 1054-1065.

55. Gonzalez,L., J.M.Freije, S.Cal, C.Lopez-Otin, M.Serrano, and I.Palmero. 2006. A functional link between the tumour suppressors ARF and p33ING1. *Oncogene* **25**: 5173-5179.

56. Gozani,O., R.Feld, and R.Reed. 1996. Evidence that sequence-independent binding of highly conserved U2 snRNP proteins upstream of the branch site is required for assembly of spliceosomal complex A. *Genes Dev.* **10**: 233-243.

57. Griffith,J.D., L.Comeau, S.Rosenfield, R.M.Stansel, A.Bianchi, H.Moss, and L.T.de. 1999. Mammalian telomeres end in a large duplex loop. *Cell* **97**: 503-514.

58. Gruenbaum,Y., K.L.Wilson, A.Harel, M.Goldberg, and M.Cohen. 2000. Review: nuclear lamins--structural proteins with fundamental functions. *J. Struct. Biol.* **129**: 313-323.

59. Haithcock,E., Y.Dayani, E.Neufeld, A.J.Zahand, N.Feinstein, A.Mattout, Y.Gruenbaum, and J.Liu. 2005. Age-related changes of nuclear architecture in Caenorhabditis elegans. *Proc. Natl. Acad. Sci. U. S. A* **102**: 16690-16695.

60. Han,X., P.Berardi, and K.Riabowol. 2006. Chromatin modification and senescence: linkage by tumor suppressors? *Rejuvenation. Res.* **9**: 69-76.

61. Haraguchi,T., T.Koujin, T.Hayakawa, T.Kaneda, C.Tsutsumi, N.Imamoto, C.Akazawa, J.Sukegawa, Y.Yoneda, and Y.Hiraoka. 2000. Live fluorescence imaging reveals early recruitment of emerin, LBR, RanBP2, and Nup153 to reforming functional nuclear envelopes. *J. Cell Sci.* **113 (Pt 5)**: 779-794.

62. Harbour,J.W. and D.C.Dean. 2000. The Rb/E2F pathway: expanding roles and emerging paradigms. *Genes Dev.* **14**: 2393-2409.

63. He,G.H., C.C.Helbing, M.J.Wagner, C.W.Sensen, and K.Riabowol. 2005. Phylogenetic analysis of the ING family of PHD finger proteins. *Mol. Biol. Evol.* **22**: 104-116.

64. Heald,R. and F.McKeon. 1990. Mutations of phosphorylation sites in lamin A that prevent nuclear lamina disassembly in mitosis. *Cell* **61**: 579-589.

65. Helbing,C.C., C.Veillette, K.Riabowol, R.N.Johnston, and I.Garkavtsev. 1997. A novel candidate tumor suppressor, ING1, is involved in the regulation of apoptosis. *Cancer Res.* **57**: 1255-1258.

66. Helsens,K., L.Martens, J.Vandekerckhove, and K.Gevaert. 2007. MascotDatfile: an open-source library to fully parse and analyse MASCOT MS/MS search results. *Proteomics.* **7**: 364-366.

67. Hinds,P.W., S.Mittnacht, V.Dulic, A.Arnold, S.I.Reed, and R.A.Weinberg. 1992. Regulation of retinoblastoma protein functions by ectopic expression of human cyclins. *Cell* **70**: 993-1006.

68. Holaska,J.M., K.K.Lee, A.K.Kowalski, and K.L.Wilson. 2003. Transcriptional repressor germ cell-less (GCL) and barrier to autointegration factor (BAF) compete for binding to emerin in vitro. *J. Biol. Chem.* **278**: 6969-6975.

69. Holmer,L. and H.J.Worman. 2001. Inner nuclear membrane proteins: functions and targeting. *Cell Mol. Life Sci.* **58**: 1741-1747.

70. Ivorra,C., M.Kubicek, J.M.Gonzalez, S.M.Sanz-Gonzalez, A.varez-Barrientos, J.E.O'Connor, B.Burke, and V.Andres. 2006. A mechanism of AP-1 suppression through interaction of c-Fos with lamin A/C. *Genes Dev.* **20**: 307-320.

71. James,T.C. and S.C.Elgin. 1986. Identification of a nonhistone chromosomal protein associated with heterochromatin in Drosophila melanogaster and its gene. *Mol. Cell Biol.* **6**: 3862-3872.

72. Janknecht,R., M.G.de, J.Lou, R.A.Hipskind, A.Nordheim, and H.G.Stunnenberg. 1991. Rapid and efficient purification of native histidine-tagged protein expressed by recombinant vaccinia virus. *Proc. Natl. Acad. Sci. U. S. A* **88**: 8972-8976.

73. Kaadige,M.R. and D.E.Ayer. 2006. The polybasic region that follows the plant homeodomain zinc finger 1 of Pf1 is necessary and sufficient for specific phosphoinositide binding. *J. Biol. Chem.* **281**: 28831-28836.

74. Kataoka,H., P.Bonnefin, D.Vieyra, X.Feng, Y.Hara, Y.Miura, T.Joh, H.Nakabayashi, H.Vaziri, C.C.Harris, and K.Riabowol. 2003. ING1 represses transcription by direct DNA binding and through effects on p53. *Cancer Res.* **63**: 5785-5792.

75. Kawaji,H., C.Schonbach, Y.Matsuo, J.Kawai, Y.Okazaki, Y.Hayashizaki, and H.Matsuda. 2002. Exploration of novel motifs derived from mouse cDNA sequences. *Genome Res.* **12**: 367-378.

76. Kennedy,B.K., D.A.Barbie, M.Classon, N.Dyson, and E.Harlow. 2000. Nuclear organization of DNA replication in primary mammalian cells. *Genes Dev.* **14**: 2855-2868.

77. Kichina,J.V., M.Zeremski, L.Aris, K.V.Gurova, E.Walker, R.Franks, A.Y.Nikitin, H.Kiyokawa, and A.V.Gudkov. 2006. Targeted disruption of the mouse ing1 locus results in reduced body size, hypersensitivity to radiation and elevated incidence of lymphomas. *Oncogene* **25**: 857-866.

78. Kobza,K., G.Camporeale, B.Rueckert, A.Kueh, J.B.Griffin, G.Sarath, and J.Zempleni. 2005. K4, K9 and K18 in human histone H3 are targets for biotinylation by biotinidase. *FEBS J.* **272**: 4249-4259.

79. Kuzmichev,A., Y.Zhang, H.Erdjument-Bromage, P.Tempst, and D.Reinberg. 2002. Role of the Sin3-histone deacetylase complex in growth regulation by the candidate tumor suppressor p33(ING1). *Mol. Cell Biol.* **22**: 835-848.

80. Lammerding,J. and R.T.Lee. 2005. The nuclear membrane and mechanotransduction: impaired nuclear mechanics and mechanotransduction in lamin A/C deficient cells. *Novartis. Found. Symp.* **264**: 264-273.

81. Lammerding,J., P.C.Schulze, T.Takahashi, S.Kozlov, T.Sullivan, R.D.Kamm, C.L.Stewart, and R.T.Lee. 2004. Lamin A/C deficiency causes defective nuclear mechanics and mechanotransduction. *J. Clin. Invest* **113**: 370-378.

82. Langland,J.O., P.N.Kao, and B.L.Jacobs. 1999. Nuclear factor-90 of activated T-cells: A double-stranded RNA-binding protein and substrate for the double-stranded RNA-dependent protein kinase, PKR. *Biochemistry* **38**: 6361-6368.

83. Lee,S.C., J.Chan, M.V.Clement, and S.Pervaiz. 2006. Functional proteomics of resveratrol-induced colon cancer cell apoptosis: caspase-6-mediated cleavage of lamin A is a major signaling loop. *Proteomics.* **6**: 2386-2394.

84. Lee,W.H., J.Y.Shew, F.D.Hong, T.W.Sery, L.A.Donoso, L.J.Young, R.Bookstein, and E.Y.Lee. 1987. The retinoblastoma susceptibility gene encodes a nuclear phosphoprotein associated with DNA binding activity. *Nature* **329**: 642-645.

85. Lin,F., D.L.Blake, I.Callebaut, I.S.Skerjanc, L.Holmer, M.W.McBurney, M.Paulin-Levasseur, and H.J.Worman. 2000. MAN1, an inner nuclear membrane protein that shares the LEM domain with lamina-associated polypeptide 2 and emerin. *J. Biol. Chem.* **275**: 4840-4847.

86. Liu,B., J.Wang, K.M.Chan, W.M.Tjia, W.Deng, X.Guan, J.D.Huang, K.M.Li, P.Y.Chau, D.J.Chen, D.Pei, A.M.Pendas, J.Cadinanos, C.Lopez-Otin, H.F.Tse, C.Hutchison, J.Chen, Y.Cao, K.S.Cheah, K.Tryggvason, and Z.Zhou. 2005. Genomic instability in laminopathy-based premature aging. *Nat. Med.* **11**: 780-785.

87. Liu,J., K.K.Lee, M.Segura-Totten, E.Neufeld, K.L.Wilson, and Y.Gruenbaum. 2003. MAN1 and emerin have overlapping function(s) essential for chromosome segregation and cell division in Caenorhabditis elegans. *Proc. Natl. Acad. Sci. U. S. A* **100**: 4598-4603.

88. Liu,J., T.Rolef Ben-Shahar, D.Riemer, M.Treinin, P.Spann, K.Weber, A.Fire, and Y.Gruenbaum. 2000. Essential roles for Caenorhabditis elegans lamin gene in nuclear organization, cell cycle progression, and spatial organization of nuclear pore complexes. *Mol. Biol. Cell* **11**: 3937-3947.

89. Lloyd,D.J., R.C.Trembath, and S.Shackleton. 2002. A novel interaction between lamin A and SREBP1: implications for partial lipodystrophy and other laminopathies. *Hum. Mol. Genet.* **11**: 769-777.

90. Loewinger,L. and F.McKeon. 1988. Mutations in the nuclear lamin proteins resulting in their aberrant assembly in the cytoplasm. *EMBO J.* **7**: 2301-2309.

91. Loewith,R., M.Meijer, S.P.Lees-Miller, K.Riabowol, and D.Young. 2000. Three yeast proteins related to the human candidate tumor suppressor p33(ING1) are associated with histone acetyltransferase activities. *Mol. Cell Biol.* **20**: 3807-3816.

92. Loftus,B.J., U.J.Kim, V.P.Sneddon, F.Kalush, R.Brandon, J.Fuhrmann, T.Mason, M.L.Crosby, M.Barnstead, L.Cronin, M.A.Deslattes, Y.Cao, R.X.Xu, H.L.Kang, S.Mitchell, E.E.Eichler, P.C.Harris, J.C.Venter, and M.D.Adams. 1999. Genome duplications and other features in 12 Mb of DNA sequence from human chromosome 16p and 16q. *Genomics* **60**: 295-308.

93. Ludlow,J.W., C.L.Glendening, D.M.Livingston, and J.A.DeCarprio. 1993. Specific enzymatic dephosphorylation of the retinoblastoma protein. *Mol. Cell Biol.* **13**: 367-372.

94. Ludlow,J.W., J.Shon, J.M.Pipas, D.M.Livingston, and J.A.DeCaprio. 1990. The retinoblastoma susceptibility gene product undergoes cell cycle-dependent dephosphorylation and binding to and release from SV40 large T. *Cell* **60**: 387-396.

95. Ma,H., J.Samarabandu, R.S.Devdhar, R.Acharya, P.C.Cheng, C.Meng, and R.Berezney. 1998. Spatial and temporal dynamics of DNA replication sites in mammalian cells. *J. Cell Biol.* **143**: 1415-1425.

96. Machiels,B.M., A.H.Zorenc, J.M.Endert, H.J.Kuijpers, G.J.van Eys, F.C.Ramaekers, and J.L.Broers. 1996. An alternative splicing product of the lamin A/C gene lacks exon 10. *J. Biol. Chem.* **271**: 9249-9253.

97. Maga,G. and U.Hubscher. 2003. Proliferating cell nuclear antigen (PCNA): a dancer with many partners. *J. Cell Sci.* **116**: 3051-3060.

98. Mai,A., S.Massa, D.Rotili, I.Cerbara, S.Valente, R.Pezzi, S.Simeoni, and R.Ragno. 2005. Histone deacetylation in epigenetics: an attractive target for anticancer therapy. *Med. Res. Rev.* **25**: 261-309.

99. Mancini,M.A., B.Shan, J.A.Nickerson, S.Penman, and W.H.Lee. 1994. The retinoblastoma gene product is a cell cycle-dependent, nuclear matrix-associated protein. *Proc. Natl. Acad. Sci. U. S. A* **91**: 418-422.

100. Manilal,S., T.M.Nguyen, C.A.Sewry, and G.E.Morris. 1996. The Emery-Dreifuss muscular dystrophy protein, emerin, is a nuclear membrane protein. *Hum. Mol. Genet.* **5**: 801-808.

101. Markiewicz,E., T.Dechat, R.Foisner, R.A.Quinlan, and C.J.Hutchison. 2002. Lamin A/C binding protein LAP2alpha is required for nuclear anchorage of retinoblastoma protein. *Mol. Biol. Cell* **13**: 4401-4413.

102. Marmorstein,R. 2004. Structural and chemical basis of histone acetylation. *Novartis. Found. Symp.* **259**: 78-98.

103. Martelli,A.M., M.Zweyer, R.L.Ochs, P.L.Tazzari, G.Tabellini, P.Narducci, and R.Bortul. 2001. Nuclear apoptotic changes: an overview. *J. Cell Biochem.* **82**: 634-646.

104. Martens,J.A. and F.Winston. 2003. Recent advances in understanding chromatin remodeling by Swi/Snf complexes. *Curr. Opin. Genet. Dev.* **13**: 136-142.

105. Massague,J. 1998. TGF-beta signal transduction. *Annu. Rev. Biochem.* **67**: 753-791.

106. Massague,J., J.Seoane, and D.Wotton. 2005. Smad transcription factors. *Genes Dev.* **19**: 2783-2810.

107. McClintock,D., L.B.Gordon, and K.Djabali. 2006. Hutchinson-Gilford progeria mutant lamin A primarily targets human vascular cells as detected by an anti-Lamin A G608G antibody. *Proc. Natl. Acad. Sci. U. S. A* **103**: 2154-2159.

108. McKeon,F.D., M.W.Kirschner, and D.Caput. 1986. Homologies in both primary and secondary structure between nuclear envelope and intermediate filament proteins. *Nature* **319**: 463-468.

109. Meier,J., K.H.Campbell, C.C.Ford, R.Stick, and C.J.Hutchison. 1991. The role of lamin LIII in nuclear assembly and DNA replication, in cell-free extracts of Xenopus eggs. *J. Cell Sci.* **98 (Pt 3)**: 271-279.

110. Mihara,K., X.R.Cao, A.Yen, S.Chandler, B.Driscoll, A.L.Murphree, A.T'Ang, and Y.K.Fung. 1989. Cell cycle-dependent regulation of phosphorylation of the human retinoblastoma gene product. *Science* **246**: 1300-1303.

111. Mislow,J.M., J.M.Holaska, M.S.Kim, K.K.Lee, M.Segura-Totten, K.L.Wilson, and E.M.McNally. 2002. Nesprin-1alpha self-associates and binds directly to emerin and lamin A in vitro. *FEBS Lett.* **525**: 135-140.

112. Moir,R.D. and R.D.Goldman. 1993. Lamin dynamics. *Curr. Opin. Cell Biol.* **5**: 408-411.

113. Moir,R.D., M.Montag-Lowy, and R.D.Goldman. 1994. Dynamic properties of nuclear lamins: lamin B is associated with sites of DNA replication. *J. Cell Biol.* **125**: 1201-1212.

114. Moir,R.D., T.P.Spann, H.Herrmann, and R.D.Goldman. 2000a. Disruption of nuclear lamin organization blocks the elongation phase of DNA replication. *J. Cell Biol.* **149**: 1179-1192.

115. Moir,R.D., M.Yoon, S.Khuon, and R.D.Goldman. 2000b. Nuclear lamins A and B1: different pathways of assembly during nuclear envelope formation in living cells. *J. Cell Biol.* **151**: 1155-1168.

116. Nagashima,M., M.Shiseki, K.Miura, K.Hagiwara, S.P.Linke, R.Pedeux, X.W.Wang, J.Yokota, K.Riabowol, and C.C.Harris. 2001. DNA damage-inducible gene p33ING2 negatively regulates cell proliferation through acetylation of p53. *Proc. Natl. Acad. Sci. U. S. A* **98**: 9671-9676.

117. Nagashima,M., M.Shiseki, R.M.Pedeux, S.Okamura, M.Kitahama-Shiseki, K.Miura, J.Yokota, and C.C.Harris. 2003. A novel PHD-finger motif protein, p47ING3, modulates p53-mediated transcription, cell cycle control, and apoptosis. *Oncogene* **22**: 343-350.

118. Nagy,A., J.Rossant, R.Nagy, W.bramow-Newerly, and J.C.Roder. 1993. Derivation of completely cell culture-derived mice from early-passage embryonic stem cells. *Proc. Natl. Acad. Sci. U. S. A* **90**: 8424-8428.

119. Nakamura,H., T.Morita, and C.Sato. 1986. Structural organizations of replicon domains during DNA synthetic phase in the mammalian nucleus. *Exp. Cell Res.* **165**: 291-297.

120. Nakayasu,H. and R.Berezney. 1989. Mapping replicational sites in the eucaryotic cell nucleus. *J. Cell Biol.* **108**: 1-11.

121. Nevins,J.R. 2001. The Rb/E2F pathway and cancer. *Hum. Mol. Genet.* **10**: 699-703.

122. Newport,J.W., K.L.Wilson, and W.G.Dunphy. 1990. A lamin-independent pathway for nuclear envelope assembly. *J. Cell Biol.* **111**: 2247-2259.

123. Nielsen,A.L., M.Oulad-Abdelghani, J.A.Ortiz, E.Remboutsika, P.Chambon, and R.Losson. 2001. Heterochromatin formation in mammalian cells: interaction between histones and HP1 proteins. *Mol. Cell* **7**: 729-739.

124. Nigg,E.A. 1992. Assembly and cell cycle dynamics of the nuclear lamina. *Semin. Cell Biol.* **3**: 245-253.

125. Nili,E., G.S.Cojocaru, Y.Kalma, D.Ginsberg, N.G.Copeland, D.J.Gilbert, N.A.Jenkins, R.Berger, S.Shaklai, N.Amariglio, F.Brok-Simoni, A.J.Simon, and G.Rechavi. 2001. Nuclear membrane protein LAP2beta mediates transcriptional repression alone and together with its binding partner GCL (germ-cell-less). *J. Cell Sci.* **114**: 3297-3307.

126. Notredame,C., D.G.Higgins, and J.Heringa. 2000. T-Coffee: A novel method for fast and accurate multiple sequence alignment. *J. Mol. Biol.* **302**: 205-217.

127. Ozaki,T., M.Saijo, K.Murakami, H.Enomoto, Y.Taya, and S.Sakiyama. 1994. Complex formation between lamin A and the retinoblastoma gene product: identification of the domain on lamin A required for its interaction. *Oncogene* **9**: 2649-2653.

128. Palacios,A., P.Garcia, D.Padro, E.Lopez-Hernandez, I.Martin, and F.J.Blanco. 2006. Solution structure and NMR characterization of the binding to methylated histone tails of the plant homeodomain finger of the tumour suppressor ING4. *FEBS Lett.* **580**: 6903-6908.

129. Parry,D.A., J.F.Conway, and P.M.Steinert. 1986. Structural studies on lamin. Similarities and differences between lamin and intermediate-filament proteins. *Biochem. J.* **238**: 305-308.

130. Paulson,J.R., J.S.Patzlaff, and A.J.Vallis. 1996. Evidence that the endogenous histone H1 phosphatase in HeLa mitotic chromosomes is protein phosphatase 1, not protein phosphatase 2A. *J. Cell Sci.* **109 (Pt 6)**: 1437-1447.

131. Pedeux,R., S.Sengupta, J.C.Shen, O.N.Demidov, S.Saito, H.Onogi, K.Kumamoto, S.Wincovitch, S.H.Garfield, M.McMenamin, M.Nagashima, S.R.Grossman, E.Appella, and C.C.Harris. 2005. ING2 regulates the onset of replicative senescence by induction of p300-dependent p53 acetylation. *Mol. Cell Biol.* **25**: 6639-6648.

132. Peixoto,P. and A.Lansiaux. 2006. [Histone-deacetylases inhibitors: from TSA to SAHA]. *Bull. Cancer* **93**: 27-36.

133. Pena,P.V., F.Davrazou, X.Shi, K.L.Walter, V.V.Verkhusha, O.Gozani, R.Zhao, and T.G.Kutateladze. 2006. Molecular mechanism of histone H3K4me3 recognition by plant homeodomain of ING2. *Nature* **442**: 100-103.

134. Pendas,A.M., Z.Zhou, J.Cadinanos, J.M.Freije, J.Wang, K.Hultenby, A.Astudillo, A.Wernerson, F.Rodriguez, K.Tryggvason, and C.Lopez-Otin. 2002. Defective prelamin A processing and muscular and adipocyte alterations in Zmpste24 metalloproteinase-deficient mice. *Nat. Genet.* **31**: 94-99.

135. Perkins,D.N., D.J.Pappin, D.M.Creasy, and J.S.Cottrell. 1999. Probability-based protein identification by searching sequence databases using mass spectrometry data. *Electrophoresis* **20**: 3551-3567.

136. Peter,M., J.Nakagawa, M.Doree, J.C.Labbe, and E.A.Nigg. 1990. In vitro disassembly of the nuclear lamina and M phase-specific phosphorylation of lamins by cdc2 kinase. *Cell* **61**: 591-602.

137. Peters,A.H., S.Kubicek, K.Mechtler, R.J.O'Sullivan, A.A.Derijck, L.Perez-Burgos, A.Kohlmaier, S.Opravil, M.Tachibana, Y.Shinkai, J.H.Martens, and T.Jenuwein. 2003. Partitioning and plasticity of repressive histone methylation states in mammalian chromatin. *Mol. Cell* **12**: 1577-1589.

138. Rao,L., D.Perez, and E.White. 1996. Lamin proteolysis facilitates nuclear events during apoptosis. *J. Cell Biol.* **135**: 1441-1455.

139. Rice,J.C., S.D.Briggs, B.Ueberheide, C.M.Barber, J.Shabanowitz, D.F.Hunt, Y.Shinkai, and C.D.Allis. 2003. Histone methyltransferases direct different degrees of methylation to define distinct chromatin domains. *Mol. Cell* **12**: 1591-1598.

140. Rober,R.A., K.Weber, and M.Osborn. 1989. Differential timing of nuclear lamin A/C expression in the various organs of the mouse embryo and the young animal: a developmental study. *Development* **105**: 365-378.

141. Roth,S.Y., J.M.Denu, and C.D.Allis. 2001. Histone acetyltransferases. *Annu. Rev. Biochem.* **70**: 81-120.

142. Roux,K.J. and B.Burke. 2007. Nuclear envelope defects in muscular dystrophy. *Biochim. Biophys. Acta* **1772**: 118-127.

143. Rusinol,A.E. and M.S.Sinensky. 2006. Farnesylated lamins, progeroid syndromes and farnesyl transferase inhibitors. *J. Cell Sci.* **119**: 3265-3272.

144. Santos-Rosa,H., R.Schneider, A.J.Bannister, J.Sherriff, B.E.Bernstein, N.C.Emre, S.L.Schreiber, J.Mellor, and T.Kouzarides. 2002. Active genes are tri-methylated at K4 of histone H3. *Nature* **419**: 407-411.

145. Scaffidi,P. and T.Misteli. 2005. Reversal of the cellular phenotype in the premature aging disease Hutchinson-Gilford progeria syndrome. *Nat. Med.* **11**: 440-445.

146. Scaffidi,P. and T.Misteli. 2006. Lamin A-dependent nuclear defects in human aging. *Science* **312**: 1059-1063.

147. Schaffer,A.A., L.Aravind, T.L.Madden, S.Shavirin, J.L.Spouge, Y.I.Wolf, E.V.Koonin, and S.F.Altschul. 2001. Improving the accuracy of PSI-BLAST protein database searches with composition-based statistics and other refinements. *Nucleic Acids Res.* **29**: 2994-3005.

148. Schuler,E., F.Lin, and H.J.Worman. 1994. Characterization of the human gene encoding LBR, an integral protein of the nuclear envelope inner membrane. *J. Biol. Chem.* **269**: 11312-11317.

149. Scott,M., F.M.Boisvert, D.Vieyra, R.N.Johnston, D.P.Bazett-Jones, and K.Riabowol. 2001a. UV induces nucleolar translocation of ING1 through two distinct nucleolar targeting sequences. *Nucleic Acids Res.* **29**: 2052-2058.

150. Scott,M., P.Bonnefin, D.Vieyra, F.M.Boisvert, D.Young, D.P.Bazett-Jones, and K.Riabowol. 2001b. UV-induced binding of ING1 to PCNA regulates the induction of apoptosis. *J. Cell Sci.* **114**: 3455-3462.

151. Senior,A. and L.Gerace. 1988. Integral membrane proteins specific to the inner nuclear membrane and associated with the nuclear lamina. *J. Cell Biol.* **107**: 2029-2036.

152. Shi,X., T.Hong, K.L.Walter, M.Ewalt, E.Michishita, T.Hung, D.Carney, P.Pena, F.Lan, M.R.Kaadige, N.Lacoste, C.Cayrou, F.Davrazou, A.Saha, B.R.Cairns, D.E.Ayer, T.G.Kutateladze, Y.Shi, J.Cote, K.F.Chua, and O.Gozani. 2006. ING2 PHD domain links histone H3 lysine 4 methylation to active gene repression. *Nature* **442**: 96-99.

153. Shumaker,D.K., T.Dechat, A.Kohlmaier, S.A.Adam, M.R.Bozovsky, M.R.Erdos, M.Eriksson, A.E.Goldman, S.Khuon, F.S.Collins, T.Jenuwein, and R.D.Goldman. 2006. Mutant nuclear lamin A leads to progressive alterations of epigenetic control in premature aging. *Proc. Natl. Acad. Sci. U. S. A* **103**: 8703-8708.

154. Simone,C. 2006. SWI/SNF: the crossroads where extracellular signaling pathways meet chromatin. *J. Cell Physiol* **207**: 309-314.

155. Skowyra,D., M.Zeremski, N.Neznanov, M.Li, Y.Choi, M.Uesugi, C.A.Hauser, W.Gu, A.V.Gudkov, and J.Qin. 2001. Differential association of products of alternative transcripts of the candidate tumor suppressor ING1 with the mSin3/HDAC1 transcriptional corepressor complex. *J. Biol. Chem.* **276**: 8734-8739.

156. Slee,E.A., C.Adrain, and S.J.Martin. 2001. Executioner caspase-3, -6, and -7 perform distinct, non-redundant roles during the demolition phase of apoptosis. *J. Biol. Chem.* **276**: 7320-7326.

157. Spann,T.P., A.E.Goldman, C.Wang, S.Huang, and R.D.Goldman. 2002. Alteration of nuclear lamin organization inhibits RNA polymerase II-dependent transcription. *J. Cell Biol.* **156**: 603-608.

158. Spann,T.P., R.D.Moir, A.E.Goldman, R.Stick, and R.D.Goldman. 1997. Disruption of nuclear lamin organization alters the distribution of replication factors and inhibits DNA synthesis. *J. Cell Biol.* **136**: 1201-1212.

159. Steen,R.L., M.Beullens, H.B.Landsverk, M.Bollen, and P.Collas. 2003. AKAP149 is a novel PP1 specifier required to maintain nuclear envelope integrity in G1 phase. *J. Cell Sci.* **116**: 2237-2246.

160. Steen,R.L. and P.Collas. 2001. Mistargeting of B-type lamins at the end of mitosis: implications on cell survival and regulation of lamins A/C expression. *J. Cell Biol.* **153**: 621-626.

161. Steen,R.L., S.B.Martins, K.Tasken, and P.Collas. 2000. Recruitment of protein phosphatase 1 to the nuclear envelope by A-kinase anchoring protein AKAP149 is a prerequisite for nuclear lamina assembly. *J. Cell Biol.* **150**: 1251-1262.

162. Sterner,D.E. and S.L.Berger. 2000. Acetylation of histones and transcription-related factors. *Microbiol. Mol. Biol. Rev.* **64**: 435-459.

163. Stierle,V., J.Couprie, C.Ostlund, I.Krimm, S.Zinn-Justin, P.Hossenlopp, H.J.Worman, J.C.Courvalin, and I.Duband-Goulet. 2003. The carboxyl-terminal region common to lamins A and C contains a DNA binding domain. *Biochemistry* **42**: 4819-4828.

164. Stuurman,N., S.Heins, and U.Aebi. 1998. Nuclear lamins: their structure, assembly, and interactions. *J. Struct. Biol.* **122**: 42-66.

165. Sullivan,T., D.Escalante-Alcalde, H.Bhatt, M.Anver, N.Bhat, K.Nagashima, C.L.Stewart, and B.Burke. 1999. Loss of A-type lamin expression compromises nuclear envelope integrity leading to muscular dystrophy. *J. Cell Biol.* **147**: 913-920.

166. Takahashi,M., N.Seki, T.Ozaki, M.Kato, T.Kuno, T.Nakagawa, K.Watanabe, K.Miyazaki, M.Ohira, S.Hayashi, M.Hosoda, H.Tokita, H.Mizuguchi, T.Hayakawa, S.Todo, and A.Nakagawara. 2002. Identification of the p33(ING1)-regulated genes that include cyclin B1 and proto-oncogene DEK by using cDNA microarray in a mouse mammary epithelial cell line NMuMG. *Cancer Res.* **62**: 2203-2209.

167. Tallen,G., K.Riabowol, and J.E.Wolff. 2003. Expression of p33ING1 mRNA and chemosensitivity in brain tumor cells. *Anticancer Res.* **23**: 1631-1635.

168. Thompson,L.J., M.Bollen, and A.P.Fields. 1997. Identification of protein phosphatase 1 as a mitotic lamin phosphatase. *J. Biol. Chem.* **272**: 29693-29697.

169. Ting,N.S., P.N.Kao, D.W.Chan, L.G.Lintott, and S.P.Lees-Miller. 1998. DNA-dependent protein kinase interacts with antigen receptor response element binding proteins NF90 and NF45. *J. Biol. Chem.* **273**: 2136-2145.

170. Toth,J.I., S.H.Yang, X.Qiao, A.P.Beigneux, M.H.Gelb, C.L.Moulson, J.H.Miner, S.G.Young, and L.G.Fong. 2005. Blocking protein farnesyltransferase improves nuclear shape in fibroblasts from humans with progeroid syndromes. *Proc. Natl. Acad. Sci. U. S. A* **102**: 12873-12878.

171. Tounekti,O., J.Belehradek, Jr., and L.M.Mir. 1995. Relationships between DNA fragmentation, chromatin condensation, and changes in flow cytometry profiles detected during apoptosis. *Exp. Cell Res.* **217**: 506-516.

172. Ulitzur,N., A.Harel, N.Feinstein, and Y.Gruenbaum. 1992. Lamin activity is essential for nuclear envelope assembly in a Drosophila embryo cell-free extract. *J. Cell Biol.* **119**: 17-25.

173. Ulitzur,N., A.Harel, M.Goldberg, N.Feinstein, and Y.Gruenbaum. 1997. Nuclear membrane vesicle targeting to chromatin in a Drosophila embryo cell-free system. *Mol. Biol. Cell* **8**: 1439-1448.

174. Vakoc,C.R., S.A.Mandat, B.A.Olenchock, and G.A.Blobel. 2005. Histone H3 lysine 9 methylation and HP1gamma are associated with transcription elongation through mammalian chromatin. *Mol. Cell* **19**: 381-391.

175. Vakoc,C.R., M.M.Sachdeva, H.Wang, and G.A.Blobel. 2006. Profile of histone lysine methylation across transcribed mammalian chromatin. *Mol. Cell Biol.* **26**: 9185-9195.

176. Vaquero,A., M.Scher, D.Lee, H.Erdjument-Bromage, P.Tempst, and D.Reinberg. 2004. Human SirT1 interacts with histone H1 and promotes formation of facultative heterochromatin. *Mol. Cell* **16**: 93-105.

177. Varela,I., J.Cadinanos, A.M.Pendas, A.Gutierrez-Fernandez, A.R.Folgueras, L.M.Sanchez, Z.Zhou, F.J.Rodriguez, C.L.Stewart, J.A.Vega, K.Tryggvason, J.M.Freije, and C.Lopez-Otin. 2005. Accelerated ageing in mice deficient in Zmpste24 protease is linked to p53 signalling activation. *Nature* **437**: 564-568.

178. Vaziri,H., S.K.Dessain, E.E.Ng, S.I.Imai, R.A.Frye, T.K.Pandita, L.Guarente, and R.A.Weinberg. 2001. hSIR2(SIRT1) functions as an NAD-dependent p53 deacetylase. *Cell* **107**: 149-159.

179. Vieyra,D., R.Loewith, M.Scott, P.Bonnefin, F.M.Boisvert, P.Cheema, S.Pastyryeva, M.Meijer, R.N.Johnston, D.P.Bazett-Jones, S.McMahon, M.D.Cole, D.Young, and K.Riabowol. 2002a. Human ING1 proteins differentially regulate histone acetylation. *J. Biol. Chem.* **277**: 29832-29839.

180. Vieyra,D., D.L.Senger, T.Toyama, H.Muzik, P.M.Brasher, R.N.Johnston, K.Riabowol, and P.A.Forsyth. 2003. Altered subcellular localization and low frequency of mutations of ING1 in human brain tumors. *Clin. Cancer Res.* **9**: 5952-5961.

181. Vieyra,D., T.Toyama, Y.Hara, D.Boland, R.Johnston, and K.Riabowol. 2002b. ING1 isoforms differentially affect apoptosis in a cell age-dependent manner. *Cancer Res.* **62**: 4445-4452.

182. Waterham,H.R., J.Koster, P.Mooyer, G.G.Noort, R.I.Kelley, W.R.Wilcox, R.J.Wanders, R.C.Hennekam, and J.C.Oosterwijk. 2003. Autosomal recessive HEM/Greenberg skeletal dysplasia is caused by 3 beta-hydroxysterol delta 14-reductase deficiency due to mutations in the lamin B receptor gene. *Am. J. Hum. Genet.* **72**: 1013-1017.

183. Worman,H.J., J.Yuan, G.Blobel, and S.D.Georgatos. 1988. A lamin B receptor in the nuclear envelope. *Proc. Natl. Acad. Sci. U. S. A* **85**: 8531-8534.

184. Xin,H., H.G.Yoon, P.B.Singh, J.Wong, and J.Qin. 2004. Components of a pathway maintaining histone modification and heterochromatin protein 1 binding at the pericentric heterochromatin in Mammalian cells. *J. Biol. Chem.* **279**: 9539-9546.

185. Yang,L., T.Guan, and L.Gerace. 1997. Lamin-binding fragment of LAP2 inhibits increase in nuclear volume during the cell cycle and progression into S phase. *J. Cell Biol.* **139**: 1077-1087.

186. Zeremski,M., J.E.Hill, S.S.Kwek, I.A.Grigorian, K.V.Gurova, I.V.Garkavtsev, L.Diatchenko, E.V.Koonin, and A.V.Gudkov. 1999. Structure and regulation of the mouse ing1 gene. Three alternative transcripts encode two phd finger proteins that have opposite effects on p53 function. *J. Biol. Chem.* **274**: 32172-32181.

187. Zhang,Q., C.Ragnauth, M.J.Greener, C.M.Shanahan, and R.G.Roberts. 2002. The nesprins are giant actin-binding proteins, orthologous to Drosophila melanogaster muscle protein MSP-300. *Genomics* **80**: 473-481.

188. Zhang,Q., C.D.Ragnauth, J.N.Skepper, N.F.Worth, D.T.Warren, R.G.Roberts, P.L.Weissberg, J.A.Ellis, and C.M.Shanahan. 2005. Nesprin-2 is a multi-isomeric protein that binds lamin and emerin at the nuclear envelope and forms a subcellular network in skeletal muscle. *J. Cell Sci.* **118**: 673-687.

189. Zhang,Q., J.N.Skepper, F.Yang, J.D.Davies, L.Hegyi, R.G.Roberts, P.L.Weissberg, J.A.Ellis, and C.M.Shanahan. 2001. Nesprins: a novel family of spectrin-repeat-containing proteins that localize to the nuclear membrane in multiple tissues. *J. Cell Sci.* **114**: 4485-4498.

190. Zhu,L. 2005. Tumour suppressor retinoblastoma protein Rb: a transcriptional regulator. *Eur. J. Cancer* **41**: 2415-2427.